Synthesis and Characterization of Linear and Heterocyclic Bis(ferrocenyl) Containing Compounds

A THESIS SUBMITTED TO THE GRADUATE SCHOOL OF

THE UNIVERSITY OF MINNESOTA BY

Wil Ryan Goetsch

IN PARTIAL FULFILLMENT OF THE REQUIREMENTS FOR THE

DEGREE OF MASTER OF SCIENCE

Advised by Dr. Victor Nemykin

November 2012

Acknowledgments

I would like to extend my gratitude to Dr. Victor Nemykin for his resourcefulness and support throughout my research as a graduate student. I would also like to extend my appreciation to Dr. Pavlo Solntsev for his endless effort in guiding, supporting, and mentoring me in academic research; in addition, I would like to thank Jared Sabin, Derrick Anderson, and Casey Van Stappen for their contributions in computational chemistry, instrumentation technique, and assistance in conducting my research. This research would not have been possible without the opportunity from the University of Minnesota Duluth Department of Chemistry and Biochemistry, funding from the National Science Foundation (Grant CHE-1110455), NSF MRI (Grant CHE-0922366, X-ray diffractometer), and support from the Minnesota Super Computing Institute.

Part One is reprinted with permission from *Organometallics*. **2011**, *30*(24), 6636-6640 and also The Abstracts of Papers, 243rd ACS National Meeting & Exposition, San Diego, CA, United States, March 25-March 29, 2012 (2012), INOR-394.

Abstract

The new and unexpected organometallic mercury compound has been identified in the palladium-catalyzed reaction between bis(ferrocenyl)mercury and dimethylacetylene-dicarboxylate along with the expected dimethyl-(*Z*)-2,3-di(ferrocenyl)-2-butenedioate and biferrocene. Dimethyl-(*Z*)-2,3-di(ferrocenyl)-2-butenedioate resulted from *syn*-addition of 1 to 2 equivalents of dimethylacetylene-dicarboxylate. Dimethyl-(*Z*)-2,3-di(ferrocenyl)-2-butenedioate has been characterized using NMR spectroscopy, while its structure was determined by X-ray crystallography. Dimethyl-(*Z*)-2,3-di(ferrocenyl)-2-butenedioate represents a rare example of an organomercury compound in which a mercury ion is coordinated to two vinylic fragments. X-ray study of the mercury-containing reaction intermediate reveals new insight on the palladium catalyzed reaction mechanism. Accurate, low-temperature experimental data for the crystal structure of biferrocene is also reported.

In addition, structural and spectroscopic study of a newly synthesized 3,4-diferrocene substituted pyrrole derivative was characterized. Electronic structures of dimethyl (Z)-2,3-bis(ferrocenyl)-2-butenedioate and 3,4-diferrocene substituted pyrrole were investigated by UV-vis spectroscopy and density functional theory (DFT) as well as time-dependent DFT (TDDFT) approaches. The calculated vertical excitation energies are consistent with the experimental data and clearly suggest the dominance of metal-to-ligand charge-transfer bands in the visible region of the UV-Vis spectra for dimethyl (Z)-2,3-bis(ferrocenyl)-2-butenedioate.

Redox properties of dimethyl (Z)-2,3-bis(ferrocenyl)-2-butenedioate and 3,4-diferrocene substituted pyrrole were investigated using cyclic voltammetry, differential

pulse voltammetry, and spectroelectrochemical oxidation approaches. In a DCM/$(NBu_4)[B(C_6F_5)_4]$ system, ferrocene-centered oxidation processes are separated by 300 mV (dimethyl (Z)-2,3-bis(ferrocenyl)-2-butenedioate) and 298 mV (3,4-diferrocene substituted pyrrole), respectively. Stepwise spectroelectrochemical oxidation of dimethyl (Z)-2,3-bis(ferrocenyl)-2-butenedioate and 3,4-diferrocene substituted pyrrole allowed us to obtain spectroscopic signatures of the mixed-valence dimethyl (Z)-2,3-bis(ferrocenyl)-2-butenedioate and 3,4-diferrocene substituted pyrrole cations. Hush analysis of the intervalence charge-transfer bands in dimethyl (Z)-2,3-bis(ferrocenyl)-2-butenedioate cation is suggestive of class II (in the Robin and Day classification) behavior.

Table of Contents

Table of Figures

Table of Tables

Table of Schemes

Table of Terms

UV-Vis-NIR: ultra-violet- visible-near infrared

IVCT: inter-valance charge transfer

NMR: nuclear magnetic resonance

TLC: thin layer chromatography

THF: tetrahydrofuran

HOMO: highest occupied molecular orbital

LUMO: lowest unoccupied molecular orbtial

TBAP: tetrabutylammonium perchlorate

TFAB: tetra(fluorophenyl) ammonium borate

Introduction:

Mixed-valence compounds represent an important class of organometallic complexes. Electron transfer between two metal centers can be induced with absorption of a photon of the appropriate energy optically; transfer of electrons can also occur thermally. Optical or thermal electron transfer is responsible for mixed-valence states[1,2,3,4]. According to the Robin and Day classification[4], mixed-valence compounds are categorized into three classes shown in Figure 1. Class I mixed-valence systems, metal ions do not communicate with each other due to differences in the ligand field strength making electron transfer between the two centers unfavorable.

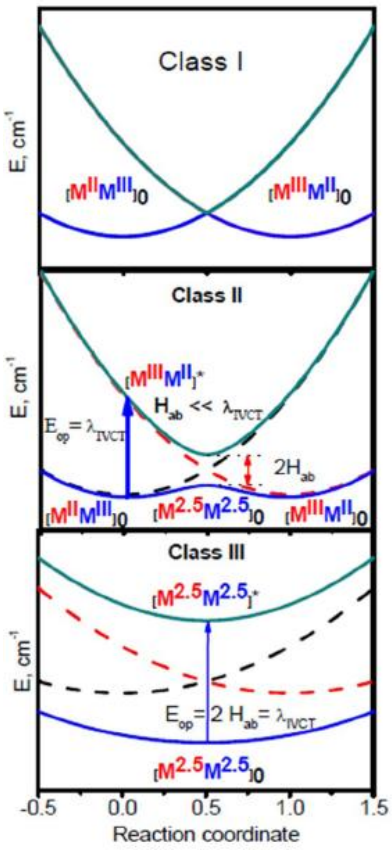

Figure 1: Robin and Day Classification for Mixed-Valence State Compounds.

In Class II mixed-valence systems, metal ions communicate with each other and as electron transfer occurs, oxidation states of the metal ions located in the same environment change. Class II Mixed-valence systems can undergo electron transfer either optically or thermally. Electron transfer is relatively slow, which allows for characterization of separate oxidation and reduction processes between metal centers to be examined. For example, when dinuclear iron complexes are considered, electron transfer to an Fe(II)/ Fe(III) center is slow, and each of these centers exhibit different spectroscopic signatures in the UV-Vis-NIR region[4].

These signatures can be characterized by solvent independent inter-valence charge transfer (IVCT) bands[4]. These bands display different energies (υ_{max}), intensities (ε) and bandwidths at half height ($\Delta\upsilon_{1/2}$),[4] which can be used for the estimation of the coupling matrix element in Class II mixed-valence systems. Class III mixed-valence electron transfer between metal centers is faster and as a result such compounds can be characterized as a valence average system. All types of behavior can be seen in Figure 1.

Ferrocene-containing conjugated compounds are of interest because of their potential applications in materials chemistry[5]. Usually, such assemblies can be prepared by a variety of cross-coupling reactions, which involve derivatives of boronic acid, organotin compounds, and quite often ferrocenyl-mercuric precursors[6,7]. Irena Beletskaya and her co-workers showed that bis(ferrocenyl)mercury could be utilized as a very convenient reagent for the preparation of a wide variety of ferrocene-containing assemblies using palladium-catalyzed cross-coupling reactions with aryl, heteroaryl, and acid halides, as well as alkynes[7].Poly-ferrocenyl conjugated compounds are capable of reversible oxidation, and electrochemical study of such compounds is important to measure separated oxidation-reduction waves of each ferrocenyl substituent. Separated oxidation waves provide concrete evidence in the establishment of a mixed-valence compound without partial oxidation of multiple ferrocene substituents. Recent study has focused on the influence that electron donating substituents have in separating reduction potentials between ferrocenyl substituents; some evidence suggests that electron withdrawing substituents provide increased separation between reduction potentials of ferrocene. The rigidity of the bridging unit also contributes to the separation between

reduction potentials; the more rigid a bridging unit the greater the separation in its reduction potential.

Saverio Santi investigated the influence of electron rich bridging units, four carbon units in length, within diferrocene-containing mixed valence compounds. He began experimenting with 1,3-alkene (3^+), 1,3-alkyne (2^+), and a 1-alken-3-yl (1^+) bridging units. Maintaining bridging units of four carbons in length provided similar contributions, i.e. electrostatic, magnetic, ion-pairing, and solvation factors, from each sample investigated. With increased electron density, the 1-aken-3-yl was hypothesized to provide the best separation of reduction potentials between ferrocenyl substituents. However, it was observed that sp^2 hybrid bridges provided the best reduction potential separation seen in the 1,3-alkene bridging unit[8]. The electronic coupling versus separation in reduction potentials are shown in Figure 2.

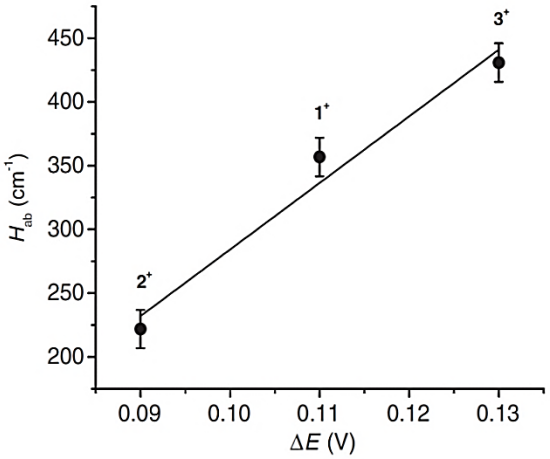

Figure 2: Electronic coupling (H_{ab}) vs. ΔE for 1^+, 2^+, and 3^+.

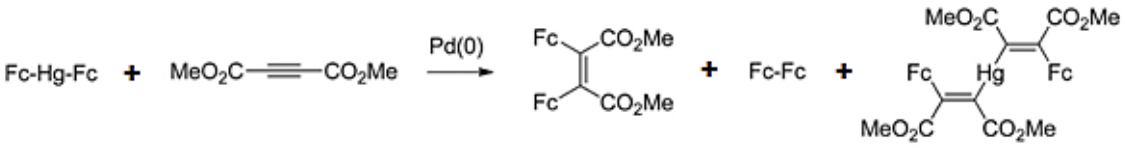

Figure 3: Reaction of bis(ferrocenyl) mercury with dimethylacetylenedicarboxylate, in the presence of palladium, and the products from their reaction.

When bis(ferrocenyl)mercury was introduced in the reaction with dimethylacetylenedicarboxylate, formation of dimethyl-(Z)-2,3-bis(ferrocenyl)-2-butenedioate and biferrocene as the major products were reported. The presence of a very unusual organometallic mercury intermediate compound was observed as a minor

product in the above mentioned reaction seen in Figure 3[9]. Detection of this complex not only provides new insight into the reaction mechanism but also points to a new potential direction for the preparation of the organomercurial compound.

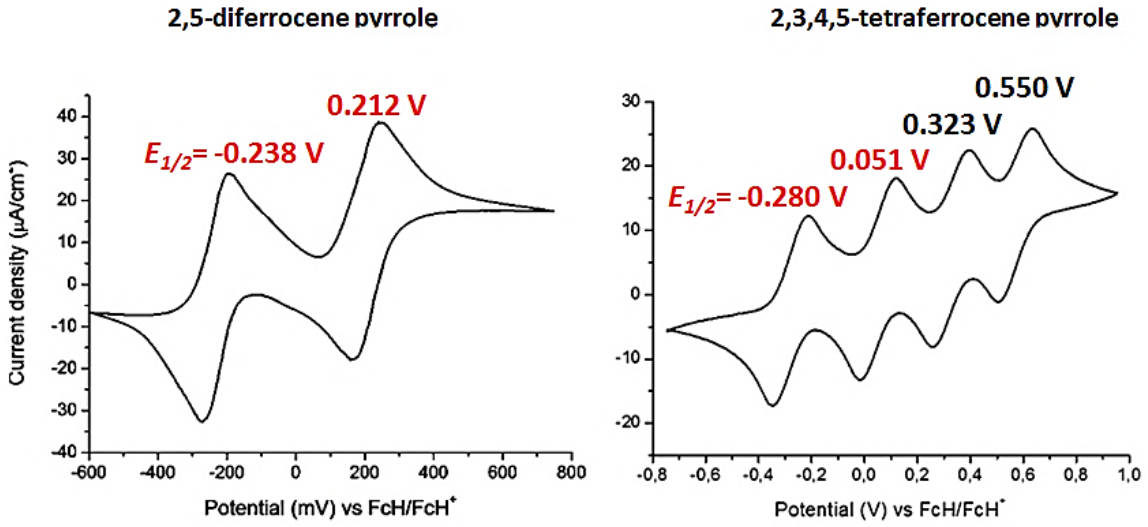

Figure 4: Electrochemical study of 2,5-bis(ferrocenyl)-1-phenyl-1H-pyrrole (**1***) and 2,3,4,5-tetraferrocenyl-1-phenyl-1H-pyrrole (**2***) in TFAB solution.

Similar work on poly-ferrocene pyrrole compounds by Alexander Hildebrandt and his co-workers reported the mixed-valence state behavior of 2,5-bisferrocenyl-1-phenyl-1H-pyrrole (**1***) and 2,3,4,5-tetraferrocenyl-1-phenyl-1H-pyrrole (**2***)[10]. Electrochemical analysis resulted in two (**1***) and four (**2***) diffusion controlled ferrocenyl-related reversible redox events (seen in Figure 4); without evidence from β-substituted(ferrocenyl)pyrrole, oxidation waves for each ferrocenyl substituent were difficult to assign. The electrochemical study of 3,4-diferrocenyl-1-(triisopropylsilyl)pyrrole, never reported previously, clarifies the assignment of each oxidation wave in a tetra(ferrocenyl)pyrrole complex.

The following two chapters report the synthesis and characterization of an unexpected organomercurial reaction intermediate along with the synthesis and

characterization of a beta-substituted pyrrole complex. Electrochemical, spectroelectrochemical, and UV-VIS-NIR analyses were performed for comparison with bis(ferrocenyl) alpha-substituted pyrrole and tetra(ferrocenyl) pyrrole for which results have been previously reported.

I. Unexpected Formation of Organomercurial Intermediate and its Characterization.

Introduction:

Despite their high toxicity, organomercurial compounds have become one of the most widely investigated organometallic reagents for the introduction of a variety of functional groups into predefined organic skeletons[11]. Organomercurial reagents have several important advantages (stability toward hydrolysis and oxygen, lower reactivity with halogen-containing compounds, etc.) over more common lithium and magnesium organometallics[12]. In recent years, organomercurial compounds have also attracted attention as soft and versatile reagents for palladium catalyzed cross-coupling reactions[13]. Organomercurial and mercury-containing heterometallic compounds were intensively tested for applications in chemo sensing devices, NLO and optical materials, catalysis, building blocks for molecular recognition, and supramolecular assemblies[14]. Ferrocene-containing conjugated assemblies in which ferrocene substituents are connected to conjugated electron-donating or electron-withdrawing groups that are of interest because of their potential applications in materials chemistry[15]. Usually, such assemblies can be prepared by a variety of cross-coupling reactions involving derivatives of boronic acid, organotin compounds, and quite often ferrocenyl-mercuric precursors[16,17]. In several

reports, Beletskaya and her co-workers showed that bis(ferrocenyl)mercury could be utilized as a very convenient reagent for the preparation of a variety of ferrocene-containing assemblies using palladium-catalyzed cross-coupling reactions with aryl, heteroaryl, and acid halides, as well as alkynes[17]. In the latter case, when bis(ferrocenyl)mercury (**1**) was introduced in the reaction with dimethylacetylenedicarboxylate (**2**), formation of dimethyl-(*Z*)-2,3-di(ferrocenyl)-2-butanedioate (**4**) and biferrocene (**5**) as the major reaction products were reported[17b]. We report the characterization of a very unusual organometallic mercury dimethyl-(Z)-2,3-bis(ferrocenyl)-2-butenedioate (**3**) in the above-mentioned reaction. Detection of this complex not only provides new insight into the reaction mechanism but also points to a new potential direction for the preparation of organomercurial compounds.

Synthesis:

As described by Beletskaya and her co-workers,[17b] the reaction between bis-(ferrocenyl)mercury (**1**, Scheme 1) and dimethylacetylenedicarboxylate (**2**, Scheme 1) in 1:2 molar ratio reproducibly results in the formation of orange dimethyl-(*Z*)-2,3-di(ferrocenyl)-2-butenedioate (**4**, Scheme 1) and orange biferrocene (**5**, Scheme 1) as the major reaction products forming only in the presence of a palladium catalyst. These stable compounds could be easily separated by column chromatography. During purification of the reaction mixture we noticed the reproducible presence of a red-colored reaction byproduct, which degraded on the column and could be eluted after the major reaction product **4**[15a].

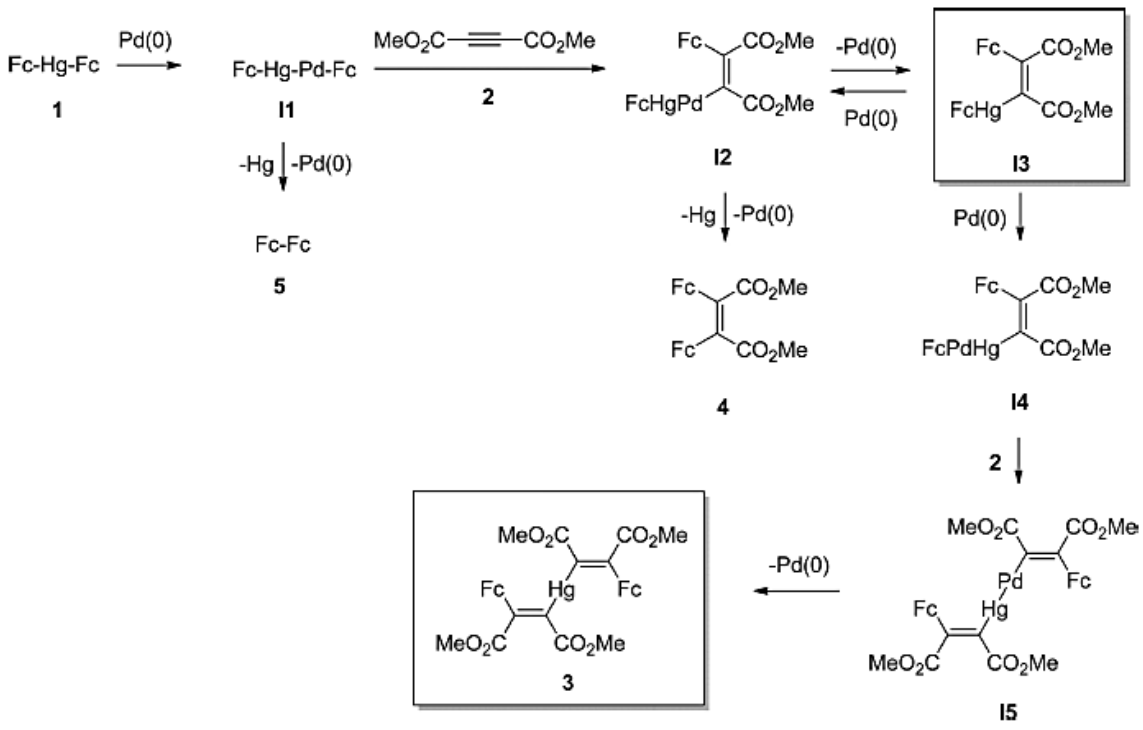

Scheme 1: One of the Possible Reaction Mechanisms for Formation of the Major Reaction Products in the Palladium-Catalyzed Reaction between bis(ferrocenyl)mercury and Dimethylacetylenedicarboxylate.

Because of the low stability of the reaction byproduct on different types of silica gel and aluminum oxide (determined by the NMR spectroscopy and color change), the purification of the reaction intermediate using standard separation methods was difficult to achieve. It was also found that red solutions of the highly unusual byproduct bis(dimethyl-(*Z*)-3-ferrocenyl-2-butenedioate)mercury (**3**, Scheme 1) in chlorinated or polar solvents quickly decolorized even at 0°C. Thus we used two other approaches for purification of complex **3**. First, a simple recrystallization method was used to purify the reaction byproduct (**3**) from the reaction mixture. Taking into consideration a very limited choice of solvents, we were able to obtain (after numerous trials) only two component mixtures of complexes **3** and **4** (Figure 6). On the other hand, purification of the target complex **3** was achieved using reverse phase thin-layer chromatography (TLC).

When complex **3** was purified using this method, only a small amount of degraded product was observed in the final NMR solution (Figure 5B).

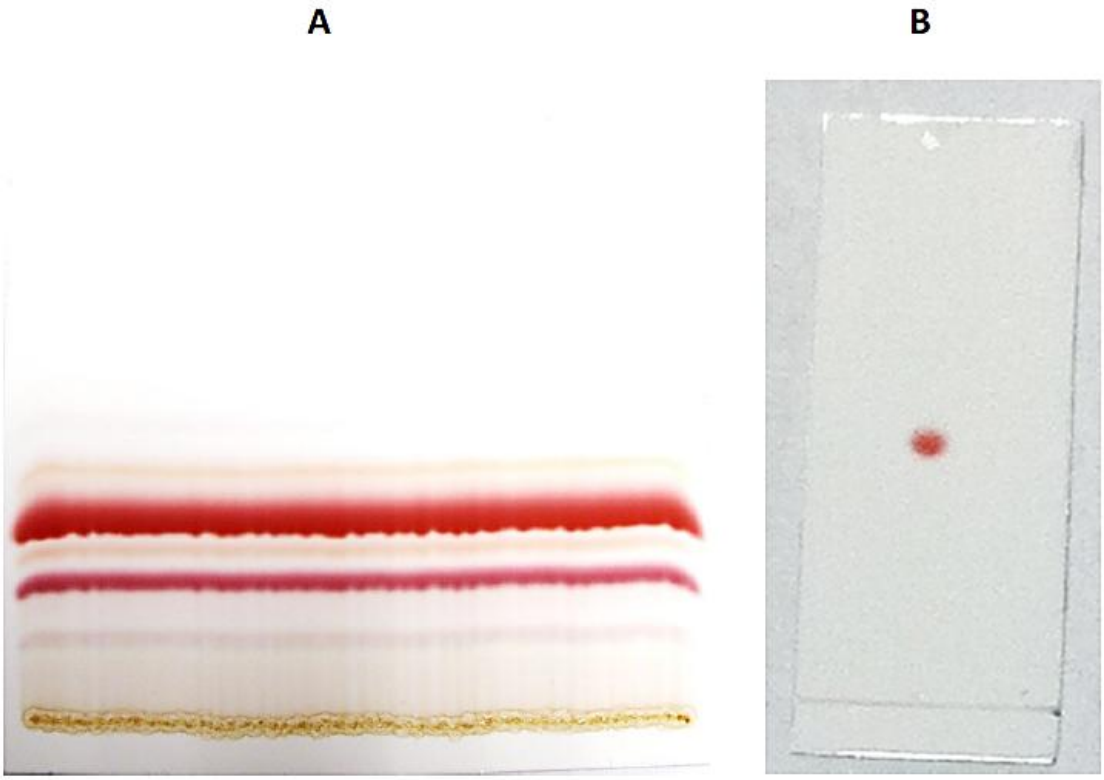

Figure 5. Reverse phase (C_{18}) TLC for the reaction mixture of **3** (**A**) and complex **3** (**B**) after purification. The unexpected product **3** is shown as the top band in A while degraded byproducts fall below.

NMR Spectroscopy:

The ^{1}H NMR spectrum of the new organomercurial compound bis(dimethyl-(*Z*)-3-ferrocenyl-2-butenedioate)mercury (**3**, Scheme 1) in benzene (C_6D_6) was first observed as a mixture with dimethyl-(*Z*)-2,3-di(ferrocenyl)-2-butanedioate (Figure 5A). Separation using C_{18} revers phase TLC resulted in a pure compound suitable for ^{1}H NMR analysis. The spectrum consists of two singlet's observed at 3.33 (6H, Figure 7) and 3.78 ppm (6H, Figure 7), originating from two types of nonequivalent ester groups, and this assignment was further confirmed by ^{1}H 2-D COSY NMR (Figure 9), 1H-13C 2-D HMQC NMR

(Figure 10), and elemental analysis experiments (Table 4). Signals originating from the ferrocenyl protons in the α-position of the substituted cyclopentadienyl ring (α-Cp) were observed as two multiplet's at 4.77 (2H, Figure 7) and 4.67 ppm (2H, Figure 7) because the large size of the mercury ion leads to hindered rotation of the ferrocenyl substituents,

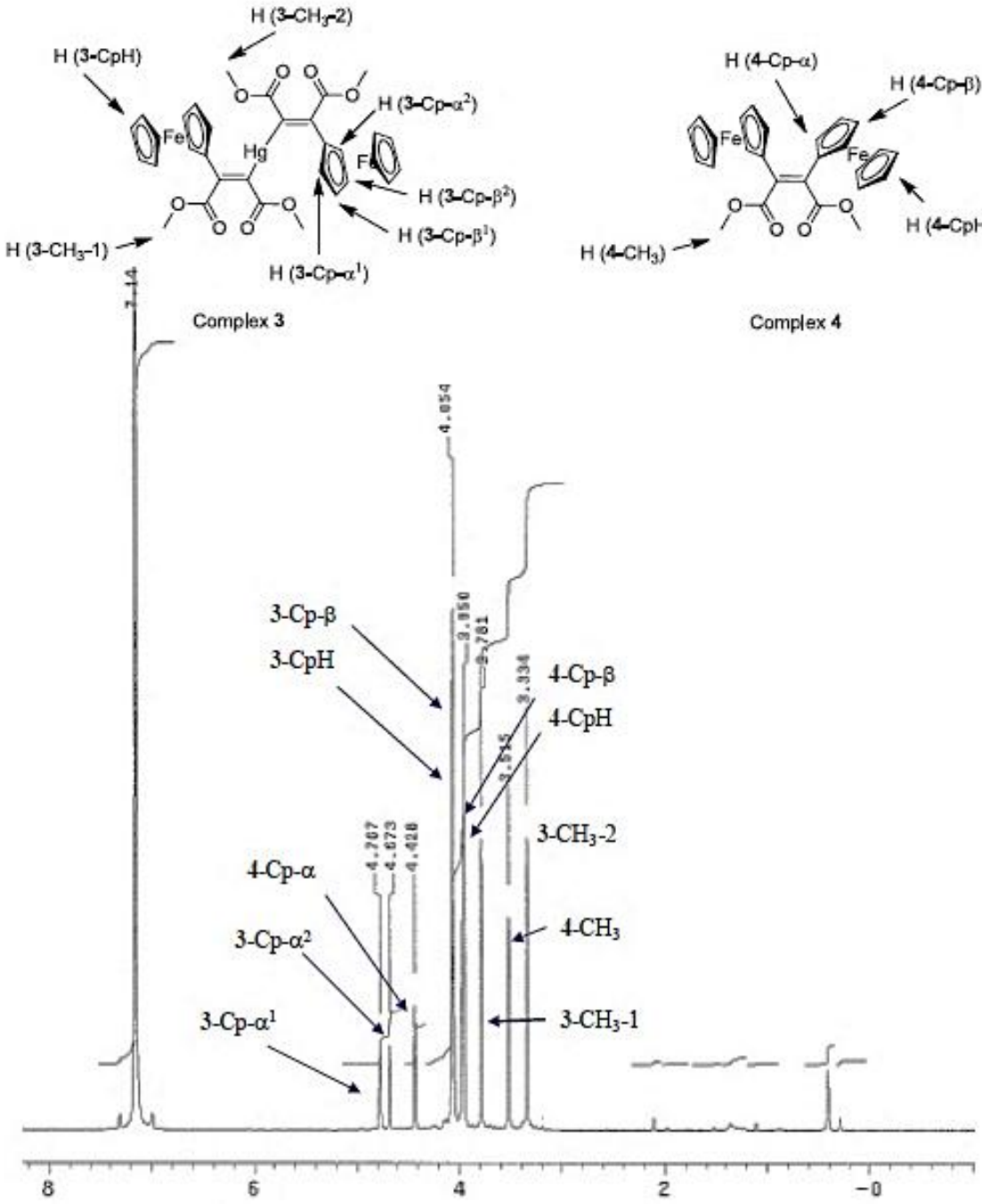

Figure 6. ^{1}H NMR (C_6D_6) spectrum of complexes **3** and **4** obtained after recrystallization of the crude reaction mixture using toluene/hexane.

which makes the two α-Cp protons diastereotopic. The diastereotopic signals originating from the protons in the β-positions of the substituted cyclopentadienyl ring (β-Cp) were observed as multiplet's at 4.07 (2H, Figure 7) and 4.05 (2H, Figure 7) ppm, which is very close to the singlet originating from the protons of un-substituted Cp ring at 4.06 ppm (10H, Figure 7). Their origins were further confirmed by HMQC 2-D NMR (Figure 10).

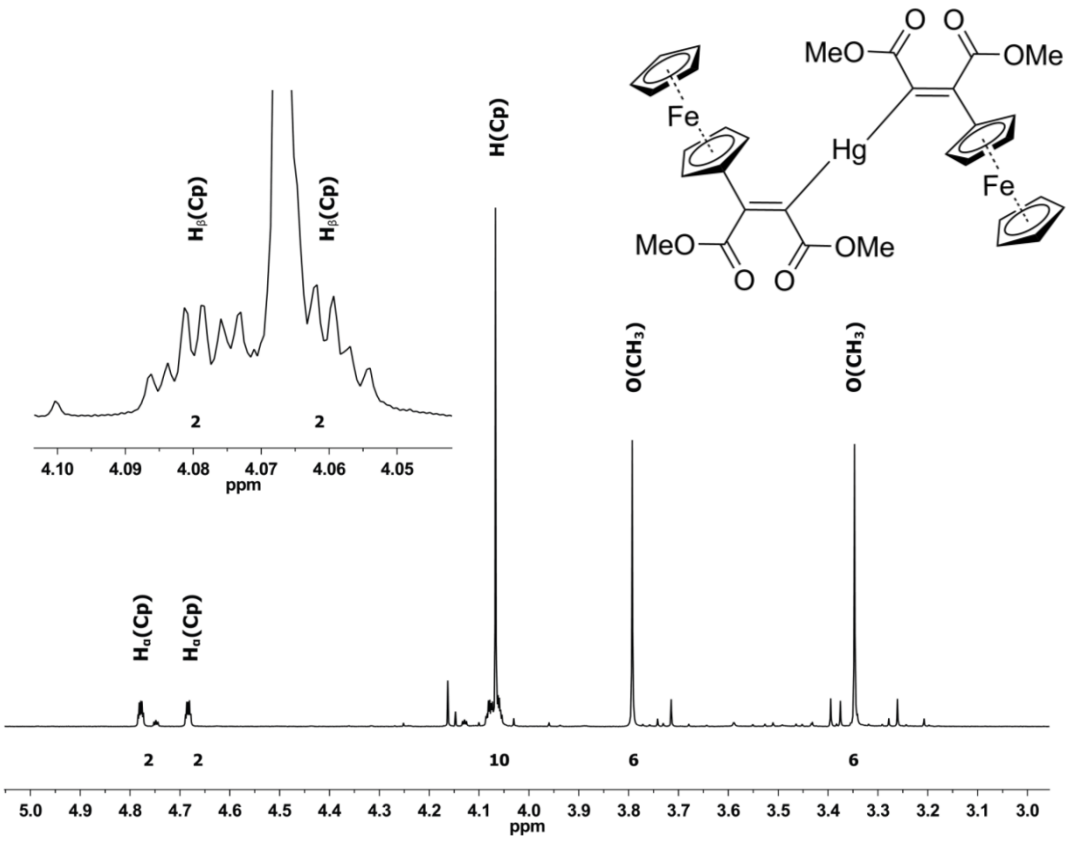

Figure 7: ^{1}H NMR Spectrum of bis(dimethyl-(*Z*)-3-ferrocenyl-2-butenedioate)mercury (**3** $(FcCOOMeC{=}C)_2Hg$, Scheme 1) obtained after reverse phase (C_{18}) TLC purification in benzene (C_6D_6).

The ^{13}C NMR spectrum of complex **3** in benzene consists of 12 distinct carbon signals with the most downfield being two nonequivalent carbonyl carbons observed at 168.65 (C_2, Figure 8) and 165.78 (C_1, Figure 8) ppm. The presence of an alkene is seen at signals 148.86 ppm (C_6, Figure 8) and 119.77 ppm (C_5, Figure 8). The presence of ferrocenyl substituents were observed as six signals resulting in the ipso cyclopentadienyl

carbon at 76.58 ppm (C_8, Figure 8), two nonequivalent α-positioned cyclopentadienyl ring carbons at 70.77 ppm (C_{11}, Figure 8) and 70.13 ppm (C_{12}, Figure 8), two nonequivalent β-positioned cyclopentadienyl ring carbons at 71.90 ppm (C_9, Figure 8) and 71.70 ppm (C_{10}, Figure 8), and last a signal representative of cyclopentadienyl carbons seen at 70.51 ppm (C_7, Figure 8). Two remaining signals seen at 52.14 ppm (C_4,

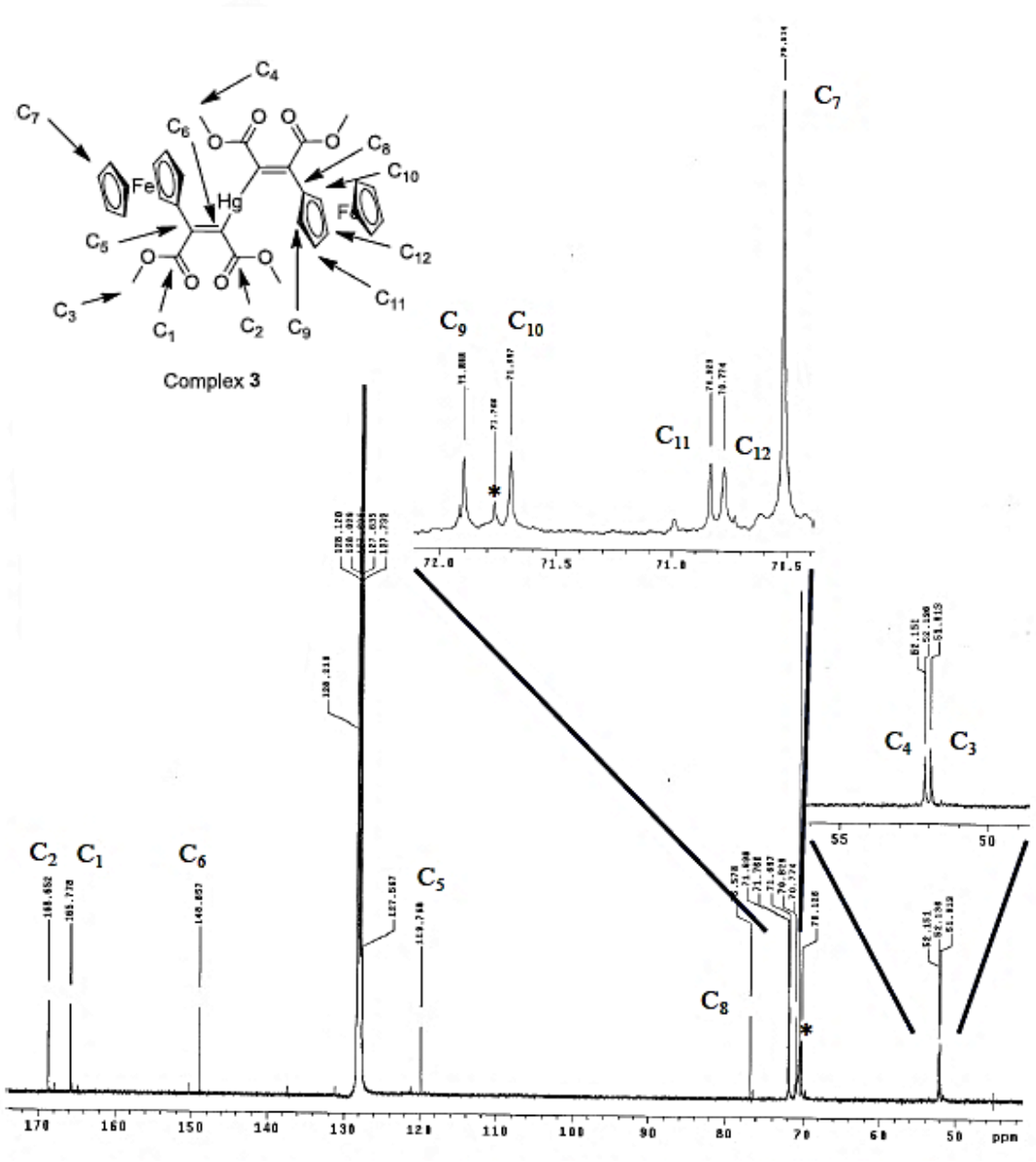

Figure 8. ^{13}C NMR spectrum of complex **3** obtained after reverse phase (C_{18}) TLC purification in benzene (C_6D_6). Degradation and solvent impurities are labeled by (*).

Figure 8) and 51.91 ppm (C_3, Figure 8).

The estimated yields of complex **3** vary between 5% and 20%, dependent on two key reaction factors: the first factor is the molar ratio of reagents bis(ferrocenyl)mercury (**1**, Scheme 1) and dimethylacetylenedicarboxylate (**2**, Scheme 1) introduced in the reaction. Increasing the molar ratio from 1:2 to 1:10 for reagents **1** and **2** favors formation of the organomercurial byproduct **3**. On the other hand, when reactant **2** was added drop wise over 10 min to the mixture of **1** and a palladium catalyst, only trace amounts of byproduct **3** and dimethyl-(*Z*)-2,3-di(ferrocenyl)-2-butenedioate (**4**, Scheme 1) were detected in the reaction mixture The main reaction product (~80% yield) was biferrocene (**5**, Scheme 1). These observations could be rationalized using one of several possible reaction mechanisms shown in Scheme 1[16b].

Oxidative insertion of the palladium catalyst into the mercury−carbon bond of **1** should result in the formation of an Fc−Hg−Pd−Fc intermediate (**I1**, Scheme 1) as proposed by Beletskaya and her co-workers[7]. In the absence (or low concentrations) of dimethylacetylenedicarboxylate (**2**), the formation of biferrocene (**5**) as the main reaction product results. If dimethylacetylenedicarboxylate (**2**) is available in the reaction mixture, carbo-palladation of the carbon−carbon triple bond leads to the formation of the intermediate **I2** (Scheme 1). Elimination of palladium and mercury from the intermediate (**I1**) results in the formation of the ester complex (**4**) as the major reaction product, as suggested by Beletskaya[16b]. Formation of the organomercuric complex **3** can be rationalized if one assumes transformation of the intermediate **I2** into intermediate **I3** (Scheme 1) upon elimination of *only* the palladium atom from **I2**. In this case, the *asymmetric* mercury-containing intermediate **I3** could again undergo oxidative insertion

of Pd(0) into the intermediate to form either intermediate **I2** or **I4** (Scheme 1). On the basis of the energetics of aryl−Hg versus vinyl−Hg bonds,[11a] it can be speculated that the preferential reaction pathway is the formation of the intermediate **I2** rather than the intermediate **I4**, which correlates with the formation of the ester complex (**4**) as the major reaction product (~50−70%) in a broad range of the molar ratios of reagents **1** and **2** (from 1:2 to 1:10). Intermediate **I4** could then be involved in the carbo-palladation reaction with the second molecule of **2** to form intermediate **I5** (Scheme 1). Finally, elimination of the palladium atom from the intermediate **I5** leads to formation of the

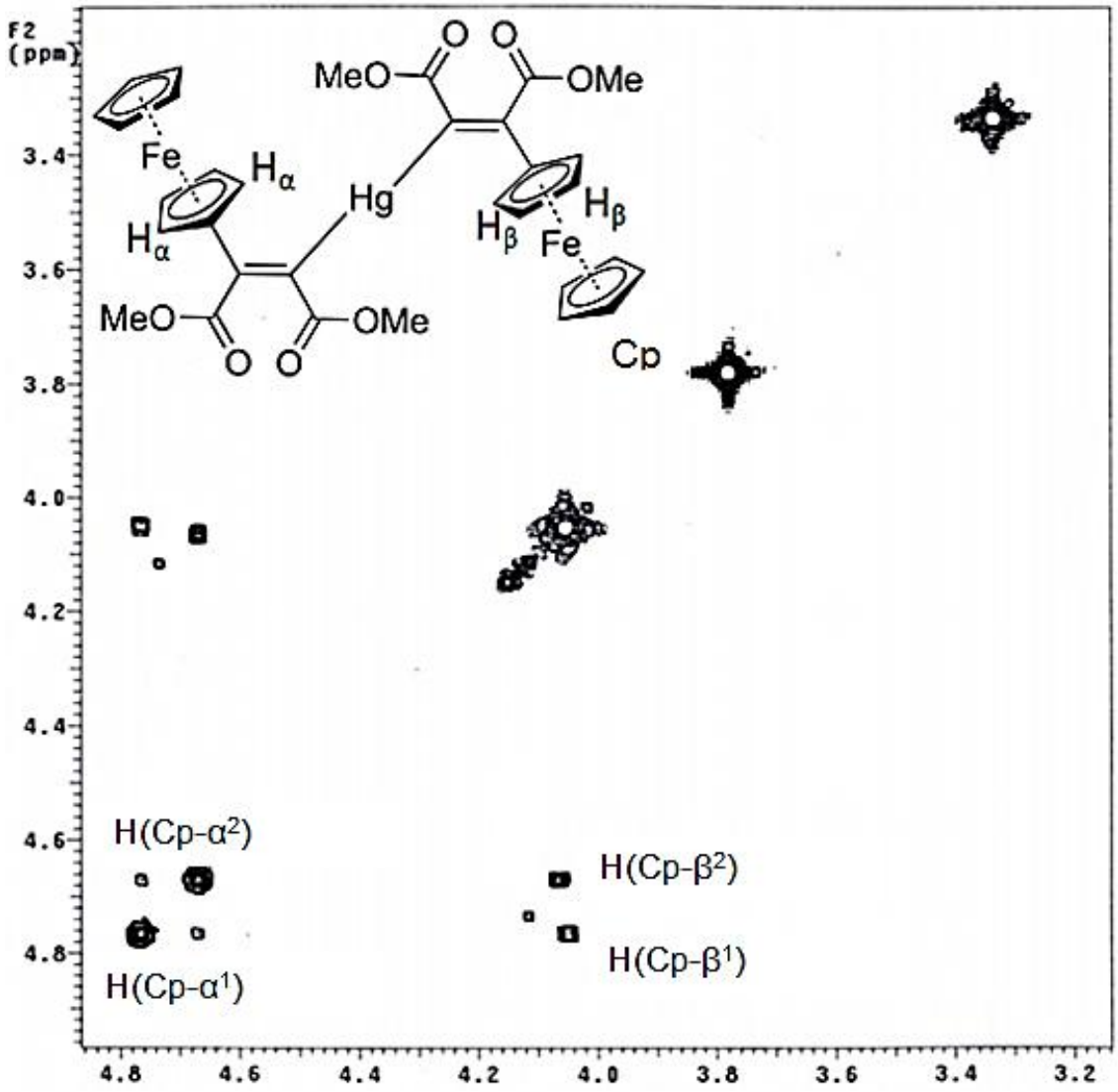

Figure 9: COSY NMR (C_6D_6) spectrum of complex **3** obtained after reverse phase (C_{18}) TLC purification.

organomercurial byproduct **3**.

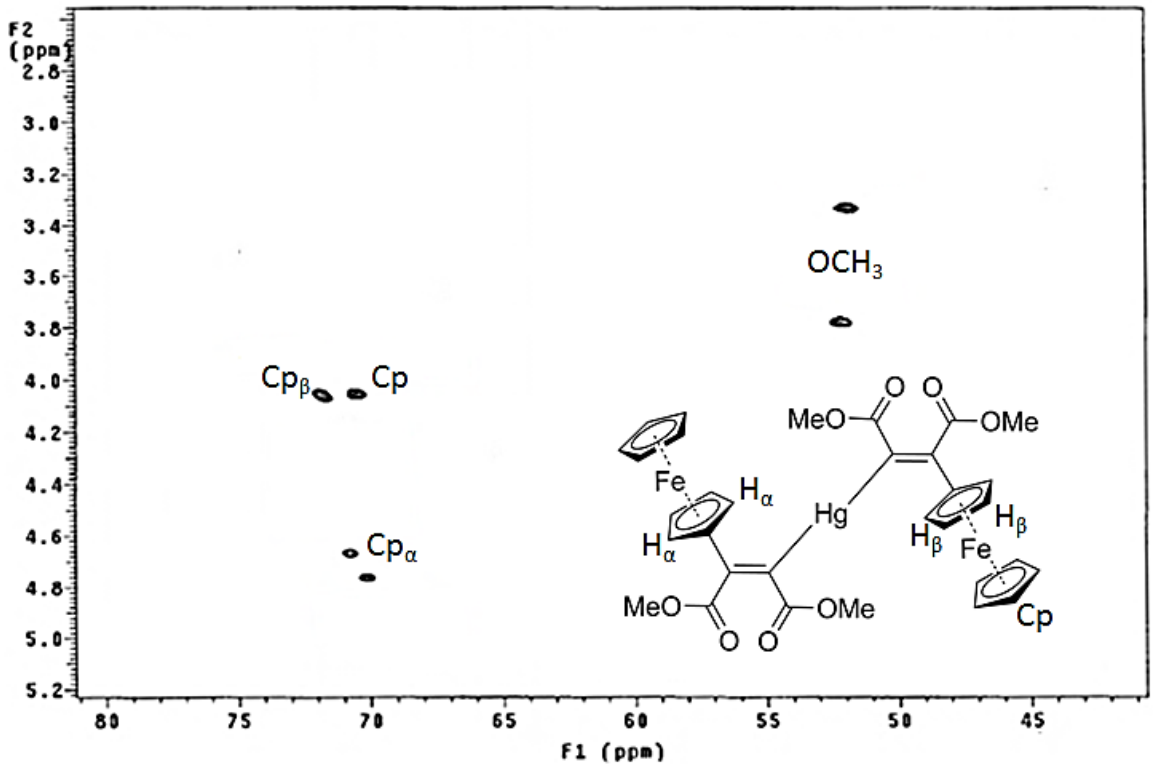

Figure 10: HMQC NMR (C_6D_6) spectrum of complex **3** obtained after reverse phase (C_{18}) TLC purification.

The key difference between the possible reaction mechanism in Scheme 1 and the one suggested earlier[17b] is that elimination of the palladium atom from the reaction intermediates **I2** and **I5** occurs *without* elimination of the mercury atom and results in formation of the corresponding organomercurial intermediate (**I3**) and complex **3**. Such formation of organomercurial compounds in palladium-catalyzed cross-coupling reactions has never been discussed before and could be potentially useful for preparation of new organomercurial compounds. In order to confirm formation of the intermediate **I3**, we investigated the reaction mixture in THF-d_8 using ^{1}H and COSY NMR spectroscopic methods. Unfortunately, the reaction mixture (Figure 11) was too complex to analyze,

and at this point we were unable to clearly identify the reaction intermediate **I3** in solution.

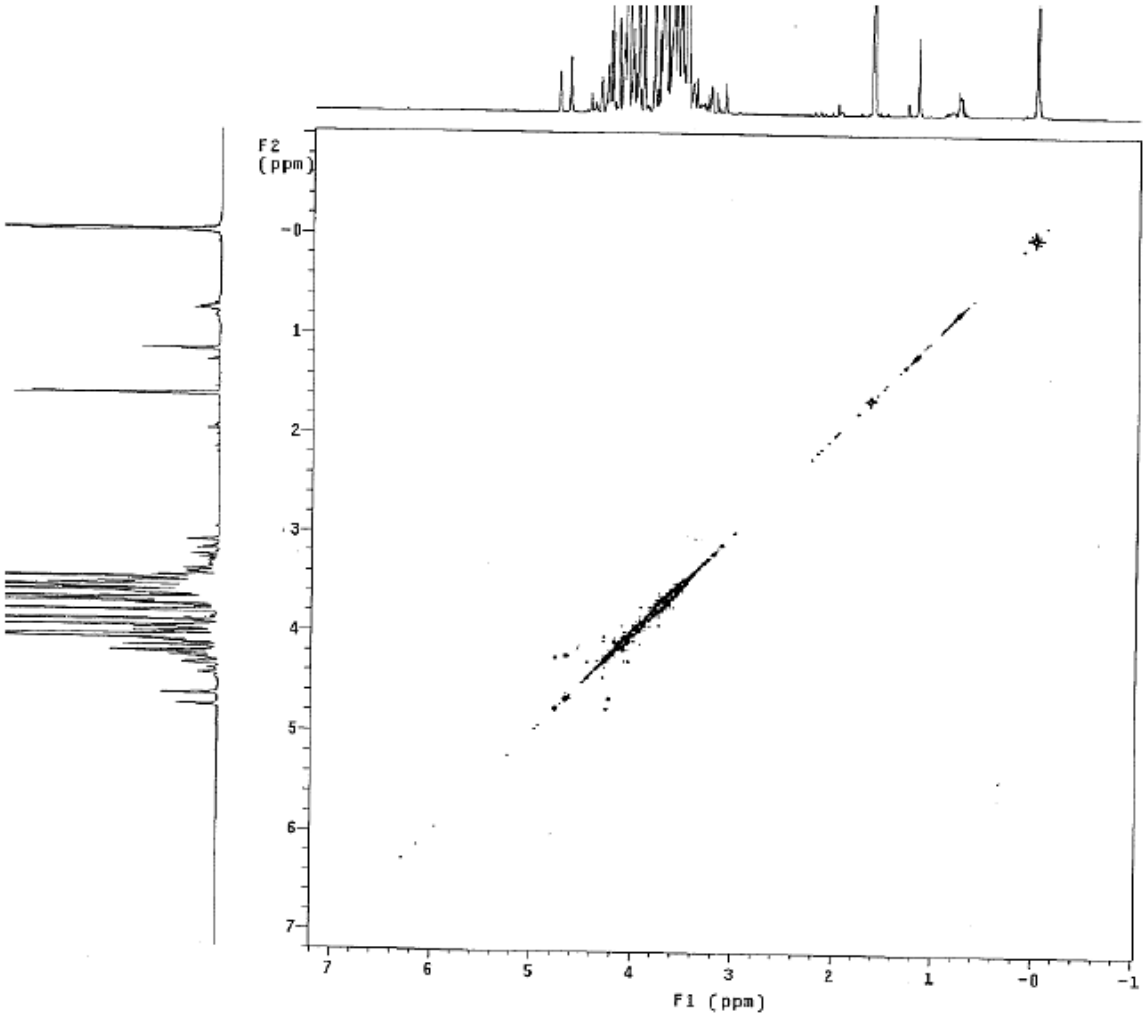

Figure 11: COSY NMR (C_6D_6) spectrum for the reaction mixture of **3** in THF-d_8/acetone-d_6.

X-Ray Analysis:

The final assignment of the structure of bis(dimethyl-(*Z*)-3-ferrocenyl-2-butenedioate)mercury (**3**, Scheme 1) was achieved by using single-crystal X-ray diffraction. The final refinement parameters and selected bond distances and angles for bis(dimethyl-(*Z*)-3-ferrocenyl-2-butenedioate)mercury are presented in Tables 1 and 2,

while an ORTEP diagram is shown in Figure 12 (Supporting Information Tables 1-6). It should be noted that the structure of **3** is a rare example of an organomercurial compound in which the mercury atom is directly connected to the vinyl fragment. Indeed, there are only three structures of general formula R− Hg−C(X)=C(Y,Z) and 11 structures of

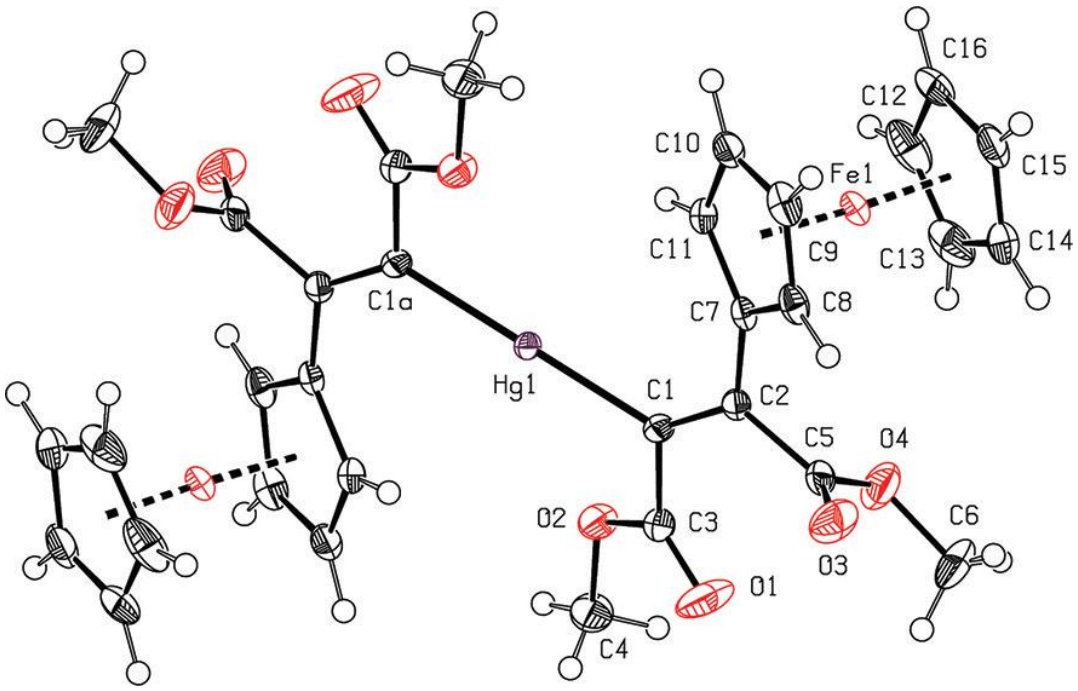

Figure 12: ORTEP diagram of bis(dimethyl-(*Z*)-3-ferrocenyl-2-butenedioate)mercury organomercurial complex **3** drawn with 50% probability ellipsoids.

general formula $Hg(C(X)=C(Y,Z))_2$ reported in the CSD with only a few of them having true bis-vinyl Hg(II) fragments[18].The two coordinated mercury atom is located on the inversion center presented in the space group *P*21/*c*, having linear geometry, and forming bonds with two sp^2 hybrid vinylic carbon atoms. The mercury−carbon bond distance (2.075(3) Å) is in the typical range for analogous compounds (1.997−2.094 Å)[18]. The alkene fragments adopt a *Z*-orientation of the ester substituents. The C=C bond distance observed in **3** (1.348(4) Å) is very close to that found in two polymorph forms of **4**[15a,17b]. The ester groups in **3** are not coplanar with the C=C bond. Interestingly, the

corresponding torsion angles O1−C3−C1−C2 and O3−C5−C2−C1 were found to be 22.8(5)° and −108.9(4)°, respectively, and are very different from each other, while those found in **4** are close to each other (−126.2(3)° and −134.6(3)°)[15a,17b].

Crystallography Collection and Refinement Data for Complexes **3** and **5**		
	Complex **3**	Complex **5**
empirical formula	$C_{32}H_{30}Fe_2HgO_8$	$C_{20}H_{18}Fe_2$
fw	854.85	370.04
cryst syst	monoclinic	monoclinic
space group, Z	$P2_1/c$, 2	$P2_1/c$, 2
a (Å)	8.902(5)	9.5320(5)
b (Å)	12.776(5)	7.7830(3)
c (Å)	13.799(5)	12.4190(11)
β (deg)	110.321(5)	126.384(5)
volume (Å^3)	1471.7(11)	741.73(8)
ρ_{calc} (g/cm^3)	1.929	1.657
μ (mm^{-1})	17.412 (Cu K_α)	1.947 (Mo K_α)
θ_{max} (deg)	68.24	27.45
GoF(F^2)	1.055	1.083
R_1 ($F^2 > 2\sigma(F^2)$)	0.0224	0.0241
wR_2 (all data)	0.0563	0.0553
$\Delta\rho_{max}/\Delta\rho_{min}$ (e/Å^3)	1.123/-0.752	0.490/-0.294

$$R_1(F) = \Sigma||F_o| - |F_c||/\Sigma|F_o|. \quad wR_2(F^2) = \{\Sigma[w(F_o^2 - F_c^2)^2]/\Sigma w(F_o^2)^2]\}^{1/2}.$$

Table 1: X-Ray Crystal Collection and refinement Data for bis(dimethyl-(*Z*)-3-ferrocenyl-2-butenedioate)mercury (**3**, Scheme 1) and biferrocene (**5**, Scheme 1).

The ester group closer to the mercury atom is more coplanar with the C=C bond plane because of the interaction between the positively polarized mercury atom and the oxygen atom (O2) of the ester group. The observed O2···Hg1 distance (3.029(3) Å) is smaller than the sum of van der Waals radii of Hg and O (3.07 Å)[19]. Similar interactions are common for organomercurial compounds and were observed before[20] with the distances ranging between 2.833(9) and 2.88(1) Å. The second ester group in **3** is almost perpendicular with respect to the C=C bond plane orientation and does not form any close contacts with the mercury atom. The torsion angle C1−C2−C7−C8 between the

substituted Cp ring and the C=C bond (148.6(3)°) is significantly larger than that reported for the **4** (130.7(3)°),[15a,17b] which can be explained on the basis of the steric interaction between ferrocene and its neighboring substituents, i.e., the ferrocenyl substituent in the ester substituent or the mercury atom in the complex **3**.

Bond Distance (Å)			Angle (deg)
Hg(1)-C(1)	2.075(3)	C(2)-C(1)-C(3)	119.5(3)
O(1)-C(3)	1.197(4)	C(2)-C(1)-Hg(1)	124.1(2)
O(2)-C(3)	1.344(4)	C(1)-C(2)-C(7)	125.1(3)
O(2)-C(4)	1.451(4)	C(1)-C(2)-C(5)	120.5(3)
O(3)-C(5)	1.204(4)	C(7)-C(2)-C(5)	114.2(3)
O(4)-C(5)	1.328(4)	C(3)-C(1)-C(2)-C(7)	177.7(3)
O(4)-C(6)	1.447(5)	Hg(1)-C(1)-C(2)-C(5)	5.8(4)
C(1)-C(2)	1.348(4)	C(3)-C(1)-C(2)-C(5)	3.1(4)
C(1)-C(3)	1.478(4)	C(2)-C(1)-C(3)-O(1)	22.8(5)
C(2)-C(7)	1.464(4)	C(1)-C(2)-C(5)-O(3)	108.9(4)
C(2)-C(5)	1.507(4)	C(1)-C(2)-C(7)-C(8)	148.6(3)
Fe-C_{av}	2.043(4)	C(1)-C(2)-C(7)-C(11)	31.9(5)

Table 2: Selected Bond Distances and Angles for bis(dimethyl-(*Z*)-3-ferrocenyl-2-butenedioate)mercury (**3**, Scheme 1).

During the crystallization of the organomercuric complex **3**, we were also able to obtain single crystals of biferrocene (**5**), which to our surprise was characterized previously with relatively low quality[21]. The best reported average threshold for carbon−carbon bonds is in the range 0.006−0.010 Å (R_1 = 0.06), and experiments were performed at room temperature, which also increases the vibronic motion of the atoms and decreases the accuracy of the measurement of the sample's geometric parameters. Since the biferrocene molecule **5** is very popular as a model for theoretical studies (mixed valence state formation, electron-transfer properties, etc.),[22] we decided to determine its structure at low temperature (Tables 1 and 3, and Figure 13).

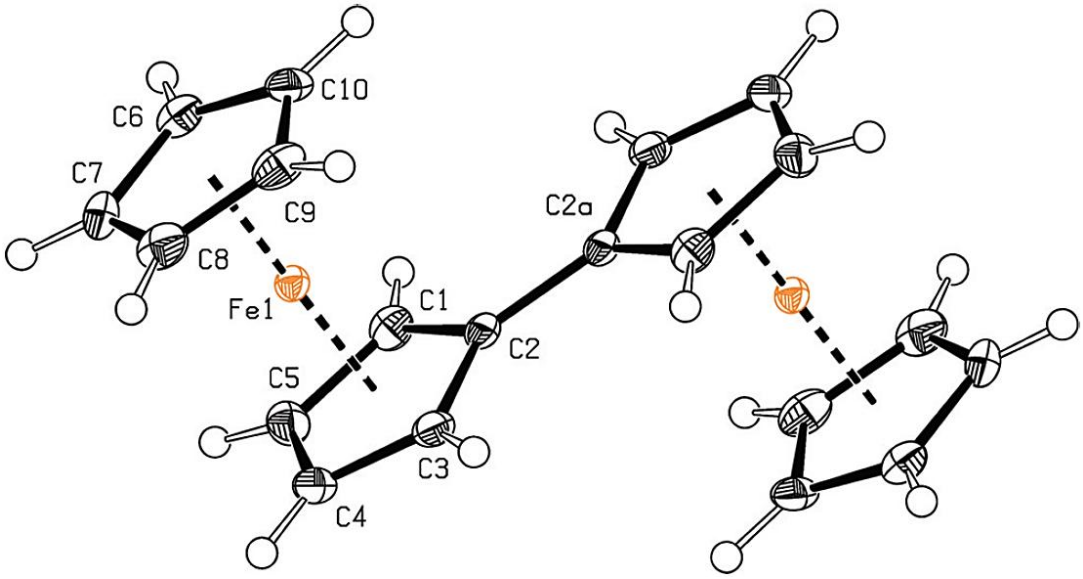

Figure 13: ORTEP diagram of biferrocene complex **5** drawn with 50% probability

The crystal structure of **5** consists of two-symmetric ferrocenyl units, connected by a single carbon−carbon bond (1.459(4) Å) seen in Figure 13 (Supporting Information Tables 7-12). Corresponding torsion angles C3−C2−C2^{a}−C1^{a} and C3−C2−C2^{a}−C3^{a} [(a) 1−*x*; −*y*; 1−*z*] are equal to 1.4(4)° and 180°, respectively. All C−C bonds within the substituted cyclopentadienyl ring (Cp) are observed in the range 1.418(3)−1.434(3) Å, while for the un-substituted Cp ring this interval is a little smaller, 1.419(3)−1.425(3) Å. The same tendency was also observed for Fe−C bonds, where they tend to be positioned in a broader range for substituted Cp rings (2.039(2)−2.057(2) Å) compared to the un-substituted Cp rings (2.042(2)−2.051(2) Å). It is of interest to note that the unit cell reported for the room-temperature crystal structure of biferrocene (**5**)[21] (*a* = 10.34(1) Å, *b* = 7.85(1) Å, *c* = 12.60(1) Å, *β* = 131.59(5)°) is quite different than that observed in our experiments. Specifically, it has a shorter dimension along the *a*-axis (*a* = 9.5320(5) Å) and smaller monoclinic angle *β*(126.384(5)°). This observation probably reflects a more dense packing mode of the biferrocene molecules in our structure (*V*= 741.73(8) Å^{3},

ρcalc = 1.657 g/cm3, Z = 2) observed in Table 1 compared to the previously reported experiment[25] (V = 764.91 Å^3, ρcalc = 1.607 g/cm^3, Z = 2).

	Bond Distance (Å)		Bond Distance (Å)
C(1)-C(5)	1.427(3)	C(6)-C(7)	1.424(3)
C(1)-C(2)	1.434(3)	C(7)-C(8)	1.421(3)
C(2)-C(3)	1.432(3)	C(8)-C(9)	1.419(3)
C(3)-C(4)	1.418(3)	C(9)-C(10)	1.425(3)
C(4)-C(5)	1.427(3)	C(2)C(2)[a]	1.459(3)
C(6)-C(10)	1.412(3)	Fe-C_{av}	2.047(2)

Table 3: Selected Bond Distances and Angles for biferrocene (**5**, Scheme 1).

Elemental Analysis		
	Theory	Found
C	58.90	58.05
H	5.11	4.80

Table 4: Elemental Analysis of bis(dimethyl-(*Z*)-3-ferrocenyl-2-butenedioate)mercury (**9**, Scheme 1).

Conclusions:

Formation of the new organomercurial byproduct bis(dimethyl-(*Z*)-3-ferrocenyl-2-butenedioate)mercury (**3**, Scheme 1) has been observed in the earlier reported reaction between bis-(ferrocenyl)mercury (**1**, Scheme 1) and dimethylacetylenedicarboxylate (**2**, Scheme 1). The rare bis(vinylic)mercury complex **3** has been characterized by NMR spectroscopy (Figures 7 and 8), elemental analysis (Table 4) and X-ray crystallography (Figure 12).

II. Preparation/Characterization of β-substituted 3,4-bis(ferrocenyl)-1-(triisopropylsilyl)pyrrole.

Introduction:

It has been long known that pyrrole undergoes predominant electrophilic aromatic substitution in the alpha (α) position. Many investigations have had a goal in mind to synthesize a less readily accessible beta (β) substituted pyrrole. A number of synthetic routes exist that provide access to such compounds[28]. Three most notably successful routes are: (a) utilization of a removable deactivating substituent (usually acyl) to direct the entry of an electrophile to the β-position,[29] (b) acid-mediated isomerization of the easily prepared α isomers,[30] and (c) direct substitution of a N-(phenylsulfonyl)pyrrole with certain electrophiles, first described by Anderson et al.[31] and Rokach et al. [32] The first method, historically,[33] is the most intensively studied of synthetic routes to produce β-substituted pyrrole complexes[28]. The scope for removal of the directing substituent is quite broad as many methods have been applied previously.

The result of acid-induced isomerization of α-substituted pyrrole complexes are inconclusive and can occur under unexpectedly mild conditions[33.] The concern is the synthesis of an equilibrium mixture of α and β isomers, although such isomers can theoretically be separated with column chromatographic techniques. Friedel-Crafts acylation of 1-(phenylsulfonyl)pyrrole and subsequent removal of the nitrogen substituent under alkaline conditions is an excellent route to 3-acylpyrroles[34]. Unfortunately some electrophilic reagents do not react with this substrate at all and others favor an unfavorable β:α product ratio[28,31].

The synthesis of a β-substituted pyrrole complex is based on the use of a large substituent at the nitrogen atom, such as N-(triisopropylsilyl), to obstruct electrophilic attack at the α-pyrrole positions[34]. Considerable selectivity for β carbons is observed and the process of removing the nitrogen substituent is easily attained with the use of tetraalkylammonium fluoride[35]With the potential coupling of ferrocene in the β-positions of the protected pyrrole, such compounds have potential in the application of ferrocenyl-substituted aromatic and heteroaromatic compounds, serving as model compounds for the investigation of metal-metal coupling. It is these π-conjugated organometallic complexes that may be suitable for the design of novel electro-active materials[36]. Varying experimental conditions in previous studies hinder the comparability of their results, i.e. several substituted ferrocenyl thiophenes with measured reduction potentials separated by less than 150 mV in cyclovoltammetric studies (bis(ferrocenyl)pyridine included[37].

In order to observe single oxidation of a ferrocenyl substituent, separation in the reversible reduction potential between each substituent must be achieved to prevent the simultaneous oxidation of multiple ferrocenyl substituents. Without separation in the reduction potentials between ferrocenyl substituents, nearly no observable metal-metal interaction will result. The highest $\Delta E_{1/2}$ values among symmetrical ferrocenyl heteroaromatic compounds, 1,3-bis(ferrocenyl)benzo[*b*]thiophene (280 mV) and 1,3-bis(ferrocenyl)benzo[*b*]selenophene (305 mV) were reported by Sato and Ogawa[38]. Winter and Kowalski synthesized azaferrocenes with heteroaromatics, using pyridine or thiophene as bridging units, studying their electrochemical and spectroelectrochemical properties, resulting in higher $\Delta E_{1/2}$ values compared to the appropriate ferrocenyl derivatives[39].

In recent years, Alexander Hildebrandt and his co-workers reported the synthesis and electrochemical results of a sterically crowded 2,3,4,5-tetraferrocenyl thiophene[40]. Since it is well known that poly-pyrroles are electro-active materials of high conductivity[41], in addition to their use as porphyrin building blocks, pyrroles were selected as organic bridging units between ferrocenyl groups and the connecting system itself. One such complex, 2,5 α-substituted bis(ferrocenyl)pyrrole was synthesized for comparison with 2,3,4,5-tetraferrocenyl pyrrole electrochemically. Results reported by Hildebrandt et al. lead to an assumption in assigning ferrocene substituents based on similarities in reduction potentials for each substituent within the 2,5-diferrocenyl pyrrole complex assigning two of the four reduction potentials in the 2,3,4,5-tetraferrocenyl pyrrole described in Figure 4.

Without any conclusive evidence from electrochemical study of a β-substituted pyrrole, the assumption that overlapping oxidation waves could not prove the assignment of reversible oxidation of α and β ferrocene substituents in a tetraferrocenyl pyrrole complex. The need for β-substituted diferrocenyl pyrrole was relevant in effort to clarify the assignment of ferrocenyl oxidation waves in 2,3,4,5-tetraferrocenyl pyrrole.

The synthesis and characterization of 3,4-bis(ferrocenyl)-1-(triisopropylsilyl)pyrrole ($Fc_2(C_4N)Si(iPr)_3$), electrochemical study in specific, provides clarification in assigning the ferrocenyl oxidation waves in 2,3,4,5-tetraferrocenyl pyrrole. Future construction of an octaferrocenyl porphyrin from the β-substituted pyrrole complex established an excellent starting point.

Synthesis:

Previously, Bray and co-workers,[33] used an *N*-(triisopropylsilyl) bulky protecting group on the pyrrole nitrogen to obstruct halogenation in the α-positions. Adding a protecting group, *N*-(triisopropylsilyl), to pyrrole succeeded by combining pyrrole with lithium bis(trimethylsilyl)amide in THF creating a lithium pyrrole salt by stirring the reaction for twenty-four hours at room temperature under Argon. The lithium pyrrole salt was isolated by evaporation under vacuum. Using THF at room temperature, *N*-(triisopropylsilyl)chloride was added drop wise to the lithium pyrrole/THF solution and stirred for one 1 hour; removing the solvent under vacuum upon completion of the reaction. Purification of 1-(triisopropylsilylpyrrole) was done by dissolving the product in ether and washing it with excess water, drying over sodium sulfate, and distilling to reveal a clear residue oil that crystallized at 0°C. ^{1}H NMR spectroscopy reveals two triplets centered at δ 6.86 (1H, α-H(C_4N)) and 6.38 (1H, β-H(C_4N)) ppm for the protected pyrrole protons, slightly downfield in comparison to pyrrole. This indicates that N-silylation has no significant electronic effect on the pyrrole system.

Reacting 1-(triisopropylsilyl)pyrrole (**7**, Scheme 2) with electrophilic reagents (bromine and iodine) in the 3,4(β) positions. The bulky protecting group favored halogenation in the β-positions at low temperature. Bray and co-workers reported 78% yield upon brominating with 2 equivalents of *N*-bromosuccinamide (NBS) in dry THF solution at -78°C with 3,4-di(bromo)pyrrole having purity in excess of 96%[33]. Separation of di-brominated pyrrole from mono-brominated pyrrole using simple column chromatographic technique was unsuccessful. However, iodination in the presence of

mercuric acetate yielded a single 3,4-bis(iodo)pyrrole that was separated by dissolving in hexane and separating via filtration to yield a crystalline 3,4-diiodo-1-(triisopropylsilyl)pyrrole (**8**) confirmed by ^{1}H NMR, shown in Scheme 2.

Coupling of ferrocene to aryl-iodides as described by Beletskaya and her co-workers,[16b] the reaction between bis-(ferrocenyl)mercury (**1**, Scheme 1) and 3,4-bis(iodo)-1-(triisopropylsilyl)pyrrole (**8**, Scheme 2) in 1:2 molar ratio in the presence of

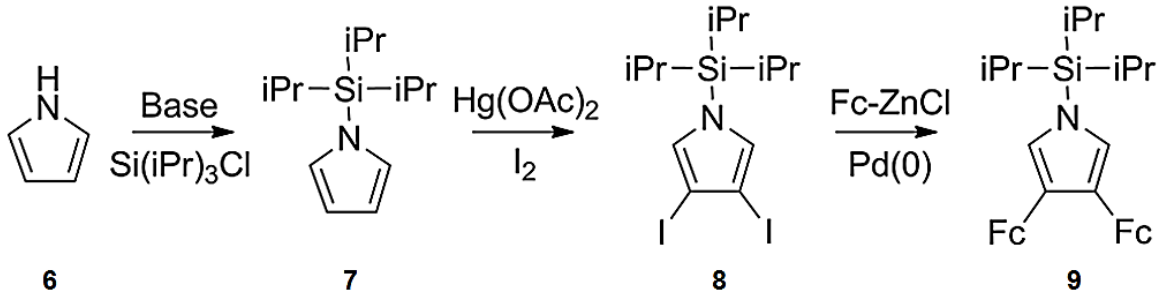

6 **7** **8** **9**

Scheme 2: Synthetic reaction scheme for the synthesis of 3,4-bis(ferrocenyl) pyrrole complex(**9**).

palladium catalyst reproducibly resulted in no reaction. Coupling of ferrocene to halogenated pyrrole was successfully reported by Hildebrandt and his co-workers[35] in their study of 2,3,4,5-tetraferrocenyl pyrrole. Creating ferrocenium zinc chloride was necessary in order to couple ferrocene to the halogenated pyrrole complex **(8)** in the presence of a palladium catalyst yielding the desired product. The purification of 3,4-bis(ferrocenyl)pyrrole (**9**, Scheme 2) was done using fractional column chromatography and recrystallization of the pure yellow-orange product in heptane.

NMR Spectroscopy:

The characterization began first with the identification of 1-(triisopropylsilyl)pyrrole and 3,4-diiodo-1-(triisopropylsilyl)pyrrole, one of the precursors required to synthesize bis(ferrocenyl) protected pyrrole. The ^{1}H NMR spectrum for compound **7** consists of four key signals; the first signal is representative of α-pyrrole protons seen as a singlet at 6.86 ppm (2H, Figure 14) and the second signal at 6.37 ppm (2H, Figure 14) represents β-pyrrole protons. The signal observed at 1.51 ppm (3H, Figure 14) represents CH protons from the isopropyl ligand within the protecting

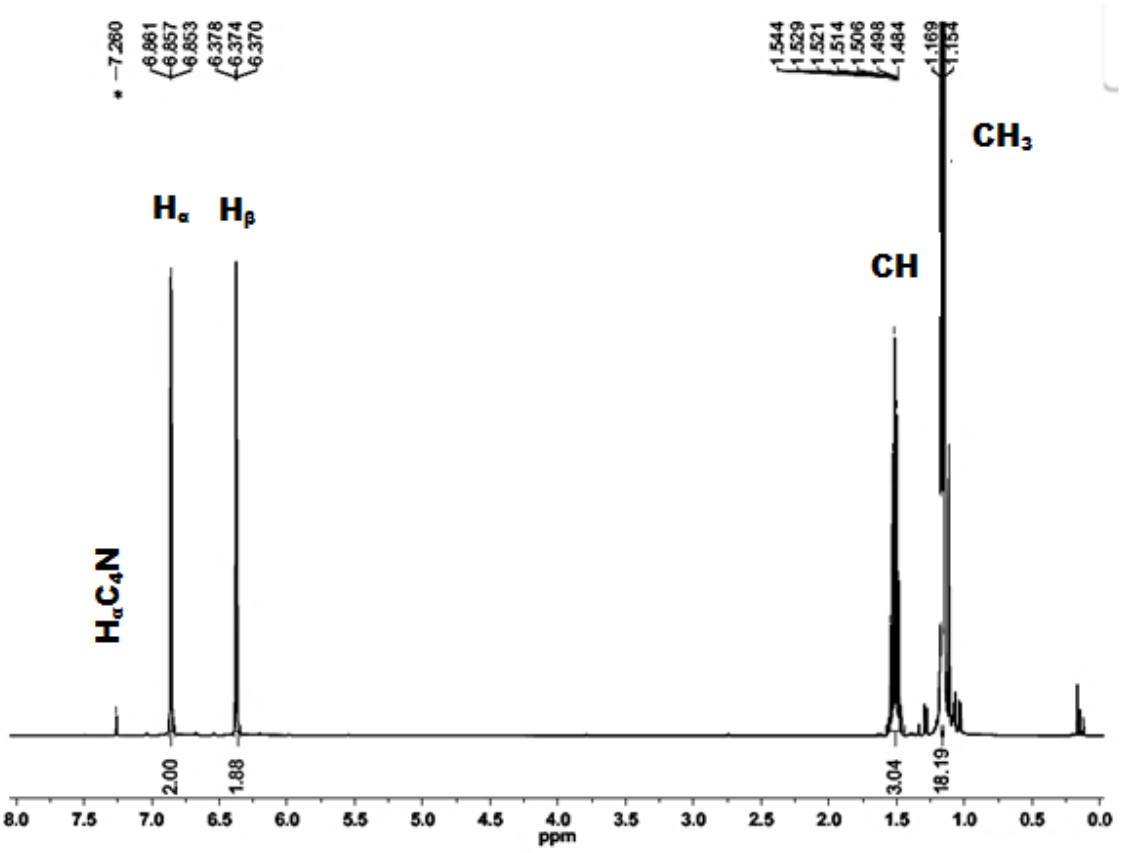

Figure 14: ^{1}H NMR ($CDCl_3$) spectrum of 1-(triisopropylsilyl)pyrrole (compound **7**, Scheme **2**).

group. The doublet at 1.16 ppm (18H, Figure 14), also caused by the protecting group, represents CH_3 protons. Compound **7** lacks β-pyrrole protons which results without the presence of a signal at 6.37 ppm; slight shifts are seen as the signals appear at 6.79, 1.40, and 1.07 ppm (Figure 14), otherwise seen in compound **8** (Scheme 2, Figure 15).

The ^{1}H NMR spectrum of the new 3,4-bis(ferrocenyl)pyrrole ($Fc_2(C_4N)Si(iPr)_3$) in deuterated chloroform ($CDCl_3$) consists of two pyrrole protons in the *α*-position as a triplet observed at 6.83 ppm (2H, Figure 16). The presence of ferrocene is indicated by two singlet's, *α* and *β*-Cp protons, at 4.33 ppm (4H, Figure 16) and 4.13 ppm (4H, Figure 16). The intense singlet at 4.03 ppm (10H, Figure 16) indicates the presence of 5 equivalent cyclopentadienyl (Cp) protons. The large protecting group containing three

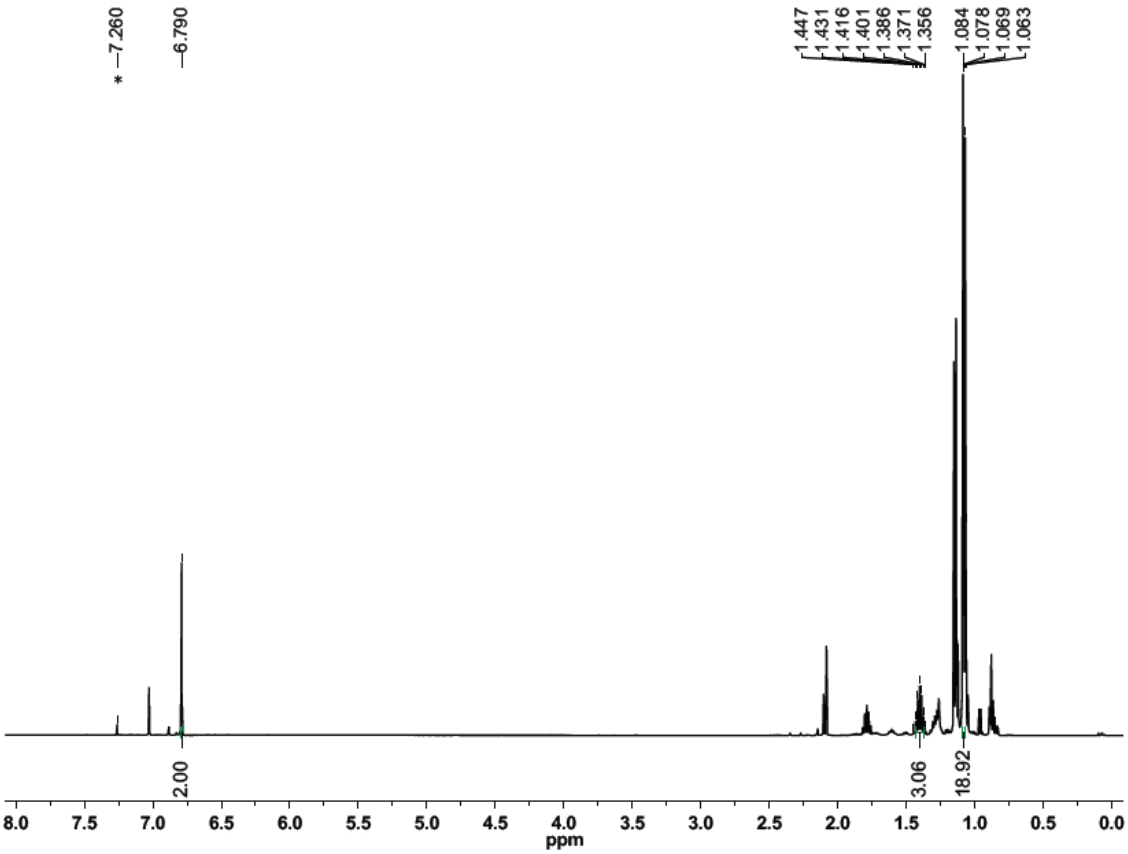

Figure 15: ^{1}H NMR ($CDCl_3$) spectrum of 3,4-diiodo-1-(triisopropylsilyl)pyrrole (compound **8**, Scheme **2**).

isopropyl central protons seen as a septet at 1.50 ppm (3H, Figure 16), the isopropyl methyl substituents in $Fc_2(C_4N)Si(iPr)_3$ are seen as a doublet at 1.19 ppm (18H, Figure 16). Signals originating from the ferrocenyl protons in the α-position of the substituted cyclopentadienyl ring (α-Cp) were observed as a multiplet at 4.33 ppm (4H, Figure 16). The (β-Cp) signal was seen at 4.13 ppm (4H, Figure 16) because it is positioned further from the electron rich nitrogen atom, being shielded, seen further downfield than the α-Cp protons. Coupling is observed between the α-Cp and β-Cp protons in the ^{1}H 2-D COSY NMR spectrum (Figure 18). The assignment of signals was further confirmed by HMQC (Figure 19), and elemental analysis (Table 7) experiments. The ^{13}C NMR spectrum of $Fc_2(C_4N)Si(iPr)_3$ in $CDCl_3$ consists of 8 distinct carbon signals with the most

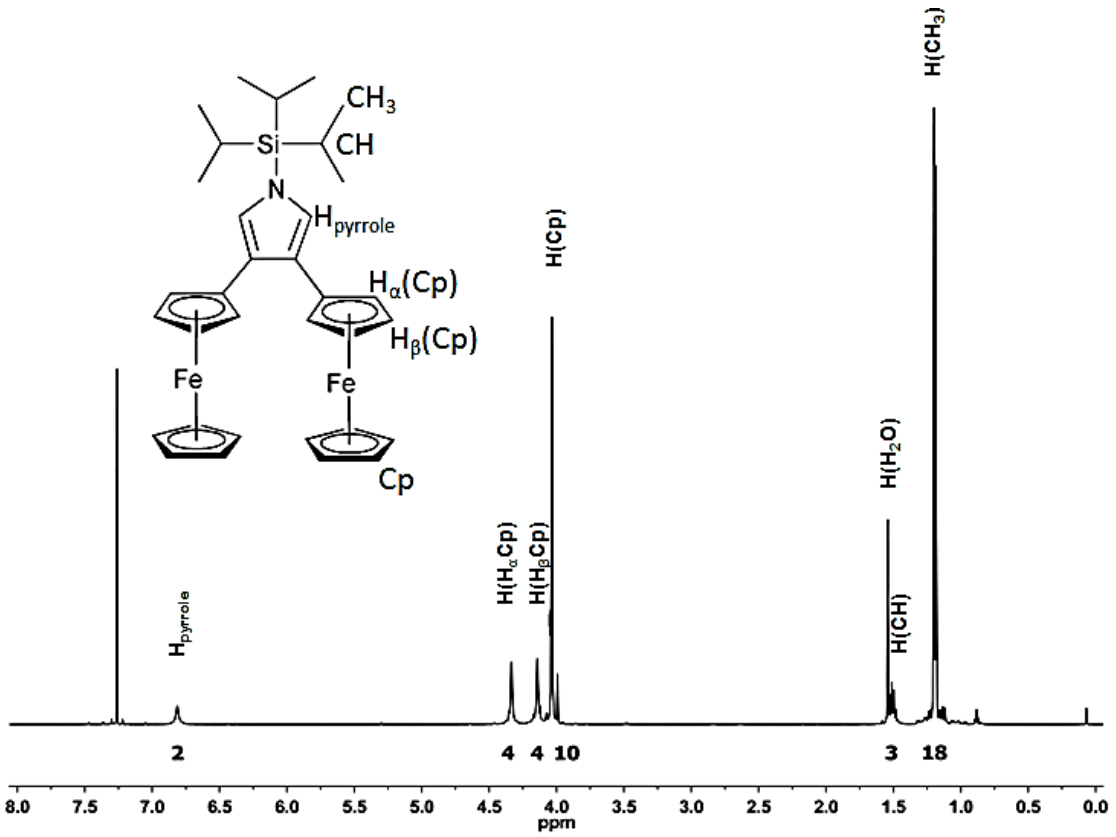

Figure 16: ^{1}H NMR ($CDCl_3$) spectrum of 3,4-diferrocene-1-(triisopropylsilyl)pyrrole (compound **9**, Scheme **2**).

downfield being the two pyrrole carbons observed at 123.53 ($C_\alpha(C_4N)$, Figure 17) and 122.07 ($C_\beta(C_4N)$, Figure 17) ppm. The ferrocenyl substituent is observed as three signals around 77.3 ppm. A shoulder is seen in the solvent region caused by the ipso cyclopentadienyl carbon within the ferrocenyl substituent at 77.52 ppm ($C_{ipso}(Cp)$, Figure 17). Two equivalent α-positioned cyclopentadienyl ring carbons seen as a single signal at 69.36 ppm ($C_\alpha(Cp)$, Figure 17) along with two equivalent β-positioned cyclopentadienyl ring carbons at 67.26 ppm ($C_\beta(Cp)$, Figure 17). Lastly, a signal representative of ten equivalent unsubstituted cyclopentadienyl carbons seen at 69.07 ppm (C(Cp), Figure 17). There were two remaining signals seen representing the isopropyl substituents within the protecting group at 18.13 ppm (C(CH), Figure 17) and 11.95 ppm ($C(CH_3)$, Figure 17).

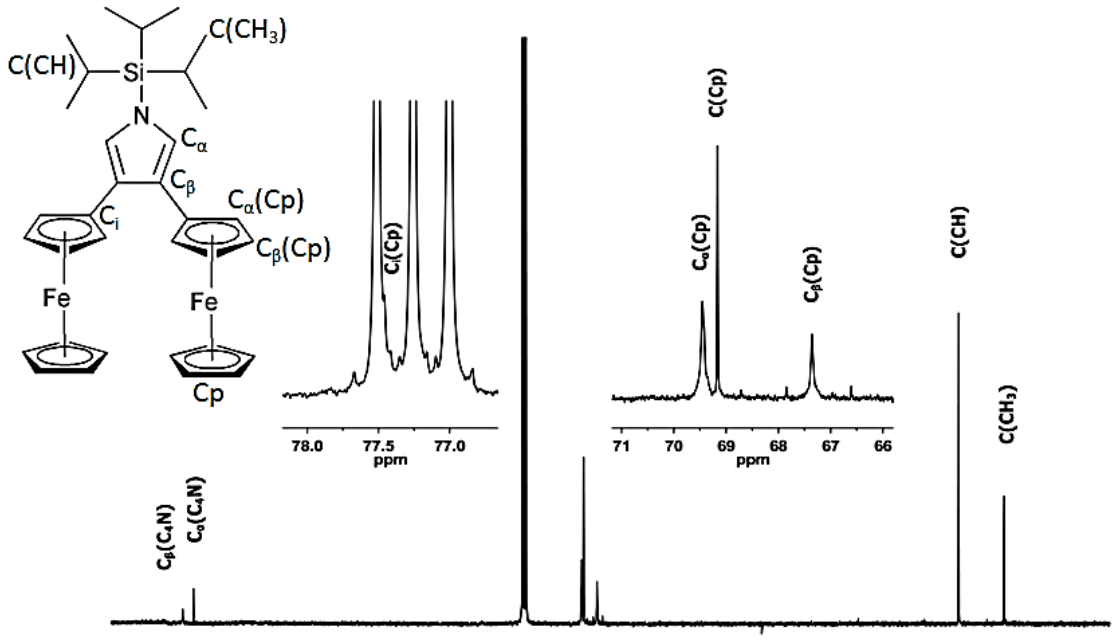

Figure 17: ^{13}C NMR Spectrum of 3,4-bis(ferrocenyl)-1-(triisopropylsilyl)pyrrole (**9** ($Fc_2(C_4N)Si(iPr)_3$, Scheme 2) in deuterated chloroform ($CDCl_3$).

The yields of $Fc_2(C_4N)Si(iPr)_3$ ranged from 7% to 52%. The major factor influencing yield was the time the reaction mixture was refluxed at 60°C. Initially it was reported that a reflux time of 48 hours would be sufficient in coupling ferrocene in the β-

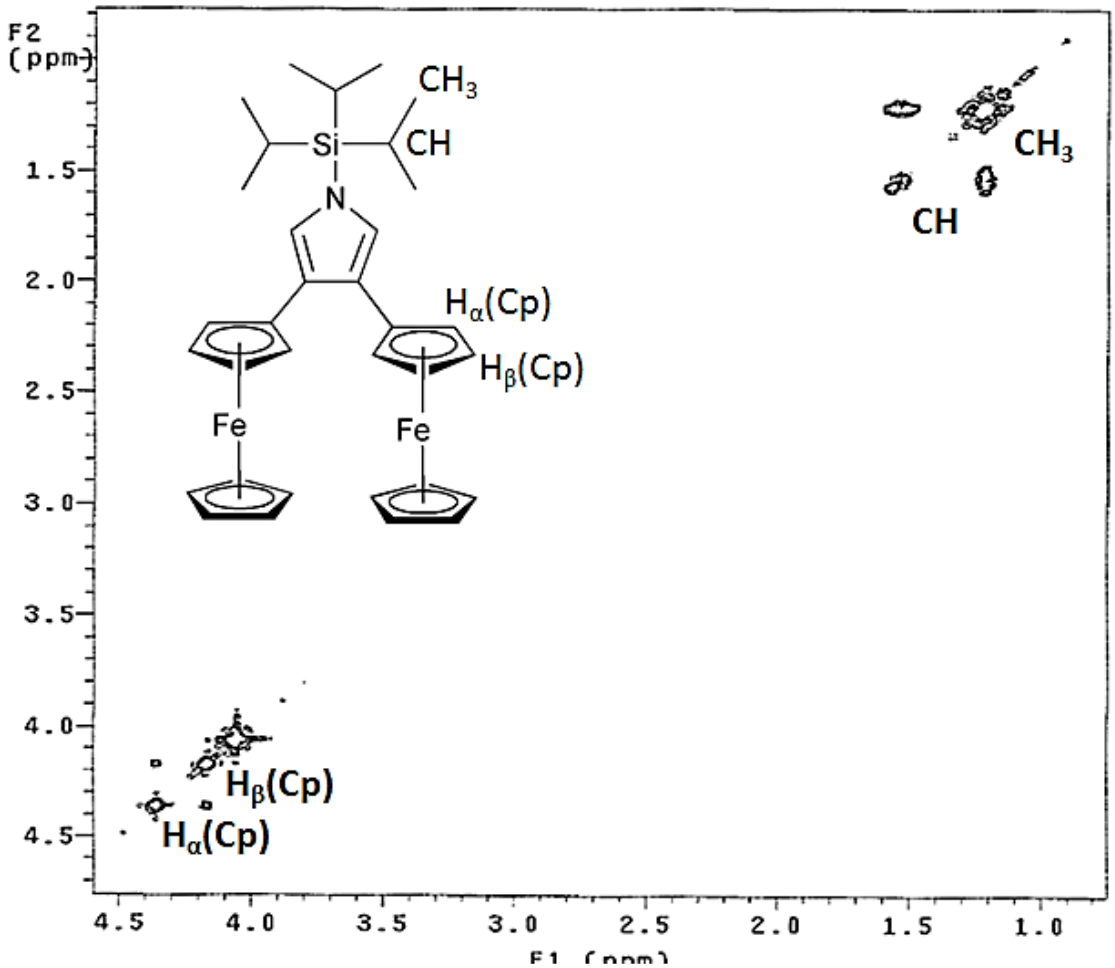

Figure 18: ^{1}H COSY 2-D NMR Spectrum of 3,4-bis(ferrocenyl)-1-(triisopropylsilyl)pyrrole (**9** ($Fc_2(C_4N)Si(iPr)_3$, Scheme 2) in deuterated chloroform ($CDCl_3$).

positions. We extended the reflux time to 72 hours and observed an improvement in the yield by a two-fold factor. Thereafter, we noticed no significant improvement in yield as a result of increasing reflux time. Trace amounts of ferrocene, bis(ferrocene), and other byproducts were detected in the reaction mixture, while the main reaction product (~52% yield) was $Fc_2(C_4N)Si(iPr)_3$. We experimented with coupling of ferrocene by means of bis(ferrocenyl)mercury in the presence of a palladium catalyst, regardless of reflux time no reaction occurred. Ferrocene was observed as the major product, and only trace amounts of unidentifiable, likely degraded initial compounds, were observed.

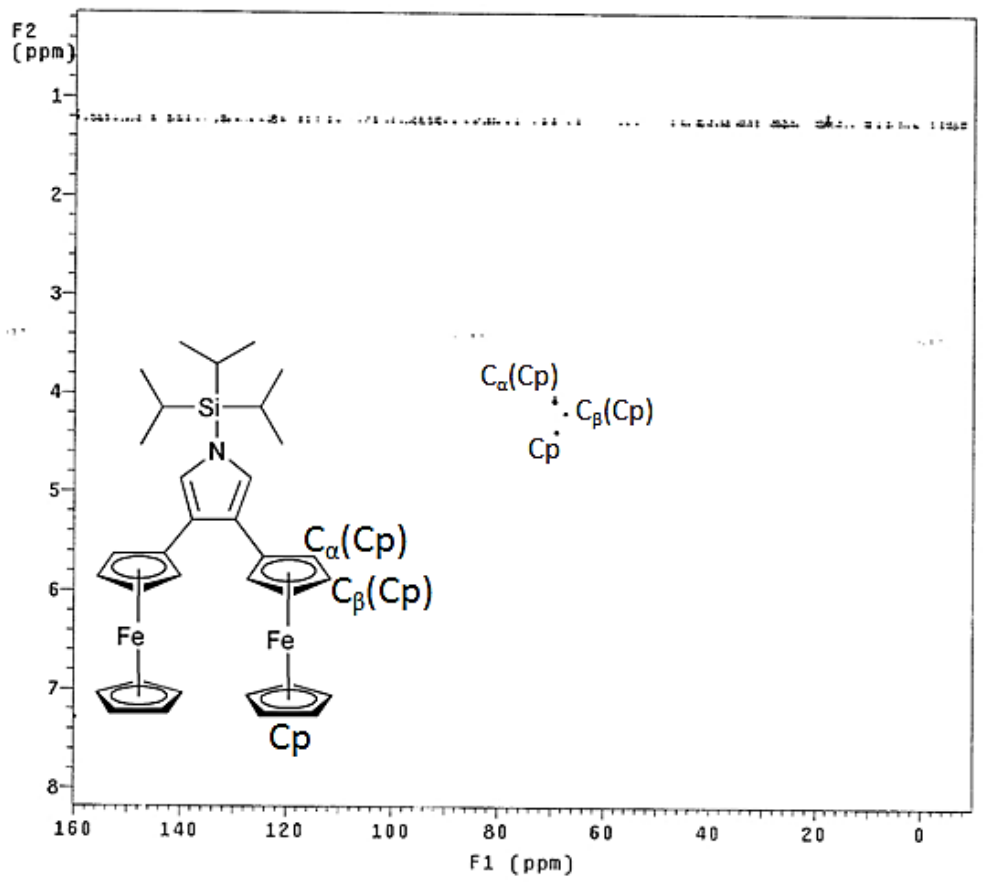

Figure 19: ^{1}H-^{13}C HMQC 2-D NMR Spectrum of 3,4-bis(ferrocenyl)-1-(triisopropylsilyl)pyrrole (**9** ($Fc_2(C_4N)Si(iPr)_3$, Scheme 2) in deuterated chloroform ($CDCl_3$).

X-Ray Analysis:

The structure (ORTEP Diagram) of 3,4-diiodo-1-(triisopropylsilyl)pyrrole (**8**, Figure 20) and the final assignment of the structure of 3,4-bis(ferrocenyl)-1-(triisopropylsilyl)pyrrole ($Fc_2(C_4N)Si(iPr)_3$, **9**, Figure 21) were achieved by using single-crystal X-ray diffraction. The final refinement parameters for complex **8** are presented in Table 5 (Supporting Information Tables 13-18), and Table 6 for complex **9** (Supporting Information Tables 19-24). Selected bond distances and angles for complex **9** are presented in Tables 7 and 8. It should be noted that the structure of $Fc_2(C_4N)Si(iPr)_3$ is a rare example of a *β*-substituted bis(ferrocenyl) heterocyclic compound in which two

ferrocenyl substituents are bridged by an electro-active pyrrole complex by only two carbon atoms. There are very few reported bis(ferrocenyl) heterocycle structures. One such example is an indirectly connected bis(heterocyclic carbene) bimetallic iron complex with 16.5 Å separating the indirectly linked ferrocenyl substituents[41]. The distance separating the two ferrocenyl substituents in 3,4-bis(ferrocenyl)-1-(triisopropylsilyl)pyrrole is 3.285(5) Å seen in Figure 21 as the distance between C5 and C15; also the distance between Fe centers within ferrocenyl substituents 5.9343(8) Å.

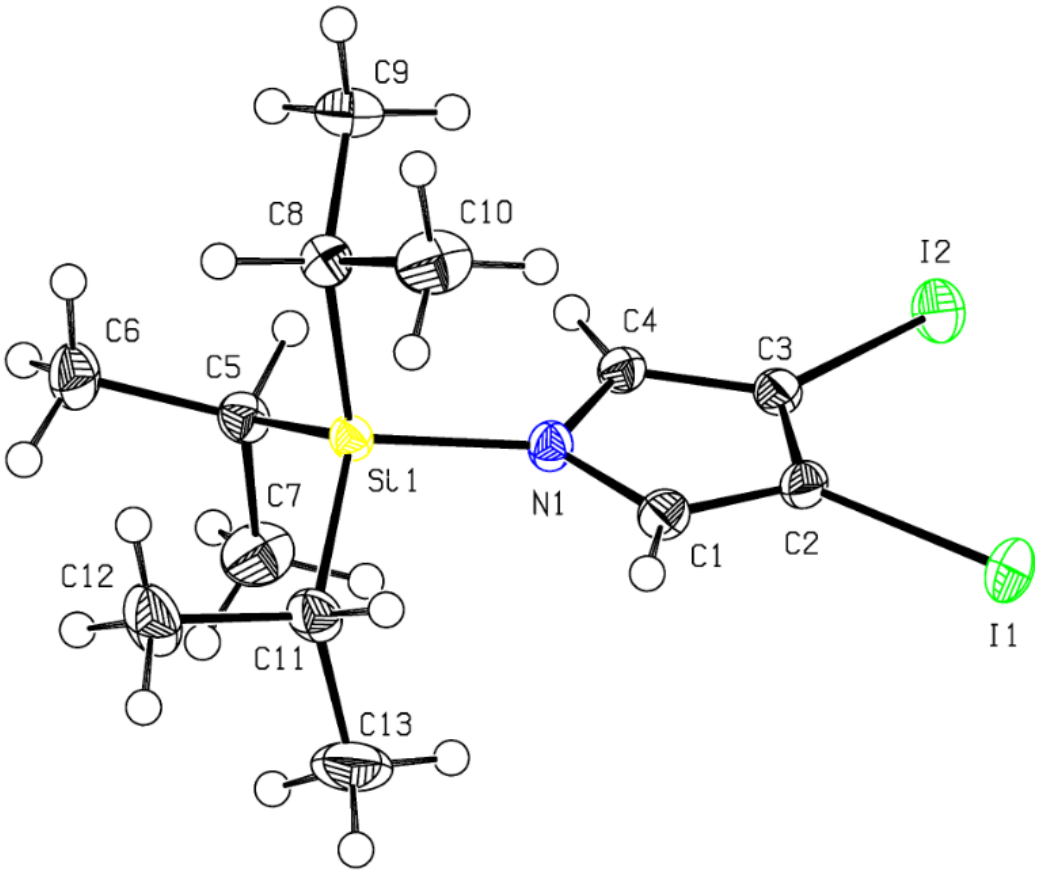

Figure 20: ORTEP diagram of 3,4-bis(ferrocenyl)-1-(triisopropylsilyl)pyrrole (Complex **9**, Scheme 2, $Fc_2(C_4N)Si(iPr)_3$) drawn with 50% probability ellipsoids.

The orientation of the two ferrocenyl substituents is similar to the 3,4-bis(ferrocenyl) ligands reported by Hildebrandt and his co-workers[35]. The torsion angles N1-C1-C2-C5 (179.9(3)°) and N1-C1-C2-C3 (-0.2(4)°) confirm the pyrrole system is

planar. $Fc_2(C_4N)Si(iPr)_3$ lacks C_2 symmetry seen in Figure 21 presented in the space group P-1. The silicone−nitrogen bond distance (1.782(3) Å) is within the typical range for analogous compounds (1.775(1) Å)[42]. The torsion angles observed for the two ferrocenyl substituents in Figure 21 is C1-C2-C5-C6 (-33.7(5))° for one ferrocenyl substituent and C2-C3-C15-C19 (67.4(5))° for the second ferrocenyl substituent. These are likely the range in which ferrocenyl substituents can rotate without influencing the properties of the compound. In an ideal sense, ferrocenyl substituents lay at a torsion angle of 45°, we see each of our substituents offset from the ideal angle ranging from 11.3-22.4°.

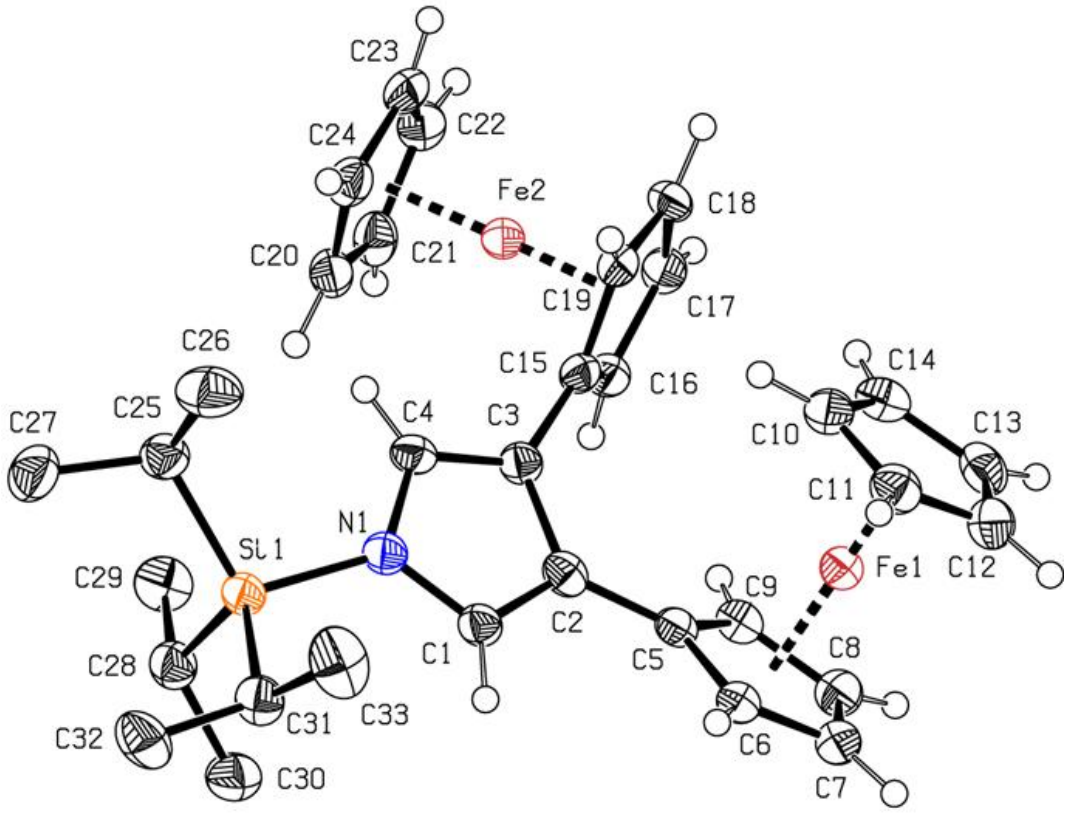

Figure 21: ORTEP diagram of 3,4-bis(ferrocenyl)-1-(triisopropylsilyl)pyrrole (Complex **9**, Scheme 2, $Fc_2(C_4N)Si(iPr)_3$) drawn with 50% probability ellipsoids.

Crystallography Collection and Refinement Data for Complex **8**	
empirical formula	$C_{33}H_{23}I_2NSi$
fw	475.21
cryst syst	monoclinic
space group, Z	P 21/c
a (Å)	9.6249(6)
b (Å)	21.7670(5)
c (Å)	8.7272(2)
α (deg)	90
β (deg)	107464(8)
γ (deg)	90
volume (Å^3)	1744.12(12)
ρ_{calc} (g/cm^3)	1.81
μ (mm^{-1})	3.659 (Mo K_α)
θ_{max} (deg)	27.29
GoF(F^2)	1.133
R_1 ($F^2 > 2\sigma(F^2)$)	0.0211
wR_2 (all data)	0.0506
$\Delta\rho_{max}/\Delta\rho_{min}$ (e/Å^3)	1.419/-0.338

$$R_1(F) = \Sigma\|F_o| - |F_c\|/\Sigma|F_o|. \quad wR_2(F^2) = \{\Sigma[w(F_o^2 - F_c^2)^2]/\Sigma w(F_o^2)^2]\}^{1/2}.$$

Table 5: X-Ray Crystal Collection and refinement Data for 3,4-diiodo-1-(triisopropylsilyl)pyrrole (**8**, Scheme 2).

The average Fe-C bond distance in $Fc_2(C_4N)Si(iPr)_3$ was 2.049(3) Å, which is in agreement with the accepted value of 2.04 Å for ferrocene. The average bond angle for nitrogen with each isopropyl ligand is 108.1(2)° similar to analogous (triisopropylsilyl)pyrrole complexes,[42] from each bond angle N1-Si1-C25 (106.5(2))°, N1-Si1-C28 (109.8(2))°, and N1-Si1-C31 (107.9(2))° seen in Table 7. This represents no condensation of bond angles as a result of coupling large ferrocenyl substituents in the *β*-positions of the pyrrole complex.

Crystallography Collection and Refinement Data for Complex **9**	
empirical formula	$C_{33}H_{41}Fe_2NSi$
fw	591.46
cryst syst	triclinic
space group, Z	P-1, 2
a (Å)	7.3670(3)
b (Å)	12.3067(5)
c (Å)	17.1322(12)
α (deg)	110.563(8)
β (deg)	98.491(7)
γ (deg)	94.446(7)
volume (Å^3)	1424.25(13)
ρ_{calc} (g/cm^3)	1.379
μ (mm^{-1})	1.083 (Mo K_α)
θ_{max} (deg)	26.37
GoF(F^2)	1.09
R_1 ($F^2 > 2\sigma(F^2)$)	0.0555
wR_2 (all data)	0.1409
$\Delta\rho_{max}/\Delta\rho_{min}$ (e/Å^3)	0.678/-0.886

$$R_1(F) = \Sigma||F_o| - |F_c||/\Sigma|F_o|. \quad wR_2(F^2) = \{\Sigma[w(F_o^2 - F_c^2)^2]/\Sigma w(F_o^2)^2]\}^{1/2}.$$

Table 6: X-Ray Crystal Collection and refinement Data for 3,4-bis(ferrocenyl)-1-(triisopropylsilyl)pyrrole (**9**, Scheme 2).

Bond Lengths (Å)		Bond Angles (deg)	
N1-Si1	1.782(3)	N1-Si1-C25	106.5(2)
Si1-C25	1.891(4)	N1-Si1-C28	109.8(2)
Si1-C28	1.883(4)	N1-Si1-C31	107.9(2)
Si1-C31	1.879(3)	N1-C1-C2	110.7(3)
Avg Fe-C	2.049	N1-C4-C3	110.8(3)

Table 7: Bond Lengths and Angles of 3,4-bis(ferrocenyl)-1-(triisopropylsilyl)pyrrole (**9**, Scheme 2).

Elemental Analysis		
	Theory	Found
C	67.01	67.84
H	7.00	7.51
N	2.37	2.16

Table 8: Elemental Analysis of 3,4-bis(ferrocenyl)-1-(triisopropylsilyl)pyrrole (**9**, Scheme 2).

UV-Vis Spectroscopy:

UV-Vis NIR spectra are shown below describing $Fc_2(C_4N)Si(iPr)_3$ (Figure 22). The bands in the UV-Vis NIR spectra seen in Figure 22 are a result of π-π* transitions. The band at 22,197 cm^{-1} (450.5 nm) is a lower energy transition, as a result of the HOMO to LUMO transition. HOMO-1 to LUMO transitions are seen in the UV-Vis-NIR

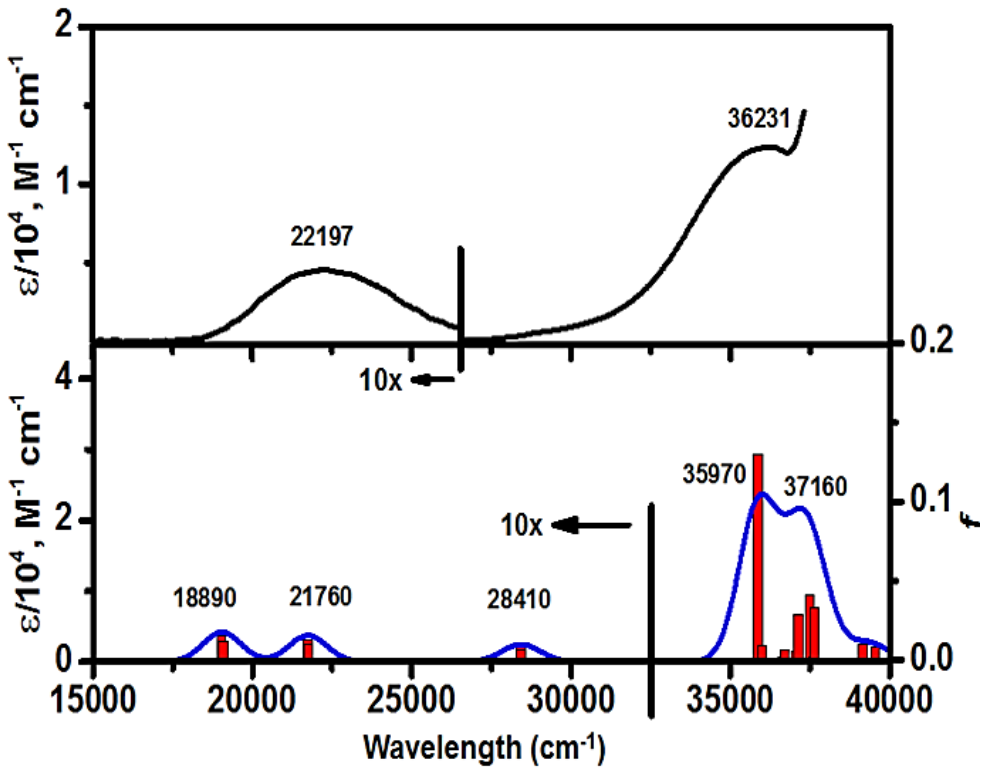

Figure 22: UV-Vis-NIR spectrum of 3,4-bis(ferrocenyl)-1-(triisopropylsilyl)pyrrole (Complex **9**, Scheme 2, $Fc_2(C_4N)Si(iPr)_3$) in DCM at 25°C.

spectrum (Figure 22) at 36,231 cm^{-1} (276 nm).

Electrochemistry:

Electrochemical study of 3,4-bis(ferrocenyl)-1-(triisopropylsilyl)pyrrole ($Fc_2(C_4N)Si(iPr)_3$) was done using cyclic voltammetry (CV), differential pulse voltammetry (DPV), and square wave voltammetry (SWV). All methods are useful for rapidly observing redox behavior over a wide range potential. As electrical current cycles from low to high voltage from its midpoint, different oxidation and reduction processes can be identified as a result of electron transfer.

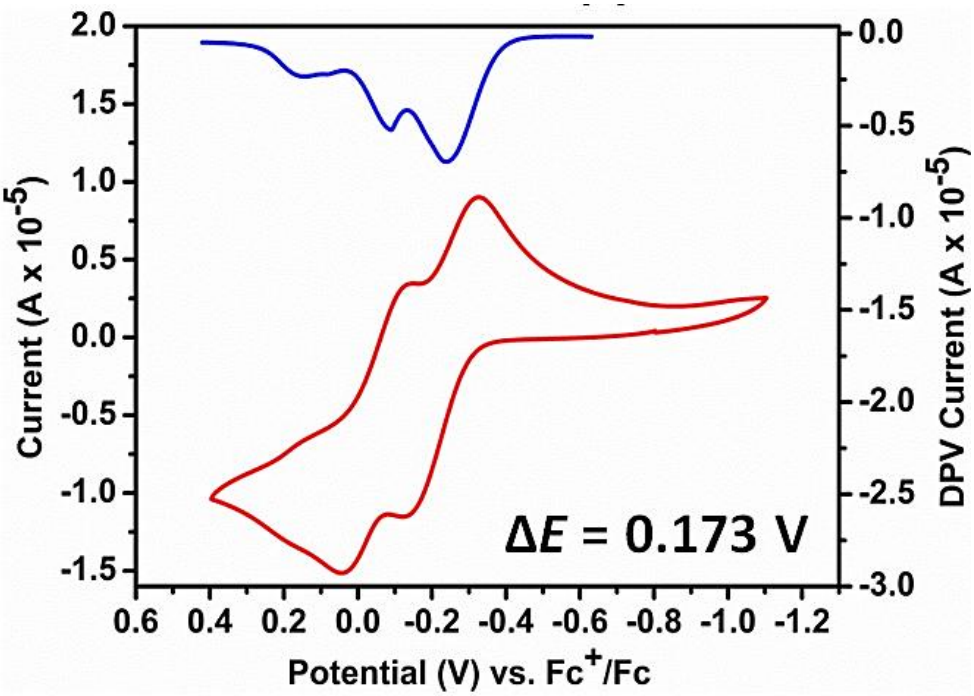

Figure 23: Electrochemical study of 3,4-bis(ferrocenyl)-1-(triisopropylsilyl)pyrrole (Complex **9**, Scheme 2, $Fc_2(C_4N)Si(iPr)_3$) in TBAP at 25°C.

The electrolyte and solvent used can influence the electron transfer process in addition to the separation in reduction potential ($\Delta E_{1/2}$) values in complexes that contain multiple nuclear transition metals.[43] Since the oxidation of the ferrocene substituents in poly-(ferrocenyl)-containing macro cycles is sensitive to the nature of the solvent and the electrolyte,[26] the redox properties of $Fc_2(C_4N)Si(iPr)_3$ were investigated by the three electrochemical methods in a low polarity solvent (DCM), coupled with either tetrabutylammonium perchlorate (TBAP) or tetrabutylammonium tetrakis(perfluorophenyl)borate (TFAB), both non-coordinating electrolytes[27].

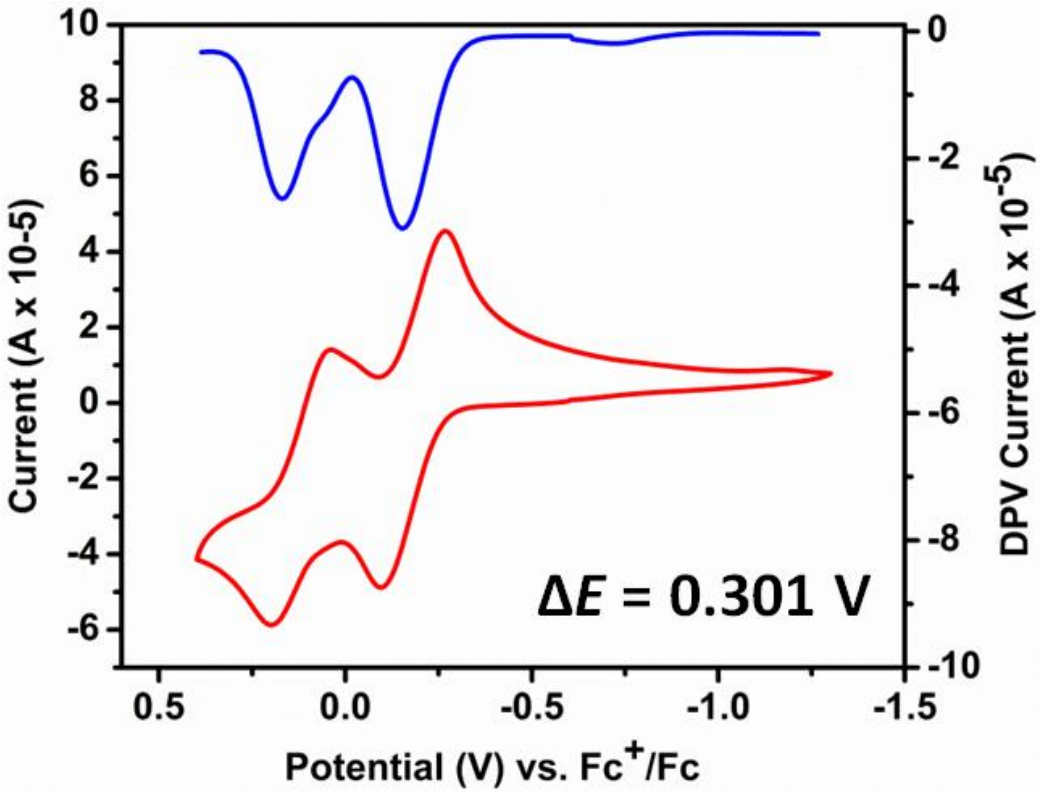

Figure 24: Electrochemical study of 3,4-bis(ferrocenyl)-1-(triisopropylsilyl)pyrrole (Complex **9**, Scheme 2, $Fc_2(C_4N)Si(iPr)_3$) in TFAB at 25°C.

Electrochemical data for $Fc_2(C_4N)Si(iPr)_3$ reveals two oxidation potentials found to be at -224 and -51 mV at 25°C in TBAP seen in Figure 23, while in TFAB the oxidation potentials were found at -182 and 119 mV (Figure 24), respectively. CV and

DPV experiments reveal two reversible oxidation processes in $Fc_2(C_4N)Si(iPr)_3$. Similar to the 2,5-bis(ferrocenyl)pyrrole system,[35] two oxidation waves were assigned to single-electron ferrocenyl-centered processes. The oxidation potentials reported in 2,5-bis(ferrocenyl)pyrrole were at -198 and 117 mV(TBAP), improvements in $\Delta E_{1/2}$ were seen by the two oxidation potentials reported at -238 and 212 mV (TFAB). Both ferrocenyl substituents in $Fc_2(C_4N)Si(iPr)_3$ could be oxidized at lower potentials compared to 2,5-bis(ferrocenyl)pyrrole. The separation between the first two oxidation waves (301 mV (TFAB)) in $Fc_2(C_4N)Si(iPr)_3$ was significantly larger than the separation

Reduction Potentials	
3,4(TBAP)	**2,5(TFAB)**
-0.051	0.212
-0.224	-0.238
3,4(TFAB)	**2,3,4,5 (TFAB)**
	0.550
	0.323
0.119	0.051
-0.182	-0.280

Table 9: Electrochemical reduction potentials of ferrocenyl substituted pyrrole complexes in solvent systems at 25°C.

observed in TBAP (173 mV), yet lower than the values reported for 2,5-bis(ferrocenyl)pyrrole system 450 mV (TFAB) [315 mV (TBAP)] or 2,3,4,5-tetraferrocenyl pyrrole 331, 272, and 227 mV (TFAB).[35] Reduction potentials are listed in Table **9**.

It was unusual to see a decrease in $\Delta E_{1/2}$ as we would expect electronic communication to be improved between the two β-substituted ferrocenyl ligands as the distance between the two substituents is much less than that of α-substituted ferrocenyl ligands. The two α-substituted ferrocenyl substituents are separated by the C-N-C heterocyclic pyrrole system, while the β-substituted ferrocenes are in closer proximity being linked by C-C bond in the heterocyclic pyrrole system.

Spectroelectrochemistry:

Spectroelectrochemistry was performed in order to obtain UV-Vis-NIR

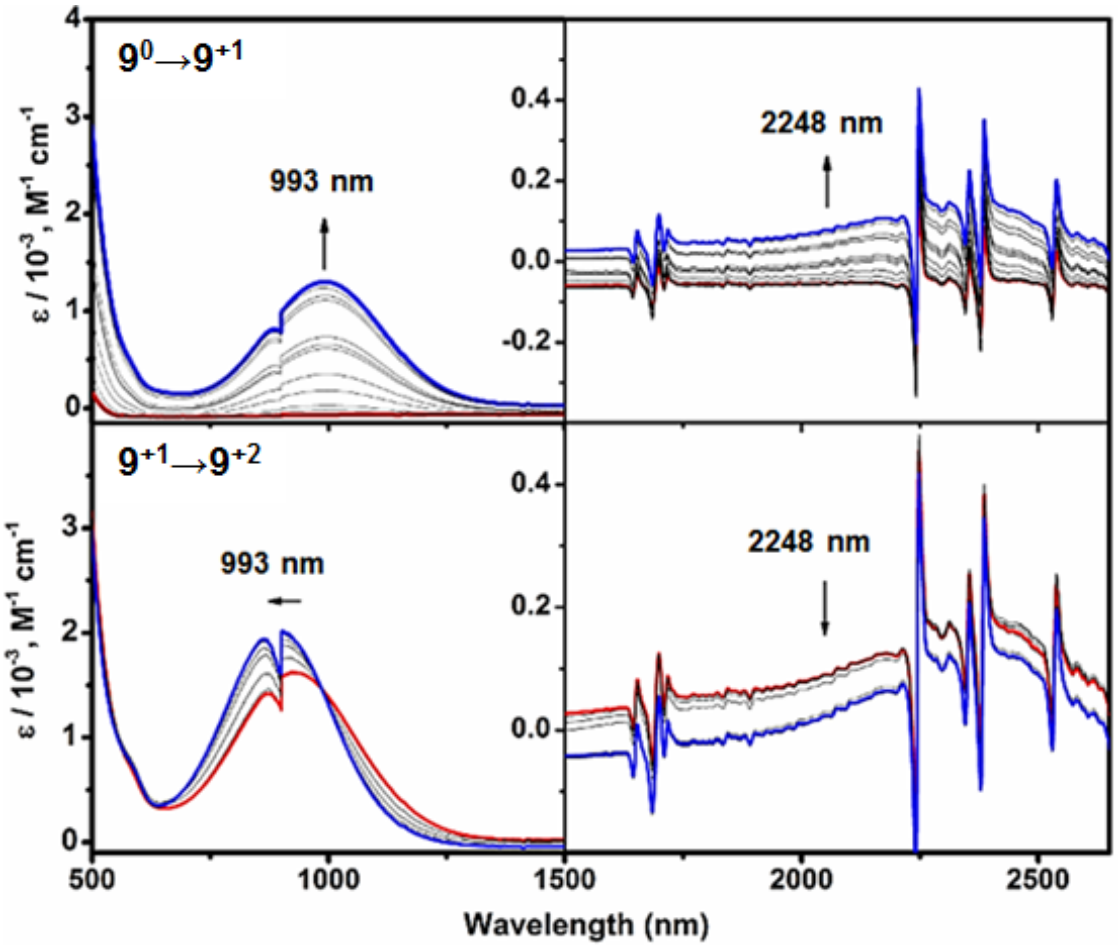

Figure 25: Spectroelectrochemical Oxidation study of 3,4-bis(ferrocenyl)-1-(triisopropylsilyl)pyrrole (Complex **9**, Scheme 2, $Fc_2(C_4N)Si(iPr)_3$) in TBAP at 25°C. Oxidation $Fc_2(C_4N)Si(iPr)_3^+$ (100-1200 mV, top) and $Fc_2(C_4N)Si(iPr)_3^{+2}$ (1300-1500 mV), bottom).

spectroscopic signatures of the different electron transfer processes that were seen with the electrochemistry for 3,4-bis(ferrocenyl)-1-(triisopropylsilyl)pyrrole ($Fc_2(C_4N)Si(iPr)_3$). Stepwise oxidation was performed in DCM and tetrabutylammonium perchlorate (TBAP) solution; the results are seen in Figure 25 and results for the completely reversible reduction of $Fc_2(C_4N)Si(iPr)_3$ seen in Figure 27.

Initial spectroelectrochemical oxidation of $Fc_2(C_4N)Si(iPr)_3$ to $Fc_2(C_4N)Si(iPr)_3^+$ showed an increasing intensity of the 993 nm band. The peak at 993 nm for $Fc_2(C_4N)Si(iPr)_3$ showed an increase in the intensity upon initial spectroelectrochemical

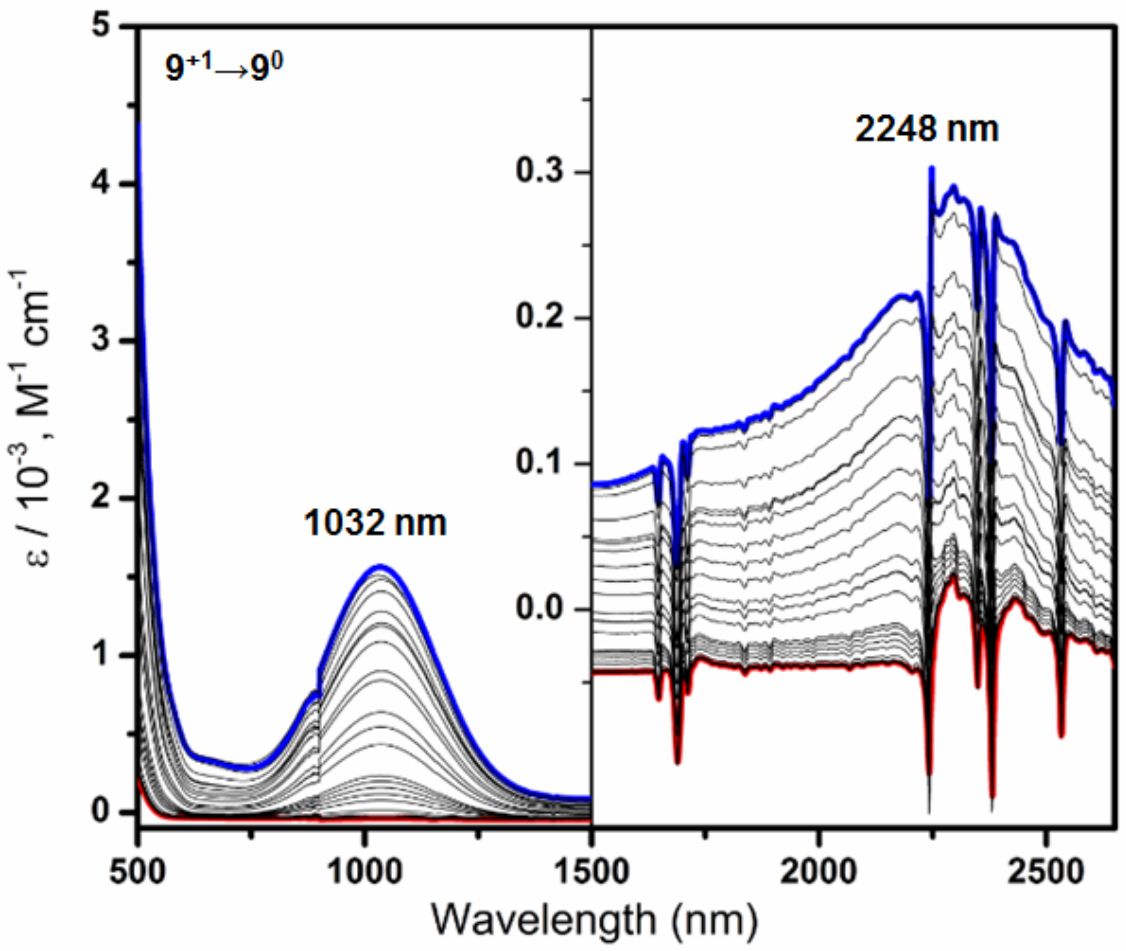

Figure 26: Spectroelectrochemical Oxidation study of 3,4-bis(ferrocenyl)-1-(triisopropylsilyl)pyrrole (Complex **9**, Scheme 2, $Fc_2(C_4N)Si(iPr)_3$) in TFAB at 25°C. Oxidation $Fc_2(C_4N)Si(iPr)_3^+$ (100-900 mV.

oxidation as did the signal at 2248 nm (Figure 25, top). The creation of a mixed valence state (Fe^{2+},Fe^{3+}) was supported by the presence of the IVCT band at 2248 nm as it increased throughout the first oxidation process.

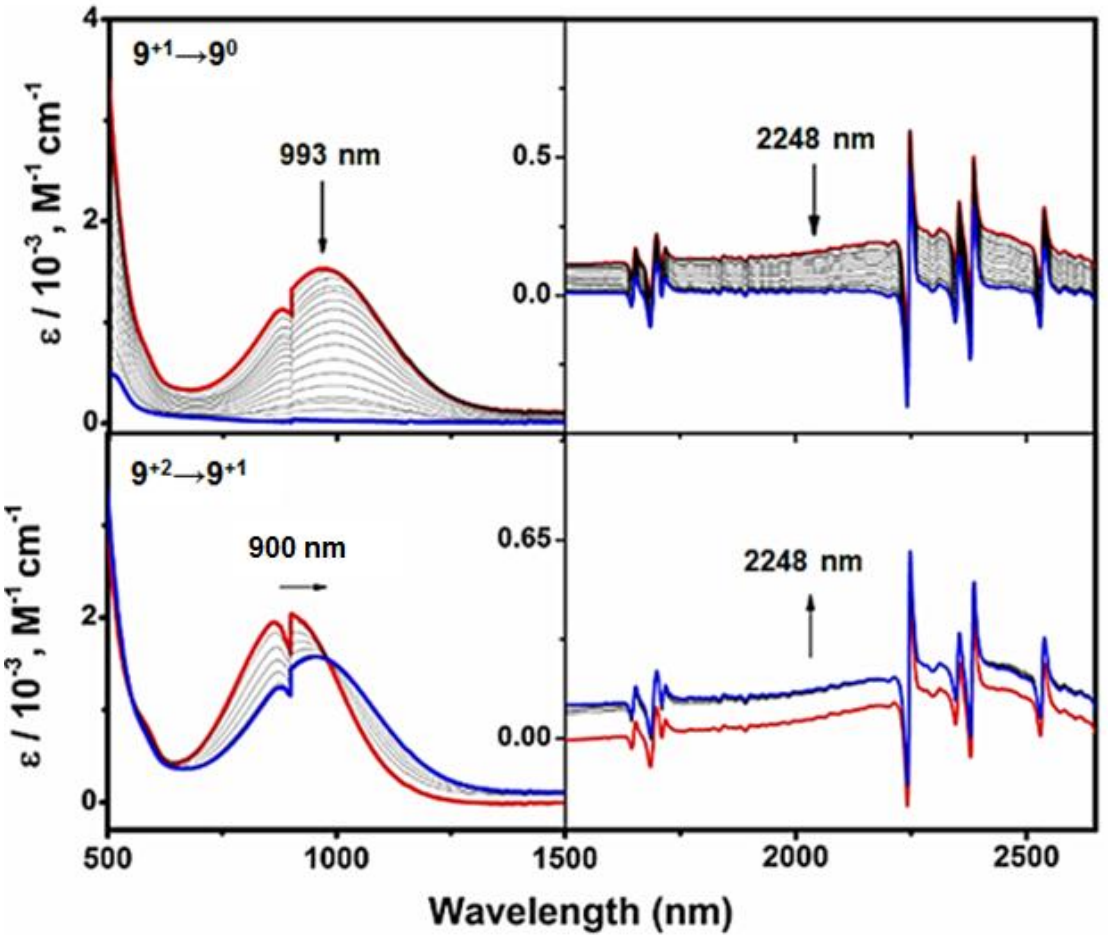

Figure 27: Spectroelectrochemical Reduction study of 3,4-bis(ferrocenyl)-1-(triisopropylsilyl)pyrrole (Complex **9**, Scheme 2, $Fc_2(C_4N)Si(iPr)_3$) in TBAP at 25°C.Reduction $Fc_2(C_4N)Si(iPr)_3^{+1}$ (-500 mV, top) and $Fc_2(C_4N)Si(iPr)_3^{+2}$ (-500 mV), bottom).

Upon entering the second oxidation process, the IVCT band would be lost upon oxidizing both metals to equivalent states (Fe^{3+},Fe^{3+}). The fall of the IVCT band was observed with no shift. The peak at 993 nm was observed to red shift to 900 nm throughout the second oxidation process (Figure 25, bottom). Our results agree with reported results in both the 2,5-bis(ferrocenyl)pyrrole and the 2,3,4,5-tetraferrocenyl pyrrole where a red shift results in the NIR region of their spectra in addition to the

decrease in the IVCT band upon removal of the second electron from the system.[35] Similar results were observed in the first oxidative process in a TFAB system; the results are seen in Figure 26. Initially, the peak at 1032 nm began increasing throughout the first oxidative process.

Reduction of the doubly oxidized $Fc_2(C_4N)Si(iPr)_3^{+2}$ complex was completely reversible as shown in Figure 27. The first reduction process results in the band at 951 nm blue shifting as it moves back to the original 993 nm position. The intensity of the IVCT band at 2248 nm begins increasing as the mixed valance state is established in the $Fc_2(C_4N)Si(iPr)_3^{+1}$ complex. The IVCT band was lost as $Fc_2(C_4N)Si(iPr)_3^{+1}$ returned to its neutral state ($Fc_2(C_4N)Si(iPr)_3$) and similar results were seen to the initial $Fc_2(C_4N)Si(iPr)_3$ complex.

Electronic Structure:

Density functional theory calculations were performed to gain understanding of the nature of the electronic structure of 3,4-bis(ferrocenyl)-1-(triisopropylsilyl)pyrrole ($Fc_2(C_4N)Si(iPr)_3$). Gas-phase geometries were optimized using B3LYP exchange-correlation function, 6-311+G basis set. The HOMO-LUMO gap shown in the molecular orbital energy diagram below (Figure 28) shows the HOMO-LUMO energy differences, in addition the images for the HOMO and LUMO are depicted at the right.

Molecular orbital contribution diagrams are also shown below (Figure 29). From the contribution diagram, the HOMO has ~84% contributions from the two ferrocene substituents, while the remainder is a due to the electro-active pyrrole system. In comparison, the HOMO has ~94-95% contributions from ferrocene substituents in

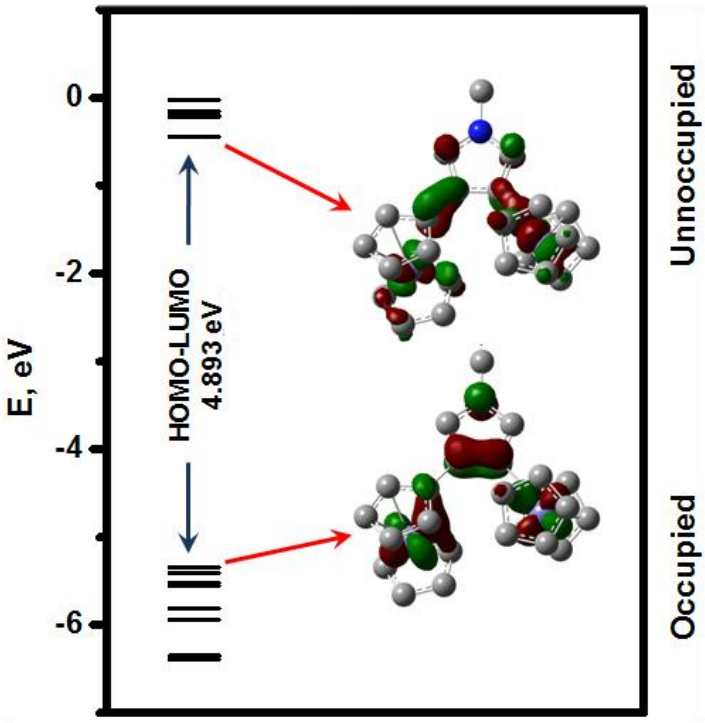

Figure 28: Molecular Orbital diagram for 3,4-bis(ferrocenyl)-1-(triisopropylsilyl)pyrrole ($Fc_2(C_4N)Si(iPr)_3$) including HOMO and LUMO images shown at right using Density Functional Theory Using B3LYP/6-311+G (Fe),6-311G(d).

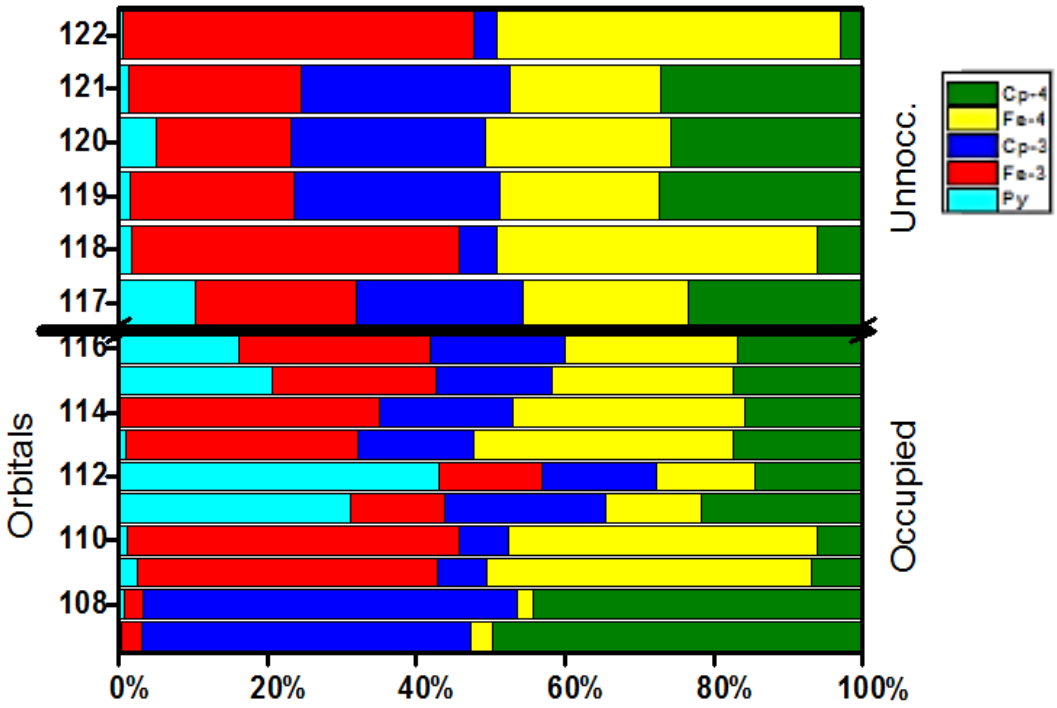

Figure 29: Molecular Orbital Contribution diagram for 3,4-bis(ferrocenyl)-1-(triisopropylsilyl)pyrrole ($Fc_2(C_4N)Si(iPr)_3$) shown at right using Density Functional Theory Using B3LYP/6-311+G (Fe),6-311G(d).

dimethyl (Z)-2,3-bis(ferrocenyl)-2-butenedioate and (Z)-2,3-bis(ferrocenyl)maleimide

systems.[5] It is clear from both the molecular contribution diagram (Figure 29) and the image from the HOMO (Figure 28) is conclusive in supporting the electron density is located around the ferrocene substituents likely due to the overlapping π-orbitals involved in the aromatic cyclopentadienyl rings (Cp). The LUMO is predominantly centered on π* orbitals of both ferrocene substituents shown in Figure 28.

Conclusions:

Formation of the new 3,4-bis(ferrocenyl)-1-(triisopropylsilyl)pyrrole (Complex **9**, Scheme 2, $Fc_2(C_4N)Si(iPr)_3$) brings attention the properties of *β*-substituted bis(ferrocenyl) heterocycles, a new class of compounds not well known. The $Fc_2(C_4N)Si(iPr)_3$ complex has been characterized by NMR spectroscopy (Figures 16 and 17), elemental analysis (Table 7) and X-ray crystallography (Figure 21).

Experimental Section:

Materials:

Caution! All organomercurials are highly toxic. Extreme care is necessary when handling all products and their solutions. All commercial reagents were ACS grade and were used without further purification. Silica gel, reverse phase (C_{18}) silica gel (60 Å, 63-100 μm), and aluminum oxide (Activity I, 50-200 μm) for column chromatography were purchased from Dynamic Adsorbents, Inc. NMR spectra were recorded on a Varian INOVA NMR spectrometer at 500 MHz using TMS as a reference and $CDCl_3$ or C_6D_6 as solvent. Single crystals suitable for X-ray crystallographic analysis of **3**, **5**, and **9**(CCDC 841448 for **3** and CCDC 841447 for **5**; these data can be obtained from the Cambridge Crystallographic Data Centre, 12 Union Road, Cambridge CB2 1EZ, UK; fax: +44-1223-

336033; e-mail: deposit@ccdc.cam.ac.uk) were obtained by slow evaporation of a concentrated hexane and toluene solution, respectively. X-ray diffraction data were collected on a Rigaku Rapid II image plate diffractometer using graphite-monochromated Mo Kα (λ = 0.71073 Å) for **5** and **9** or Cu Kα radiation (λ = 1.54178 Å) for **3** at 123 K. Multiscan absorption corrections were applied to the data using the CrystalClear 2.0 program.[22] The structures were solved by direct methods implemented in SIR-92[23] (**3**, **5**, and **9**) and refined by full-matrix least squares based on F^2 using SHELXL software[25]. Distances between Fe atoms and η^5-C_5H_5 ring centroids were calculated using PLATON[26] software. PLATON software was also used for visualization of the results. All reactions were performed under dry argon atmosphere with flame-dried glassware. Dry toluene was obtained by distillation over sodium and benzophenone indicator, dry DCM was obtained by distillation over calcium hydride prior to experiments, and dry THF was obtained by distillation over Na/K alloy with diphenylketone. The compounds tetrabutylammonium perchlorate (TBAP) and tetrabutylammonium tetrakis(pentafluorophenyl)borate (TFAB) was used in anhydrous DCM for electrochemical studies, after preparation according to literature[44].

Synthesis:

Preparation of Complex 3. Bis(ferrocenyl)mercury (**1**) (856 mg, 1.49 mmol), dimethylacethylenedicarboxylate (**2**) (416 mg, 2.98 mmol), sodium iodide (905 mg, 4.47 mmol), 24.5 mL of THF, and 24.5 mL of dry acetone were added to a flask equipped with a reflux condenser and gas inlet. The reaction mixture was heated to reflux and 34 mg (0.15 mmol) of $Pd(OAc)_2$ catalyst was added to the reaction mixture refluxing for 30 min. The reaction mixture was cooled and filtered through a thin layer of silica gel

The filtrate was evaporated under reduced pressure. The resulting residue was washed several times with cold hexane, and the remaining residue was recrystallized several times from a toluene/hexane mixture. Based on ^{1}H NMR spectroscopy, organomercuric compound **3** always co-crystallized with ester **4** in close to equimolar amounts. Since all attempts to purify organomercuric compound **3** using chromatographic methods on silica gel and aluminum oxide failed because of product degradation on the column, compound **3** was purified using reversed phase (C_{18}) TLC plates. In spite of its purity detected by TLC, compound **3** still slightly degrades during its removal from TLC plates (because of the polar solvent use), as evident from NMR spectra (Figures 5, 6−11). Data for **3**: ^{1}H NMR (500 MHz, C_6D_6, TMS): δ 4.77 (m, 2H, H_α(Cp)), 4.67 (m, 2H, H_α(Cp)), 4.05 (m, 2H, H_β(Cp)), 4.07 (m, 2H, H_β(Cp)), 4.06 (s, 10H, Cp), 3.78 (s, 6H, (O)CH3), 3.34 (s, 6H, (O)CH3). ^{13}C NMR (125 MHz, C_6D_6, TMS): δ 168.65 C(=O)), 165.78 (C(C=O)), 148.86 (C(=C)), 119.77 (C(Hg)), 76.58 (C_{ipso}(Cp)), 71.90 (C_β(Cp)), 71.70 (C_β(Cp)), 70.77 (C_α(Cp)), 70.13 (C_α(Cp)), 70.51 (C(Cp)), 52.14 (C(OCH3)), 51.91 (C-(OCH3)). Anal. Calcd for $C_{32}H_{30}O_8Fe_2Hg\cdot 4C_7H_8$ ($C_{60}H_{62}O_8Fe_2Hg$): C(58.90), H(5.11). Found: C(58.05), H(4.8).

Preparation of Complex 7. A solution of potassium-bis-trimethylsilyl amide(16.72g, 83.8 mmol) in anhydrous THF and pyrrole (6.04g, 84.4 mmol) added drop wise were combined under Argon atmosphere. The reaction mixture was stirred for 18 hours, afterwards the solvent was evaporated in vacuum to reveal a dry potassium pyrrole salt. Triisopropylsilyl chloride (16.49g, 85.5 mmol) was added drop wise to dry potassium pyrrole salt (83.8 mmol) in anhydrous THF and stirred for 1 hour. The solvent was evaporated under vacuum; ether was added to the reaction mixture, and washed with

water. The ether layer was dried over sodium sulfate and via Kugelrohr distillation the purified product was obtained as a clear oil (12.73g, 68% yield). Data for **7**: ^{1}H NMR (500 MHz, $CDCl_3$, TMS): δ1.09 (d, 18 H, J = 7.4 Hz, CH_3), 1.45 (m, 3 H, J = 7.4 Hz, CH), 6.32 (t, 2 H, $H_\alpha(C_4N)$), 6.80 (t, 2 H, $H_\beta(C_4N)$).

Preparation of Complex 8. Iodine, (0.95g, 4 mmol) in 200mL of anhydrous DCM was added drop wise to a mixture of mercuric acetate (1.28g, 4 mmol) and **7** (0.51g, 2 mmol) in DCM at 0°C over a period of 1 hour. The reaction mixture was stirred for 3.5 hours, and the solvent was removed in vacuum. Hexane was added to dissolve the product, and it was later evaporated to obtain the yellow crystalline product (0.494g, 69% yield). Data for **8**: ^{1}H NMR (500 MHz, $CDCl_3$, TMS): δ1.08 (d, 18 H, J = 7.49 Hz, CH_3), 1.41 (sept, 3 H, J = 7.49 Hz, CH), 6.79 (s, 2 H, $H_\alpha(C_4N)$).

Preparation of Complex 9. In a Schlenck flask, (2.79 g, 15 mmol) ferrocene and (0.17 g, 1.5 mmol) potassium tert-butoxide were combined in 50 mL of dry THF under Argon atmosphere, the reaction mixture was then cooled to -38°C. Drop wise tert-butyl lithium, 1.7 M in pentane (13.8 mL, 23.5 mmol), was added to the reaction mixture kept at -38°C. After being stirred for 1 hour, (6.76 g, 24.1 mmol) of [$ZnCl_2 \cdot 2THF$] was added and stirred for an additional 1 hour at -38°C;the reaction mixture was returned to room temperature being stirred for an additional 1 hour. Palladium triphenylphosphate (0.104 g, 0.09 mmol) was added along with **8** (2.39 g, 5 mmol) to the reaction mixture. The reaction mixture was refluxed at 60°C for 72 hours. Evaporating all volatile solvents under vacuum, the red-orange precipitate was dissolved in 500 mL of dichloromethane and washed with water (150 mL) three times. The organic layer was dried over $MgSO_4$,

and the solvent was removed under vacuum revealing a dark orange solid product separated by column chromatography using alumina and hexane: toluene (9:1) as the eluent. Purification of the product was done using fractional crystallization in heptane to obtain red-orange crystals (0.421 g, 52% yield) Data for 9: ^{1}H NMR (500 MHz, $CDCl_3$, TMS): δ 6.81 (s, 2H, $H_{\alpha}(C_4N)$), 4.33 (s, 4H, $H_{\alpha}(Cp)$), 4.14 (s, 4H, $H_{\beta}(Cp)$), 4.03 (s, 10H, Cp), 1.52 (m, 3H, CH), 1.19 (d, 18H, CH_3). ^{13}C (125 MHz, $CDCl_3$, TMS): δ123.5 ($C_{\alpha}(C_4N)$), 122.1 ($C_{\beta}(Cp)$), 77.37 ($C_{ipso}(Cp)$), 69.4 ($C_{\alpha}(Cp)$), 69.1 ($C_{\beta}(Cp)$), 67.3 (C(Cp)), 18.1 (CH), 12.0 (CH_3). Anal. Calcd for $C_{33}H_{41}Fe_2N$ (593.46 g/mol): C, 67.00; H, 7.00; N, 2.37. Found: C, 67.85; H, 7.51; N, 2.16.

Instrumentation:

A Varian Unity INOVA NMR instrument was used to evaluate spectra taken at 500 MHz frequency for protons and 125 MHz for carbons. Each were referenced to TMS as an internal standard and chemical shifts were recorded in parts per million. All UV-Vis data was obtained on a JASCO-720 spectrophotometer at room temperature. Electrochemical measurements were conducted using a CHI620C electrochemical analyzer utilizing the three-electrode scheme. Either carbon or platinum working, auxiliary and reference electrodes were used in 0.05 M solution of TFAB (or 0.1 M TBAP) in DCM with redox potentials corrected using internal standard (decamethylferrocene) in all cases. Spectroelectrochemical data was collected using a custom-made 1 mm cell, a working electrode made of platinum mesh, and a 0.15 M solution of TBAP or TFAB in DCM. Fluorescence techniques were performed using a

Varian Cary Eclipse Fluorescence Spectrometer. Elemental analysis was performed by Atlantic Microlab, Inc. in Atlanta, Georgia.

Computational Aspects:

All computations were performed using Gaussian09 software package supported by the Minnesota Super Computing Institute. Molecular orbital contributions were compiled from 74 single point calculations using the VMOdes program[53]. TDDFT calculated excitation energies were found where the lowest 150 singlet excited states had been considered. In all calculations, Becke, 3-parameter, Lee-Yang-Parr correlation functional (B3LYP) were used. Wachter's full-electron basis set was used for iron (6-311+G), while for all other atoms 6-311G(d) basis set was employed. The percentage of atomic orbital contributions to their respective molecular orbitals was calculated by using the VMOdes program. In all cases, frequency calculations were performed to ensure that the optimized structures represent potential energy surface minima. It has been shown that B3LYP exchange-correlation functional coupled with the mentioned above basis set could accurately predict MLCT and π-π^* in variety of ferrocene-containing compounds, porphyrins, and phthalocyanines[45]. The typical errors for the TDDFT predicted by the mentioned above combination of the exchange-correlation functional and basis set method are within ~0.1 eV.

X-Ray Crystallography:

X-ray quality single crystals of **3** were obtained by recrystallization of product residue several times from a toluene/hexane mixture. Single crystals of **5** were obtained

by recrystallization of product from a DCM/hexane mixture, and single crystals of **9** were obtained by recrystallization of product residue from slow diffusion of heptane solution. Experimental data for all compounds were collected using Rigaku Rapid II X-ray diffractometer with curved IPDS detector using graphite-monochromatized Mo Kα (λ = 0.71073 Å) for **5** and **9** or Cu Kα radiation (λ = 1.54178 Å) for **3** at 123 K. Structure **3** were solved by direct method implemented into SHELXS-97[25] program and structures **5** and **9** were solved by direct method using SIR-92 program[23]. All missed non hydrogen atoms were located from analysis of a difference Fourier-map and refined in an isotropic and then in the anisotropic approximations. All aromatic hydrogen atoms were placed geometrically while hydrogen's for methyl group were located from the difference Fourier-map analysis and were constrained. Structures were completely refined using a full-matrix least square method using SHELXL-97 program[25]. The best values for R_1 were 0.0224 (**5**), 0.0241 (**3**), and 0.0555 (**9**). All information about the refinement of crystal structures is presented in Tables 1 and 4; the corresponding CIF files are presented in the Supplemental Section.

References:

1) D'Alessandro, D.; Keene, R. *Chem. Soc. Rev.*, **2006**, *35*, 424.

2) Hush, N. S. *Prog. Inorg. Chem.* **1967**, *8*, 391.

3) Creutz, C. *Prog. Inor. Chem.*, **1983**, *30*, 1.

4) Robin, M.; Day, P. *Advances in Radiochemistry*. **1967,** *10*, 248.

5) Solntsev, P.; Dudkin, S.; Sabin, J.; Nemykin, V. N. *Organometallics* 2011, *30*, 3037.

6) Knapp, R.; Rehahn, M. *J. Organomet. Chem.* 1993, *452*, 235.

7) Beletskaya, I.; Tsvetkov, A.; Latyshev, G.; Tafeenko, V.; Lukashev, N. *J. Organomet. Chem.* 2001, *637−639*, 653.

8) S. Santi *et al.*, *Inorganica Chimica Acta*, 2011, **374**, 442-446

9) Goetsch, W.; Solntsev, P.; Nemykin, V. *Organometallics* 2011, *30*, 6636.

10) Hildebrandt, A.; Schaarschmidt, D.; Lang, H. Organometallics 2011, *30*, 556.

11) (a) Makarova, L. G.; Nesmeyanov, A. N. *Methods of Elementorganic Chemistry: Mercury* (Russian); Nauka: Moscow, 1965. (b) Sokolov, V. I.; Reutov, O. A. *Coord. Chem. Rev.* 1978, *27*, 89. (c) Sharma, S.; Chakraborty, T.; Srivastava, K.; Singh, H. B. *J. Chem. Sci.* 2011, *123*, 113. (d) Kurmaz, V. A.; Gul'tyai, V. P. *Russ. Chem. Rev.* 2010, *79*, 307. (e) Parkin, G. *New J. Chem.* 2007, *31*, 1996. (f) Taylor, T. J.; Burress, C. N.; Gabbaie, F. P. *Organometallics* 2007, *26*, 5252. (g) Wong, W.-Y. *Coord. Chem. Rev.* 2007, *251*, 2400. (h) Milaeva, E.; Petrosyan, V.; Berberova, N.; Pimenov, Y.; Pellerito, L. *Bioinorg. Chem. Appl.* 2004, *2*, 69. (i) Kitching, W.; Glenn, M. *Sci. Synth.* 2004, *3*, 133. (j) Boev, V. I.; Moskalenko, A. I.; Boev, A. *Usp. Khim.* 1997, *66*, 874.

12) (a) Kocovsky, P. *J. Organomet. Chem.* 2003, *687*, 256. (b) Kotora, M.; Takahashi, T. In *Handbook of Organopalladium Chemistry for Organic Synthesis*; Negishi, E., Ed.; John Wiley & Sons, Inc.: Hoboken, NJ, 2002; Vol. *1*, pp 973−993.

13) (a) *Metal-catalyzed Cross-Coupling Reactions*; Diederich, F.; Stang, P. J., Eds.; Wiley-VCH: Weinheim, 1998. (b) Reutov, O. A.; Beletskaya, I. P. *Reaction Mechanism of Organometallic Compounds*; North-Holland: Amsterdam, 1968.

14) (a) Qin, J.; Wu, X.; Zhang, X.; Zhan, C.; Liu, D. *Synth. Met.* 1995, *71*, 1711. (b) Klapoetke, T. M.; Krumm, B.; Moll, R. *Eur. J. Inorg. Chem.* 2011, 422. (c) More, P. G.; Dalave, N. V.; Lawand, A. S.; Nalawade, A. M. *J. Indian Chem. Soc.* 2009, *86*, 68. (d) Namba, K.; Yamamoto, H.; Sasaki, I.; Mori, K.; Imagawa, H.; Nishizawa, M. *Org. Lett.* 2008, *10*, 1767. (e) More, P. G.; Dalave, N. V.; Lawand, A. S.; Nalawade, A. M. *J. Indian Chem. Soc.* 2007, *84*, 394. (f) Kurmaz, V. A.; Ershler, A. B. *Mendeleev Commun.* 2006, 234. (g) Soro, B.; Stoccoro, S.; Minghetti, G.; Zucca, A.; Cinellu, M. A.; Manassero, M.; Gladiali, S. *Inorg. Chim. Acta* 2006, *359*, 1879. (h) King, J. B.; Gabbaie, F. P. *Organometallics* 2003, *22*, 1275.

15) (a) Solntsev, P. V.; Dudkin, S. V.; Sabin, J. R.; Nemykin, V. N. *Organometallics* 2011, *30*, 3037. (b) Santi, S.; Orian, L.; Donoli, A.; Bisello, A.; Scapinello, M.; Benetollo, F.; Ganis, P.; Ceccon, A. *Angew. Chem., Int. Ed.* 2008, *47*, 5331. (c) Cowan, D. O.; LeVanda, C.; Park, J.; Kaufman, F. *Acc. Chem. Res.* 1973, *6*, 1−7. (d) Barlow, S.; O'Hare, D. *Chem. Rev.* 1997, *97*, 637. (e) Miller, J. S.; Epstein, A. J. *Angew. Chem., Int. Ed.* 1994, *33*, 385. (f) *Ferrocenes: Ligands, Materials and Biomolecules*; Stepnicka, P., Ed.; John Wiley & Sons, Ltd.: Chichester, England, 2008. (g) Vlcek, A. Jr. *Chemtracts* 2001, *14*, 1. (h) Dong, T.-Y.; Ho, P.-H.; Lai, X.-Q.; Lin, Z.-W.; Lin, K.-J. *Organometallics* 2000, *19*, 1096. (i) Venkatasubbaiah, K.; Doshi, A.; Nowik, I.; Herber, R. H.; Rheingold, A. L.; Jakle, F. *Chem.□Eur. J.* 2008, *14*, 444. (j) Chen, Y. J.; Pan, D.-S.; Chiu, C.-F.; Su, J.-X.; Lin, S. J.; Kwan, K. S. *Inorg. Chem.* 2000, *39*, 953. (k) Patoux, C.; Coudret, C.; Launay, J.-P.; Joachim, C.; Gourdon, A. *Inorg. Chem.* 1997, *36*, 5037. (l) Solntsev, P. V.; Sabin, J. R.; Dammer, S. J.; Gerasimchuk, N. N.; Nemykin, V. N. *Chem. Commun.* 2010, 6581. (m) Bucher, C.; Devillers, C. H.; Moutet, J.-C.; Royal, G.; Saint-Aman, E. *Coord. Chem. Rev.* 2009, *253*, 21. (n) Burrell, A. K.; Campbell, W. M.; Jameson, G. B.; Officer, D. L.; Boyd, P. D. W.; Zhao, Z.; Cocks, P. A.; Gordon, K. C. *Chem. Commun.* 1999, 637. (o) Nemykin, V. N.; Barrett, C. D.; Hadt, R. G.; Subbotin, R. I.; Maximov, A. Y.; Polshin, E. V.; Koposov, A. Y. *Dalton Trans.* 2007, 3378. (p) Nemykin, V. N.; Galloni, P.; Floris, B.; Barrett, C. D.; Hadt, R. G.; Subbotin, R. I.; Marrani, A. G.; Zanoni, R.; Loim, N. M. *Dalton Trans.* 2008, 4233. (q) Nemykin, V. N.; Rohde, G. T.; Barrett, C. D.; Hadt, R. G.; Bizzarri, C.; Galloni, P.; Floris, B.; Nowik, I.; Herber, R. H.; Marrani, A. G.; Zanoni, R.; Loim, N. M. *J. Am. Chem. Soc.* 2009, *131*, 14969. (r) Nemykin, V. N.; Rohde, G. T.; Barrett, C. D.; Hadt, R. G.; Sabin, J. R.; Reina, G.; Galloni, P.; Floris, B. *Inorg. Chem.* 2010, *49*, 7497. (s) Nemykin, V. N.; Kobayashi, N. *Chem. Commun.* 2001, 165. (t) Herber, R. H.; Nowik, I.; Grosland, J. O.; Hadt, R. G..; Nemykin, V. N. *J. Organomet. Chem.* 2008, *693*, 1850−1856. (u) Nemykin, V. N.; Makarova, E. A.; Grosland, J. O.; Hadt, R. G.; Koposov, A. Y. *Inorg. Chem.* 2007, *46*,

9591. (v) Nemykin, V. N.; Maximov, A. Y.; Koposov, A. Y. *Organometallics* 2007, *26*, 3138. (w) Nemykin, V. N.; Hadt, R. G. *Inorg. Chem.* 2006, *45*, 8297.

16) (a) Knapp, R.; Rehahn, M. *J. Organomet. Chem.* 1993, *452*, 235. (b) Foxman, B. M.; Rosenblum, M. *Organometallics* 1993, *12*, 4805. (c) Huttenloch, M. E.; Diebold, J.; Rief, U.; Brintzinger, H. H. *Organometallics* 1992, *11*, 3607. (d) Iyoda, M.; Kondo, T.; Okabe, T.; Matsuyama, H.; Sasaki, S.; Kuwatani, Y. *Chem. Lett.* 1997, 35. (e) Liu, C.-M.; Guo, Y.-L.; Wu, X.-L.; Liang, L.-M.; Ma, Y.-H. *J. Organomet. Chem.* 2000, *612*, 172. (f) Guillaneux, D.; Kagan, H. B. *J. Org. Chem.* 1995, *60*, 2502. (g) Lin, J. T.; Sun, S.-S.; Wu, J. J.; Lee, L; Lin, K.-J.; Huang, Y. F. *Inorg. Chem.* 1995, *34*, 2323. (h) Tsukazaki, M.; Tinkl, M.; Roglans, A.; Chapell, B. J.; Taylor, N. J.; Snieckus, V. *J. Am. Chem. Soc.* 1996, *118*, 685. (i) Imrie, C.; Luobser, C.; Engelbrecht, P.; McCleland, C. W. *J. Chem. Soc., Perkin Trans. 1* 1999, 2513. (j) Iyoda, M.; Okabe, T.; Katada, M.; Kuwatani, Y. *J. Organomet. Chem.* 1996, *569*, 225.

17) (a) Tsvetkov, A. V.; Latyshev, G. V.; Lukashev, N. V.; Beletskaya I. P. *Tetrahedron Lett.* 2000, *41*, 3987. (b) Beletskaya, I. P.; Tsvetkov, A. V.; Latyshev, G. V.; Tafeenko, V. A; Lukashev, N. V. *J. Organomet. Chem.* 2001, *637−639*, 653.

18) (a) Cambridge Structural Database. Allen, F. H. *Acta Crystallogr.*, 2002, *B58*, 380. (b) Brisdon, A. K.; Crossley, I. R.; Pritchard, R. G.; Sadiq, G. *J. Organomet. Chem.* 2007, *692*, 2125. (c) Sikirica, M.; Grdenic, D.; Cimas, S. *Acta Crystallogr.* 1982, *B38*, 926. (d) Tecle, B.; Siddiqui, K. F.; Ceccarelli, C.; Oliver, J. P. *J. Organomet. Chem.* 1983, *255*, 11. (e) Banger, K. K.; Brisdon, A. K.; Brain, P. T.; Parsons, S.; Rankin, D. W. H.; Robertson, H. E.; Smart, B. A.; Buhl, M. *Inorg. Chem.* 1999, *38*, 5894. (f) Maas, G.; Bruckmann, R.; Lorenz, W. *J. Organomet. Chem.* 1985, *289*, 9. (g) Grdenic, D.; Kamenar, B.; Zezelj, V. *Acta Crystallogr.* 1979, *B35*, 1889. (h) Crouch, D. J.; Hatton, P. M.; Helliwell, M.; O'Brien, P.; Raftery, J. *Dalton Trans.* 2003, 2761. (i) Begum, R. A.; Sharp, P. R. *Organometallics* 2005, *24*, 2670. (j) Zamora, F.; Sabat, M.; Lippert, B. *Inorg. Chem.* 1996, *35*, 4858. (k) Bois d'Enghien-Peteau, M.; Meunier-Piret, J.; van Meerssche, M. *Cryst. Struct. Commun.* 1975, *4*, 383. (l) Clark, G. R.; Ng, M. M. P.; Roper, W. R.; Wright, L. J. *J. Organomet. Chem.* 1995, *491*, 219.

19) Bondi, A. *J. Phys. Chem.* 1964, *68*, 441.

20) Clark, G. R.; Ng, M. M. P; Roper, W. R.; Wright, L. J. *J. Organomet. Chem.* 1995, *491*, 219.

21) (a) Macdonald, A. C.; Trotter, J. *Acta Crystallogr.* 1964, *17*, 872. (b) Boeyens, J. C. A.; Neuse, E. W.; Levendis, D. C. *S. Afr. J. Chem.* 1982, *35*, 57. (c) Kaluski, Z. L.; Struchkov, Yu.T.; Avoyan, R. L. *Zh. Strukt. Khim. (Russ.)* 1964, *5*, 743.

22) (a) Powers, M. J. ; Meyer, T. J. *J. Am. Chem. Soc.* 1978, *100*, 4393. (b) Dong, T.-Y.; Chang, C.-K.; Cheng, C.-H. *J. Org. Chem.* 1999, *587*, 46. (c) Williams, R. D.; Petrov, V. I.; Lu, H. P.; Hupp, J. T. *J. Phys. Chem. A* 1997, *101*, 8070. (d) Hadt, R. G.; Nemykin, V. N. *Inorg. Chem.* 2009, *48*, 3982. (e) Cowan, D. O.; Kaufman, F. *J. Am. Chem. Soc.* 1970, *92*, 219. (f) Cowan, D. O.; Levanda, C. *J. Am. Chem. Soc.* 1972, *94*, 9271. (g) Iijima, S.; Saida, R.; Motoyama, I.; Sano, H. *Bull. Chem. Soc. Jpn.* 1981, *54*, 1375. (h) Boehm, M. C.; Gleiter, R.; Delgado-Pena, F.; Cowan, D. O. *J. Chem. Phys.* 1983, *79*, 1154. (i) Dong, T. Y.; Hendrickson, D. N.; Iwai, K.; Cohn, M. J.; Geib, S. J.; Rheingold, A. L.; Sano, H.; Motoyama, I.; Nakashima, S. *J. Am. Chem. Soc.* 1985, *107*, 7996. (j) Morrison, W. H. Jr.; Hendrickson, D. N. *J. Chem. Phys.* 1973, *59*, 380. (k) Delgado-Pena, F.; Talham, D. R.; Cowan, D. O. *J. Organomet. Chem.* 1983, *253*, C43. (l) Cohn, M. J.; Timken, M. D.; Hendrickson, D. N. *J. Am. Chem. Soc.* 1984, *106*, 6683.

23) *CrystalClear-SM Expert 2.0* r4, Rigaku Inc., 2009.

24) Altomare, A.; Cascarano, G.; Giacovazzo, C.; Guagliardi, A.; Burla, M. C.; Polidori, G.; Camalli, M. *J. Appl. Crystallogr.* 1994, *27*, 435.

25) Beurskens, P. T.; Beurskens, G.; de Gelder, R.; Garcia-Granda, S.; Gould, R. O.; Smits, J. M. M. *DIRDIF*; 2008.

26) Sheldrick, G. M. *Acta Crystallogr.* 2008, *A64*, 112.

27) Spek, A. L. *J. Appl. Crystallogr.* 2003, *36*, 7−13.

28) Anderson, H. J.; Loader, C. E. *Synthesis* 1985, 353.

29) Loader, C. E.; Anderson, H. J. *Can. J. Chem.* **1981**, *59*, 2673 and references therein.

30) Desales, J.; Greenhouse, R.; Muchowski, J. M. *J. Org. Chem.* **1982**, *47*, 3668 and references therein.

31) Anderson, H. J.; Loader, C. E.; Xu, R.; Le, N.;Gogan, N. J.; McDonald, R.; Edwards, L. G. *Can. J. Chem.* **1985**, *63*, 896.

32) (a) Rokach, J.; Hamel, P.; Kakushima, M.; Smith, G. M. *Tetrahedron Lett.* **1981**, *22*, 4899. (b) Kakushima, M.; Hamel, P.; Frenette, R.; Rokach, J. *J. Org. Chem.* **1983**, *48*, 3214.

33) Carmona, O.; Greenhouse, R.; Landeros, R.; Muchowski, J. M. *J. Org. Chem.* **1980**, *45*, 5336.

34) Bray, B. L.; Mathies, P. H.; Naef, R.; Solas, D. R.; Tidwell, Thomas T.; Artis, D. R.; Muchowski, J. M. *Journal of Org. Chem.* **1990**, *55*, 6317-28.

35) Corey, E. J.; Snider, B. B. *J. Am. Chem. Soc.* **1972**, *94*, 6190.

36) Hildebrandt, A.; Schaarschmidt, D.; Lang, H. *Organometallics* **2011**, *30*(3), 556-563.

37) (a) Jones, S. C.; Barlow, S.; O'Hare, D. *Chem.-Eur. J.* **2005**, *11*, 4473. (b) Barlow, S.; O'Hare, D. *Chem. Rev.* **1997**, 97, 637. (c) Bruce, I. M. *Coord. Chem. Rev.* **1997**, *166*, 91. (d) Ratner, M.; Jortner, J. *Molecular Electronics*; Blackwell Science: Malden, MA, 1997. (e) Tour, M. *J. Acc. Chem. Res.* **2000**, ***33***, 791. (f) Collier, P. C.; Wong,W. E.; Belohradsky, M.; Raymo, M. F.; Stoddart, F. J.; Kuekes, J. P.; Williams, S. R.; Heath, R. J. *Science* **1999**, *285*, 391. (g) Carroll, R. L.; Gorman, Ch. B. *Angew. Chem., Int. Ed.* **2002**, *41*, 4378. (h) Robertson, N.; McGowan, C. A. *Chem. Soc. Rev.* **2003**, *32*, 96. (i) Diallo, A. K.; Daran, J.-C.; Varret, F.; Ruiz, J.; Astruc, D. *Angew. Che.,, Int. Ed.* **2009**, *48*, 3141.

38) Ogawa, S.; Muraoka, H.; Kikuta, K.; Saito, F.; Sato, R. *J. Organomet. Chem.* **2007**, *692*, 60.

39) Kowalsi, K.; Winter, R. F. *J. Organomet. Chem.* **2009**, *694*, 1041.

40) Hildebrandt, A.; Ruffer, T.; Erasmus, E.; Swarts, J. C.; Lang, H. *Organometallics* **2010**, *29*, 4900.

41) (a) Curran, D.; Grimshaw, J.; Perera, S. D. *Chem. Soc. Rev.* **1991**, *20*, 391. (b) Li, S.; Macosko, C. W.; White, H. S. *Adv. Mater.* **1993**, *5*, 575. (c) Fabre, B.; Simonet, J. *Coord. Chem. Rev.* **1998**, *178-180*, 1211. (d) Reddinger, J. L.; Reynolds, J. R. *Adv. Polym. Sci.* **1999**, *145*, 57. (e) MacDiarmid, A. G. Angew. *Chem., Int. Ed.* **2001**, *40*, 2581.

42) Tennyson, A. G.; Khramov, D. M.; Varnado, C. D.; Creswell, P. T.; Kamplain, J. W.; Lynch, V. M.; Bielawski, C. W. *Organometallics* **2009**, *28*(17), 5142-5147.

43) Chen, J.; Too, C. O.; Wallace, G. G.; Swiegers, G. F.; Skelton, B. W.; White, A. H. *Electrochimica Acta.* **2002**, *47*, 4227-4238.

44) Barriere, F.; Geiger, W. E. *J. Am. Chem. Soc.* **2006**, *128*, 3980.

45) (a) Waluk, J.; Michl, J. *J. Org. Chem*. **1991**, 56, 2729; (b) Gorski, A.; Vogel, E.; Sessler, J. L.; Waluk J. *J. Phys. Chem. A.* **2002**, 106, 8139; (c) Mack, J.; Stillman, M.;J. Kobayashi, N. *Coord. Chem. Rev*. **2007**, 251, 429.

Supplemental Information:

Supporting Information Table 1

Crystal data and structure refinement for bis(dimethyl-(*Z*)-3-ferrocenyl-2-butenedioate)mercury.

Identification code	redhg_p21c
Empirical formula	C32 H30 Fe2 Hg O8
Formula weight	854.85
Temperature	123(2) K
Wavelength	1.54178 A
Crystal system, space group	Monoclinic, $P2_1/c$
Unit cell dimensions	a = 8.902(5) A alpha = 90 deg. b = 12.776(5) A beta = 110.321(5) deg. c = 13.799(5) A gamma = 90 deg.
Volume	1471.7(11) A^3
Z, Calculated density	2, 1.929 Mg/m^3
Absorption coefficient	17.412 mm^{-1}
F(000)	836
Crystal size	0.22 x 0.20 x 0.18 mm
Theta range for data collection	6.84 to 68.24 deg.

Limiting indices	-10<=h<=10, -13<=k<=15, -15<=l<=16
Reflections collected / unique	16500 / 2689 [R(int) = 0.0330]
Completeness to theta = 68.24	99.4 %
Absorption correction	Semi-empirical from equivalents
Max. and min. transmission	0.1456 and 0.1143
Refinement method	Full-matrix least-squares on F^2
Data / restraints / parameters	2689 / 0 / 198
Goodness-of-fit on F^2	1.055
Final R indices [I>2sigma(I)]	R_1 = 0.0224, wR_2 = 0.0549
R indices (all data)	R_1 = 0.0240, wR_2 = 0.0563
Largest diff. peak and hole	1.123 and -0.752 $e.A^{-3}$

Supporting Information Table 2

Atomic coordinates (x 10^4) and equivalent isotropic displacement parameters (A^2 x 10^3) for bis(dimethyl-(*Z*)-3-ferrocenyl-2-butenedioate)mercury.

U(eq) is defined as one third of the trace of the orthogonalized Uij tensor.

	x	y	z	U(eq)
Hg(1)	10000	5000	5000	15(1)
Fe(1)	10469(1)	8532(1)	6676(1)	19(1)
O(1)	5459(3)	6167(2)	3450(2)	49(1)
O(2)	6409(3)	4668(2)	4249(2)	27(1)
O(3)	6935(3)	8474(2)	3687(2)	39(1)
O(4)	5946(3)	7844(2)	4853(2)	41(1)
C(1)	8155(4)	6086(2)	4650(2)	17(1)
C(2)	8377(4)	7122(2)	4828(2)	17(1)
C(3)	6539(4)	5688(3)	4052(3)	23(1)
C(4)	4870(4)	4187(3)	3703(3)	35(1)
C(5)	7012(4)	7878(3)	4378(2)	23(1)
C(6)	4520(5)	8463(4)	4369(4)	55(1)
C(7)	9918(4)	7623(2)	5374(2)	16(1)
C(8)	10390(4)	8658(3)	5185(2)	22(1)
C(9)	11963(4)	8846(3)	5877(3)	26(1)
C(10)	12500(4)	7947(3)	6505(3)	25(1)
C(11)	11252(4)	7189(3)	6205(2)	21(1)
C(12)	9968(6)	8155(3)	7963(3)	41(1)
C(13)	8566(5)	8550(4)	7191(3)	41(1)
C(14)	8903(5)	9580(3)	6931(3)	35(1)
C(15)	10506(5)	9822(3)	7559(3)	33(1)
C(16)	11155(5)	8938(3)	8196(3)	34(1)

Supporting Information Table 3

Bond lengths [A] and angles [deg] for bis(dimethyl-(*Z*)-3-ferrocenyl-2-butenedioate)mercury.

Hg(1)-C(1)#1	2.075(3)
Hg(1)-C(1)	2.075(3)
Fe(1)-C(12)	2.034(4)
Fe(1)-C(16)	2.038(3)
Fe(1)-C(8)	2.039(3)
Fe(1)-C(9)	2.041(3)
Fe(1)-C(11)	2.041(3)
Fe(1)-C(15)	2.044(4)
Fe(1)-C(10)	2.045(4)
Fe(1)-C(14)	2.050(4)
Fe(1)-C(7)	2.050(3)
Fe(1)-C(13)	2.052(4)
O(1)-C(3)	1.197(4)
O(2)-C(3)	1.344(4)
O(2)-C(4)	1.451(4)
O(3)-C(5)	1.204(4)
O(4)-C(5)	1.328(4)
O(4)-C(6)	1.447(5)
C(1)-C(2)	1.348(4)
C(1)-C(3)	1.478(4)
C(2)-C(7)	1.464(4)
C(2)-C(5)	1.507(4)
C(4)-H(4A)	0.9800
C(4)-H(4B)	0.9800
C(4)-H(4C)	0.9800
C(6)-H(6A)	0.9800
C(6)-H(6B)	0.9800
C(6)-H(6C)	0.9800
C(7)-C(8)	1.439(4)
C(7)-C(11)	1.444(4)
C(8)-C(9)	1.415(5)
C(8)-H(8)	0.9500
C(9)-C(10)	1.419(5)
C(9)-H(9)	0.9500
C(10)-C(11)	1.423(5)
C(10)-H(10)	0.9500
C(11)-H(11)	0.9500
C(12)-C(16)	1.409(6)
C(12)-C(13)	1.423(6)
C(12)-H(12)	0.9500

C(13)-C(14)	1.422(6)
C(13)-H(13)	0.9500
C(14)-C(15)	1.422(6)
C(14)-H(14)	0.9500
C(15)-C(16)	1.424(6)
C(15)-H(15)	0.9500
C(16)-H(16)	0.9500

C(1)#1-Hg(1)-C(1)	179.999(1)
C(12)-Fe(1)-C(16)	40.48(16)
C(12)-Fe(1)-C(8)	163.38(16)
C(16)-Fe(1)-C(8)	155.62(15)
C(12)-Fe(1)-C(9)	154.16(17)
C(16)-Fe(1)-C(9)	119.15(16)
C(8)-Fe(1)-C(9)	40.58(14)
C(12)-Fe(1)-C(11)	106.35(16)
C(16)-Fe(1)-C(11)	121.88(15)
C(8)-Fe(1)-C(11)	69.00(13)
C(9)-Fe(1)-C(11)	68.60(14)
C(12)-Fe(1)-C(15)	68.45(17)
C(16)-Fe(1)-C(15)	40.84(16)
C(8)-Fe(1)-C(15)	121.71(16)
C(9)-Fe(1)-C(15)	106.55(16)
C(11)-Fe(1)-C(15)	158.62(15)
C(12)-Fe(1)-C(10)	119.00(17)
C(16)-Fe(1)-C(10)	104.51(15)
C(8)-Fe(1)-C(10)	68.59(14)
C(9)-Fe(1)-C(10)	40.65(14)
C(11)-Fe(1)-C(10)	40.76(13)
C(15)-Fe(1)-C(10)	122.12(16)
C(12)-Fe(1)-C(14)	68.64(18)
C(16)-Fe(1)-C(14)	68.59(16)
C(8)-Fe(1)-C(14)	109.56(15)
C(9)-Fe(1)-C(14)	125.04(16)
C(11)-Fe(1)-C(14)	158.70(15)
C(15)-Fe(1)-C(14)	40.67(16)
C(10)-Fe(1)-C(14)	160.07(16)
C(12)-Fe(1)-C(7)	124.95(15)
C(16)-Fe(1)-C(7)	160.22(14)
C(8)-Fe(1)-C(7)	41.19(12)
C(9)-Fe(1)-C(7)	68.96(13)
C(11)-Fe(1)-C(7)	41.35(12)
C(15)-Fe(1)-C(7)	158.28(15)
C(10)-Fe(1)-C(7)	69.15(13)
C(14)-Fe(1)-C(7)	123.43(14)
C(12)-Fe(1)-C(13)	40.75(17)

C(16)-Fe(1)-C(13)	68.21(16)
C(8)-Fe(1)-C(13)	127.23(16)
C(9)-Fe(1)-C(13)	162.98(17)
C(11)-Fe(1)-C(13)	122.28(16)
C(15)-Fe(1)-C(13)	68.18(17)
C(10)-Fe(1)-C(13)	155.99(17)
C(14)-Fe(1)-C(13)	40.58(17)
C(7)-Fe(1)-C(13)	109.57(14)
C(3)-O(2)-C(4)	116.0(3)
C(5)-O(4)-C(6)	114.7(3)
C(2)-C(1)-C(3)	119.5(3)
C(2)-C(1)-Hg(1)	124.1(2)
C(3)-C(1)-Hg(1)	116.0(2)
C(1)-C(2)-C(7)	125.1(3)
C(1)-C(2)-C(5)	120.5(3)
C(7)-C(2)-C(5)	114.2(3)
O(1)-C(3)-O(2)	122.1(3)
O(1)-C(3)-C(1)	127.0(3)
O(2)-C(3)-C(1)	110.9(3)
O(2)-C(4)-H(4A)	109.5
O(2)-C(4)-H(4B)	109.5
H(4A)-C(4)-H(4B)	109.5
O(2)-C(4)-H(4C)	109.5
H(4A)-C(4)-H(4C)	109.5
H(4B)-C(4)-H(4C)	109.5
O(3)-C(5)-O(4)	123.9(3)
O(3)-C(5)-C(2)	123.2(3)
O(4)-C(5)-C(2)	112.9(3)
O(4)-C(6)-H(6A)	109.5
O(4)-C(6)-H(6B)	109.5
H(6A)-C(6)-H(6B)	109.5
O(4)-C(6)-H(6C)	109.5
H(6A)-C(6)-H(6C)	109.5
H(6B)-C(6)-H(6C)	109.5
C(8)-C(7)-C(11)	106.6(3)
C(8)-C(7)-C(2)	126.1(3)
C(11)-C(7)-C(2)	127.3(3)
C(8)-C(7)-Fe(1)	69.02(17)
C(11)-C(7)-Fe(1)	69.00(17)
C(2)-C(7)-Fe(1)	126.5(2)
C(9)-C(8)-C(7)	108.5(3)
C(9)-C(8)-Fe(1)	69.75(19)
C(7)-C(8)-Fe(1)	69.79(17)
C(9)-C(8)-H(8)	125.8
C(7)-C(8)-H(8)	125.8
Fe(1)-C(8)-H(8)	126.3

C(8)-C(9)-C(10)	108.6(3)
C(8)-C(9)-Fe(1)	69.67(19)
C(10)-C(9)-Fe(1)	69.83(19)
C(8)-C(9)-H(9)	125.7
C(10)-C(9)-H(9)	125.7
Fe(1)-C(9)-H(9)	126.4
C(9)-C(10)-C(11)	108.1(3)
C(9)-C(10)-Fe(1)	69.52(19)
C(11)-C(10)-Fe(1)	69.48(19)
C(9)-C(10)-H(10)	126.0
C(11)-C(10)-H(10)	126.0
Fe(1)-C(10)-H(10)	126.6
C(10)-C(11)-C(7)	108.3(3)
C(10)-C(11)-Fe(1)	69.75(19)
C(7)-C(11)-Fe(1)	69.65(17)
C(10)-C(11)-H(11)	125.9
C(7)-C(11)-H(11)	125.9
Fe(1)-C(11)-H(11)	126.3
C(16)-C(12)-C(13)	108.2(4)
C(16)-C(12)-Fe(1)	69.9(2)
C(13)-C(12)-Fe(1)	70.3(2)
C(16)-C(12)-H(12)	125.9
C(13)-C(12)-H(12)	125.9
Fe(1)-C(12)-H(12)	125.4
C(14)-C(13)-C(12)	108.0(4)
C(14)-C(13)-Fe(1)	69.6(2)
C(12)-C(13)-Fe(1)	68.9(2)
C(14)-C(13)-H(13)	126.0
C(12)-C(13)-H(13)	126.0
Fe(1)-C(13)-H(13)	127.0
C(13)-C(14)-C(15)	107.6(4)
C(13)-C(14)-Fe(1)	69.8(2)
C(15)-C(14)-Fe(1)	69.4(2)
C(13)-C(14)-H(14)	126.2
C(15)-C(14)-H(14)	126.2
Fe(1)-C(14)-H(14)	126.1
C(14)-C(15)-C(16)	108.0(4)
C(14)-C(15)-Fe(1)	69.9(2)
C(16)-C(15)-Fe(1)	69.4(2)
C(14)-C(15)-H(15)	126.0
C(16)-C(15)-H(15)	126.0
Fe(1)-C(15)-H(15)	126.3
C(12)-C(16)-C(15)	108.1(4)
C(12)-C(16)-Fe(1)	69.6(2)
C(15)-C(16)-Fe(1)	69.8(2)
C(12)-C(16)-H(16)	125.9

C(15)-C(16)-H(16)	125.9
Fe(1)-C(16)-H(16)	126.3

Symmetry transformations used to generate equivalent atoms:
#1 -x+2,-y+1,-z+1

Supporting Information Table 4

Anisotropic displacement parameters ($A^2 \times 10^3$) for bis(dimethyl-(*Z*)-3-ferrocenyl-2-butenedioate)mercury. The anisotropic displacement factor exponent takes the form:

$-2\ pi^2\ [\ h^2\ a^{*2}\ U11 + ... + 2\ h\ k\ a^*\ b^*\ U12\ ]$

	U11	U22	U33	U23	U13	U12
Hg(1)	16(1)	11(1)	17(1)	-0(1)	3(1)	1(1)
Fe(1)	25(1)	16(1)	17(1)	-4(1)	9(1)	-2(1)
O(1)	28(2)	31(2)	65(2)	13(1)	-14(1)	1(1)
O(2)	22(1)	17(1)	36(1)	-1(1)	2(1)	-4(1)
O(3)	39(2)	30(2)	42(2)	14(1)	6(1)	7(1)
O(4)	36(2)	53(2)	37(1)	7(1)	17(1)	22(1)
C(1)	17(2)	17(2)	16(1)	2(1)	3(1)	2(1)
C(2)	24(2)	16(2)	12(1)	3(1)	7(1)	5(1)
C(3)	23(2)	19(2)	22(2)	-2(1)	5(1)	3(1)
C(4)	24(2)	29(2)	46(2)	-10(2)	3(2)	-7(2)
C(5)	28(2)	16(2)	22(2)	-3(1)	5(1)	4(1)
C(6)	36(2)	65(3)	58(3)	-3(2)	11(2)	31(2)
C(7)	22(2)	12(2)	16(1)	-1(1)	10(1)	0(1)
C(8)	35(2)	14(2)	22(2)	-1(1)	15(1)	-1(1)
C(9)	32(2)	21(2)	30(2)	-4(1)	19(2)	-6(1)
C(10)	24(2)	26(2)	25(2)	-9(1)	9(1)	0(2)
C(11)	24(2)	16(2)	24(2)	-3(1)	8(1)	3(1)
C(12)	70(3)	38(2)	26(2)	-8(2)	30(2)	-10(2)
C(13)	37(2)	61(3)	33(2)	-20(2)	24(2)	-13(2)
C(14)	35(2)	42(2)	30(2)	-11(2)	12(2)	11(2)
C(15)	39(2)	30(2)	32(2)	-16(2)	14(2)	-0(2)
C(16)	43(2)	40(2)	17(2)	-10(2)	9(2)	2(2)

Supporting Information Table 5

Hydrogen coordinates (x 10^4) and isotropic displacement parameters (A^2 x 10^3) for bis(dimethyl-(*Z*)-3-ferrocenyl-2-butenedioate)mercury.

	x	y	z	U(eq)
H(4A)	4039	4527	3907	53
H(4B)	4916	3441	3876	53
H(4C)	4615	4267	2957	53
H(6A)	4826	9186	4287	82
H(6B)	3851	8454	4803	82
H(6C)	3916	8169	3689	82
H(8)	9753	9134	4681	27
H(9)	12560	9471	5915	31
H(10)	13516	7865	7034	30
H(11)	11289	6513	6501	25
H(12)	10083	7480	8269	49
H(13)	7578	8189	6899	49
H(14)	8188	10025	6429	42
H(15)	11048	10461	7555	40
H(16)	12205	8886	8692	41

Supporting Information Table 6

Torsion angles [deg] for bis(dimethyl-(*Z*)-3-ferrocenyl-2-butenedioate)mercury.

C(1)#1-Hg(1)-C(1)-C(2)	54(8)
C(1)#1-Hg(1)-C(1)-C(3)	-134(8)
C(3)-C(1)-C(2)-C(7)	-177.7(3)
Hg(1)-C(1)-C(2)-C(7)	-5.8(4)
C(3)-C(1)-C(2)-C(5)	-3.1(4)
Hg(1)-C(1)-C(2)-C(5)	168.8(2)
C(4)-O(2)-C(3)-O(1)	-1.1(5)
C(4)-O(2)-C(3)-C(1)	-179.9(3)
C(2)-C(1)-C(3)-O(1)	22.8(5)
Hg(1)-C(1)-C(3)-O(1)	-149.7(3)
C(2)-C(1)-C(3)-O(2)	-158.5(3)
Hg(1)-C(1)-C(3)-O(2)	29.0(3)
C(6)-O(4)-C(5)-O(3)	9.7(5)
C(6)-O(4)-C(5)-C(2)	-172.8(3)
C(1)-C(2)-C(5)-O(3)	-108.9(4)
C(7)-C(2)-C(5)-O(3)	66.3(4)
C(1)-C(2)-C(5)-O(4)	73.6(4)
C(7)-C(2)-C(5)-O(4)	-111.2(3)
C(1)-C(2)-C(7)-C(8)	148.6(3)
C(5)-C(2)-C(7)-C(8)	-26.3(4)
C(1)-C(2)-C(7)-C(11)	-31.9(5)
C(5)-C(2)-C(7)-C(11)	153.2(3)
C(1)-C(2)-C(7)-Fe(1)	-122.1(3)
C(5)-C(2)-C(7)-Fe(1)	63.0(3)
C(12)-Fe(1)-C(7)-C(8)	167.6(2)
C(16)-Fe(1)-C(7)-C(8)	-155.5(4)
C(9)-Fe(1)-C(7)-C(8)	-37.2(2)
C(11)-Fe(1)-C(7)-C(8)	-118.3(3)
C(15)-Fe(1)-C(7)-C(8)	44.7(5)
C(10)-Fe(1)-C(7)-C(8)	-80.9(2)
C(14)-Fe(1)-C(7)-C(8)	81.6(2)
C(13)-Fe(1)-C(7)-C(8)	124.7(2)
C(12)-Fe(1)-C(7)-C(11)	-74.1(3)
C(16)-Fe(1)-C(7)-C(11)	-37.1(5)
C(8)-Fe(1)-C(7)-C(11)	118.3(3)
C(9)-Fe(1)-C(7)-C(11)	81.1(2)
C(15)-Fe(1)-C(7)-C(11)	163.0(4)
C(10)-Fe(1)-C(7)-C(11)	37.43(19)
C(14)-Fe(1)-C(7)-C(11)	-160.0(2)
C(13)-Fe(1)-C(7)-C(11)	-117.0(2)
C(12)-Fe(1)-C(7)-C(2)	47.5(3)

C(16)-Fe(1)-C(7)-C(2)	84.5(5)
C(8)-Fe(1)-C(7)-C(2)	-120.1(3)
C(9)-Fe(1)-C(7)-C(2)	-157.3(3)
C(11)-Fe(1)-C(7)-C(2)	121.6(3)
C(15)-Fe(1)-C(7)-C(2)	-75.4(5)
C(10)-Fe(1)-C(7)-C(2)	159.0(3)
C(14)-Fe(1)-C(7)-C(2)	-38.4(3)
C(13)-Fe(1)-C(7)-C(2)	4.6(3)
C(11)-C(7)-C(8)-C(9)	0.2(3)
C(2)-C(7)-C(8)-C(9)	179.8(3)
Fe(1)-C(7)-C(8)-C(9)	59.2(2)
C(11)-C(7)-C(8)-Fe(1)	-59.0(2)
C(2)-C(7)-C(8)-Fe(1)	120.6(3)
C(12)-Fe(1)-C(8)-C(9)	-157.8(5)
C(16)-Fe(1)-C(8)-C(9)	40.4(4)
C(11)-Fe(1)-C(8)-C(9)	-81.2(2)
C(15)-Fe(1)-C(8)-C(9)	78.1(3)
C(10)-Fe(1)-C(8)-C(9)	-37.3(2)
C(14)-Fe(1)-C(8)-C(9)	121.5(2)
C(7)-Fe(1)-C(8)-C(9)	-119.7(3)
C(13)-Fe(1)-C(8)-C(9)	163.5(2)
C(12)-Fe(1)-C(8)-C(7)	-38.1(6)
C(16)-Fe(1)-C(8)-C(7)	160.1(3)
C(9)-Fe(1)-C(8)-C(7)	119.7(3)
C(11)-Fe(1)-C(8)-C(7)	38.52(18)
C(15)-Fe(1)-C(8)-C(7)	-162.2(2)
C(10)-Fe(1)-C(8)-C(7)	82.4(2)
C(14)-Fe(1)-C(8)-C(7)	-118.8(2)
C(13)-Fe(1)-C(8)-C(7)	-76.7(3)
C(7)-C(8)-C(9)-C(10)	-0.1(4)
Fe(1)-C(8)-C(9)-C(10)	59.2(2)
C(7)-C(8)-C(9)-Fe(1)	-59.2(2)
C(12)-Fe(1)-C(9)-C(8)	165.7(3)
C(16)-Fe(1)-C(9)-C(8)	-162.2(2)
C(11)-Fe(1)-C(9)-C(8)	82.3(2)
C(15)-Fe(1)-C(9)-C(8)	-119.7(2)
C(10)-Fe(1)-C(9)-C(8)	119.9(3)
C(14)-Fe(1)-C(9)-C(8)	-79.0(2)
C(7)-Fe(1)-C(9)-C(8)	37.79(19)
C(13)-Fe(1)-C(9)-C(8)	-50.5(6)
C(12)-Fe(1)-C(9)-C(10)	45.8(4)
C(16)-Fe(1)-C(9)-C(10)	77.9(2)
C(8)-Fe(1)-C(9)-C(10)	-119.9(3)
C(11)-Fe(1)-C(9)-C(10)	-37.60(19)
C(15)-Fe(1)-C(9)-C(10)	120.4(2)
C(14)-Fe(1)-C(9)-C(10)	161.1(2)

C(7)-Fe(1)-C(9)-C(10)	-82.1(2)
C(13)-Fe(1)-C(9)-C(10)	-170.4(5)
C(8)-C(9)-C(10)-C(11)	-0.1(4)
Fe(1)-C(9)-C(10)-C(11)	59.0(2)
C(8)-C(9)-C(10)-Fe(1)	-59.1(2)
C(12)-Fe(1)-C(10)-C(9)	-159.1(2)
C(16)-Fe(1)-C(10)-C(9)	-118.1(2)
C(8)-Fe(1)-C(10)-C(9)	37.3(2)
C(11)-Fe(1)-C(10)-C(9)	119.5(3)
C(15)-Fe(1)-C(10)-C(9)	-77.6(3)
C(14)-Fe(1)-C(10)-C(9)	-51.2(5)
C(7)-Fe(1)-C(10)-C(9)	81.6(2)
C(13)-Fe(1)-C(10)-C(9)	173.1(3)
C(12)-Fe(1)-C(10)-C(11)	81.4(2)
C(16)-Fe(1)-C(10)-C(11)	122.4(2)
C(8)-Fe(1)-C(10)-C(11)	-82.3(2)
C(9)-Fe(1)-C(10)-C(11)	-119.5(3)
C(15)-Fe(1)-C(10)-C(11)	162.9(2)
C(14)-Fe(1)-C(10)-C(11)	-170.7(4)
C(7)-Fe(1)-C(10)-C(11)	-37.95(19)
C(13)-Fe(1)-C(10)-C(11)	53.5(4)
C(9)-C(10)-C(11)-C(7)	0.2(4)
Fe(1)-C(10)-C(11)-C(7)	59.2(2)
C(9)-C(10)-C(11)-Fe(1)	-59.0(2)
C(8)-C(7)-C(11)-C(10)	-0.2(3)
C(2)-C(7)-C(11)-C(10)	-179.8(3)
Fe(1)-C(7)-C(11)-C(10)	-59.3(2)
C(8)-C(7)-C(11)-Fe(1)	59.0(2)
C(2)-C(7)-C(11)-Fe(1)	-120.6(3)
C(12)-Fe(1)-C(11)-C(10)	-115.7(2)
C(16)-Fe(1)-C(11)-C(10)	-74.4(2)
C(8)-Fe(1)-C(11)-C(10)	81.2(2)
C(9)-Fe(1)-C(11)-C(10)	37.5(2)
C(15)-Fe(1)-C(11)-C(10)	-43.2(5)
C(14)-Fe(1)-C(11)-C(10)	171.3(4)
C(7)-Fe(1)-C(11)-C(10)	119.5(3)
C(13)-Fe(1)-C(11)-C(10)	-157.2(2)
C(12)-Fe(1)-C(11)-C(7)	124.8(2)
C(16)-Fe(1)-C(11)-C(7)	166.1(2)
C(8)-Fe(1)-C(11)-C(7)	-38.38(18)
C(9)-Fe(1)-C(11)-C(7)	-82.0(2)
C(15)-Fe(1)-C(11)-C(7)	-162.7(4)
C(10)-Fe(1)-C(11)-C(7)	-119.5(3)
C(14)-Fe(1)-C(11)-C(7)	51.8(5)
C(13)-Fe(1)-C(11)-C(7)	83.2(2)
C(8)-Fe(1)-C(12)-C(16)	-168.6(5)

C(9)-Fe(1)-C(12)-C(16)	45.7(5)
C(11)-Fe(1)-C(12)-C(16)	120.3(2)
C(15)-Fe(1)-C(12)-C(16)	-37.8(2)
C(10)-Fe(1)-C(12)-C(16)	78.0(3)
C(14)-Fe(1)-C(12)-C(16)	-81.6(3)
C(7)-Fe(1)-C(12)-C(16)	161.7(2)
C(13)-Fe(1)-C(12)-C(16)	-118.9(4)
C(16)-Fe(1)-C(12)-C(13)	118.9(4)
C(8)-Fe(1)-C(12)-C(13)	-49.6(7)
C(9)-Fe(1)-C(12)-C(13)	164.7(3)
C(11)-Fe(1)-C(12)-C(13)	-120.8(2)
C(15)-Fe(1)-C(12)-C(13)	81.1(3)
C(10)-Fe(1)-C(12)-C(13)	-163.1(2)
C(14)-Fe(1)-C(12)-C(13)	37.3(2)
C(7)-Fe(1)-C(12)-C(13)	-79.3(3)
C(16)-C(12)-C(13)-C(14)	1.1(4)
Fe(1)-C(12)-C(13)-C(14)	-58.8(2)
C(16)-C(12)-C(13)-Fe(1)	59.9(3)
C(12)-Fe(1)-C(13)-C(14)	119.8(3)
C(16)-Fe(1)-C(13)-C(14)	82.1(2)
C(8)-Fe(1)-C(13)-C(14)	-76.1(3)
C(9)-Fe(1)-C(13)-C(14)	-37.0(6)
C(11)-Fe(1)-C(13)-C(14)	-163.1(2)
C(15)-Fe(1)-C(13)-C(14)	38.0(2)
C(10)-Fe(1)-C(13)-C(14)	158.5(3)
C(7)-Fe(1)-C(13)-C(14)	-118.9(2)
C(16)-Fe(1)-C(13)-C(12)	-37.7(2)
C(8)-Fe(1)-C(13)-C(12)	164.1(2)
C(9)-Fe(1)-C(13)-C(12)	-156.8(5)
C(11)-Fe(1)-C(13)-C(12)	77.1(3)
C(15)-Fe(1)-C(13)-C(12)	-81.9(3)
C(10)-Fe(1)-C(13)-C(12)	38.7(5)
C(14)-Fe(1)-C(13)-C(12)	-119.8(3)
C(7)-Fe(1)-C(13)-C(12)	121.2(2)
C(12)-C(13)-C(14)-C(15)	-1.0(4)
Fe(1)-C(13)-C(14)-C(15)	-59.4(3)
C(12)-C(13)-C(14)-Fe(1)	58.4(3)
C(12)-Fe(1)-C(14)-C(13)	-37.5(2)
C(16)-Fe(1)-C(14)-C(13)	-81.1(2)
C(8)-Fe(1)-C(14)-C(13)	124.9(2)
C(9)-Fe(1)-C(14)-C(13)	167.6(2)
C(11)-Fe(1)-C(14)-C(13)	42.7(5)
C(15)-Fe(1)-C(14)-C(13)	-118.8(3)
C(10)-Fe(1)-C(14)-C(13)	-154.1(4)
C(7)-Fe(1)-C(14)-C(13)	81.2(3)
C(12)-Fe(1)-C(14)-C(15)	81.4(3)

C(16)-Fe(1)-C(14)-C(15)	37.8(2)
C(8)-Fe(1)-C(14)-C(15)	-116.3(3)
C(9)-Fe(1)-C(14)-C(15)	-73.6(3)
C(11)-Fe(1)-C(14)-C(15)	161.5(4)
C(10)-Fe(1)-C(14)-C(15)	-35.3(6)
C(7)-Fe(1)-C(14)-C(15)	-160.0(2)
C(13)-Fe(1)-C(14)-C(15)	118.8(3)
C(13)-C(14)-C(15)-C(16)	0.5(4)
Fe(1)-C(14)-C(15)-C(16)	-59.1(3)
C(13)-C(14)-C(15)-Fe(1)	59.6(3)
C(12)-Fe(1)-C(15)-C(14)	-81.9(3)
C(16)-Fe(1)-C(15)-C(14)	-119.3(4)
C(8)-Fe(1)-C(15)-C(14)	83.4(3)
C(9)-Fe(1)-C(15)-C(14)	125.0(3)
C(11)-Fe(1)-C(15)-C(14)	-161.6(4)
C(10)-Fe(1)-C(15)-C(14)	166.6(2)
C(7)-Fe(1)-C(15)-C(14)	50.4(5)
C(13)-Fe(1)-C(15)-C(14)	-37.9(3)
C(12)-Fe(1)-C(15)-C(16)	37.5(3)
C(8)-Fe(1)-C(15)-C(16)	-157.3(2)
C(9)-Fe(1)-C(15)-C(16)	-115.7(3)
C(11)-Fe(1)-C(15)-C(16)	-42.3(5)
C(10)-Fe(1)-C(15)-C(16)	-74.1(3)
C(14)-Fe(1)-C(15)-C(16)	119.3(4)
C(7)-Fe(1)-C(15)-C(16)	169.8(3)
C(13)-Fe(1)-C(15)-C(16)	81.5(3)
C(13)-C(12)-C(16)-C(15)	-0.8(4)
Fe(1)-C(12)-C(16)-C(15)	59.4(3)
C(13)-C(12)-C(16)-Fe(1)	-60.2(3)
C(14)-C(15)-C(16)-C(12)	0.2(4)
Fe(1)-C(15)-C(16)-C(12)	-59.2(3)
C(14)-C(15)-C(16)-Fe(1)	59.4(3)
C(8)-Fe(1)-C(16)-C(12)	172.1(3)
C(9)-Fe(1)-C(16)-C(12)	-159.1(2)
C(11)-Fe(1)-C(16)-C(12)	-77.4(3)
C(15)-Fe(1)-C(16)-C(12)	119.4(4)
C(10)-Fe(1)-C(16)-C(12)	-117.9(3)
C(14)-Fe(1)-C(16)-C(12)	81.8(3)
C(7)-Fe(1)-C(16)-C(12)	-49.4(5)
C(13)-Fe(1)-C(16)-C(12)	38.0(3)
C(12)-Fe(1)-C(16)-C(15)	-119.4(4)
C(8)-Fe(1)-C(16)-C(15)	52.7(5)
C(9)-Fe(1)-C(16)-C(15)	81.6(3)
C(11)-Fe(1)-C(16)-C(15)	163.2(2)
C(10)-Fe(1)-C(16)-C(15)	122.7(2)
C(14)-Fe(1)-C(16)-C(15)	-37.6(3)

C(7)-Fe(1)-C(16)-C(15)	-168.8(4)
C(13)-Fe(1)-C(16)-C(15)	-81.4(3)

Symmetry transformations used to generate equivalent atoms:
#1 -x+2,-y+1,-z+1

Supporting Information Table 7

Crystal data and structure refinement for biferrocene.

Identification code	p21c
Empirical formula	C20 H18 Fe2
Formula weight	370.04
Temperature	123(2) K
Wavelength	0.71075 A
Crystal system, space group	Monoclinic, $P2_1/c$
Unit cell dimensions	a = 9.5320(5) A alpha = 90 deg. b = 7.7830(3) A beta = 126.384(5) deg. c = 12.4190(11) A gamma = 90 deg.
Volume	741.73(8) A^3
Z, Calculated density	2, 1.657 Mg/m^3
Absorption coefficient	1.947 mm^{-1}
F(000)	380
Crystal size	? x ? x ? mm
Theta range for data collection	3.29 to 27.45 deg.
Limiting indices	-11<=h<=12, -10<=k<=10, -16<=l<=14
Reflections collected / unique	6255 / 1683 [R(int) = 0.0304]
Completeness to theta = 27.45	99.6 %
Refinement method	Full-matrix least-squares on F^2
Data / restraints / parameters	1683 / 0 / 100
Goodness-of-fit on F^2	1.083

Final R indices [I>2sigma(I)]	$R_1 = 0.0241$, $wR_2 = 0.0510$
R indices (all data)	$R_1 = 0.0350$, $wR_2 = 0.0553$
Largest diff. peak and hole	0.490 and -0.294 $e.A^{-3}$

Supporting Information Table 8

Atomic coordinates (x 10^4) and equivalent isotropic displacement parameters (A^2 x 10^3) for biferrocene.

U(eq) is defined as one third of the trace of the orthogonalized Uij tensor.

	x	y	z	U(eq)
C(1)	6802(2)	-644(2)	4778(2)	19(1)
C(2)	5330(2)	162(2)	4609(2)	16(1)
C(3)	4646(2)	1376(2)	3541(2)	18(1)
C(4)	5673(3)	1321(3)	3058(2)	20(1)
C(5)	7010(3)	71(2)	3822(2)	20(1)
C(6)	9639(2)	2333(2)	6776(2)	20(1)
C(7)	9380(3)	3378(3)	5730(2)	24(1)
C(8)	7929(3)	4464(2)	5275(2)	25(1)
C(9)	7296(3)	4093(2)	6036(2)	23(1)
C(10)	8364(3)	2775(3)	6967(2)	21(1)
Fe(1)	7196(1)	1944(1)	5049(1)	13(1)

Supporting Information Table 9

Bond lengths [A] and angles [deg] for biferrocene.

C(1)-C(5)	1.427(3)
C(1)-C(2)	1.434(3)
C(1)-Fe(1)	2.0400(18)
C(1)-H(1)	0.9500
C(2)-C(3)	1.432(3)
C(2)-C(2)#1	1.459(4)
C(2)-Fe(1)	2.0573(18)
C(3)-C(4)	1.418(3)
C(3)-Fe(1)	2.0518(18)
C(3)-H(3)	0.9500
C(4)-C(5)	1.427(3)
C(4)-Fe(1)	2.0487(18)
C(4)-H(4)	0.9500
C(5)-Fe(1)	2.0393(19)
C(5)-H(5)	0.9500
C(6)-C(10)	1.412(3)
C(6)-C(7)	1.424(3)
C(6)-Fe(1)	2.0465(18)
C(6)-H(6)	0.9500
C(7)-C(8)	1.421(3)
C(7)-Fe(1)	2.0505(19)
C(7)-H(7)	0.9500
C(8)-C(9)	1.419(3)
C(8)-Fe(1)	2.0447(19)
C(8)-H(8)	0.9500
C(9)-C(10)	1.425(3)
C(9)-Fe(1)	2.0415(19)
C(9)-H(9)	0.9500
C(10)-Fe(1)	2.0460(18)
C(10)-H(10)	0.9500
C(5)-C(1)-C(2)	108.32(17)
C(5)-C(1)-Fe(1)	69.49(10)
C(2)-C(1)-Fe(1)	70.16(10)
C(5)-C(1)-H(1)	125.8
C(2)-C(1)-H(1)	125.8
Fe(1)-C(1)-H(1)	126.1
C(3)-C(2)-C(1)	106.99(17)
C(3)-C(2)-C(2)#1	126.3(2)
C(1)-C(2)-C(2)#1	126.7(2)
C(3)-C(2)-Fe(1)	69.39(10)

C(1)-C(2)-Fe(1)	68.86(10)
C(2)#1-C(2)-Fe(1)	125.84(17)
C(4)-C(3)-C(2)	108.79(17)
C(4)-C(3)-Fe(1)	69.65(11)
C(2)-C(3)-Fe(1)	69.81(10)
C(4)-C(3)-H(3)	125.6
C(2)-C(3)-H(3)	125.6
Fe(1)-C(3)-H(3)	126.5
C(3)-C(4)-C(5)	107.95(17)
C(3)-C(4)-Fe(1)	69.88(10)
C(5)-C(4)-Fe(1)	69.22(10)
C(3)-C(4)-H(4)	126.0
C(5)-C(4)-H(4)	126.0
Fe(1)-C(4)-H(4)	126.5
C(4)-C(5)-C(1)	107.95(18)
C(4)-C(5)-Fe(1)	69.92(11)
C(1)-C(5)-Fe(1)	69.54(10)
C(4)-C(5)-H(5)	126.0
C(1)-C(5)-H(5)	126.0
Fe(1)-C(5)-H(5)	126.1
C(10)-C(6)-C(7)	108.28(17)
C(10)-C(6)-Fe(1)	69.79(11)
C(7)-C(6)-Fe(1)	69.82(11)
C(10)-C(6)-H(6)	125.9
C(7)-C(6)-H(6)	125.9
Fe(1)-C(6)-H(6)	126.1
C(8)-C(7)-C(6)	107.70(18)
C(8)-C(7)-Fe(1)	69.48(11)
C(6)-C(7)-Fe(1)	69.51(11)
C(8)-C(7)-H(7)	126.1
C(6)-C(7)-H(7)	126.1
Fe(1)-C(7)-H(7)	126.4
C(9)-C(8)-C(7)	108.16(17)
C(9)-C(8)-Fe(1)	69.55(11)
C(7)-C(8)-Fe(1)	69.92(11)
C(9)-C(8)-H(8)	125.9
C(7)-C(8)-H(8)	125.9
Fe(1)-C(8)-H(8)	126.2
C(8)-C(9)-C(10)	107.82(18)
C(8)-C(9)-Fe(1)	69.79(11)
C(10)-C(9)-Fe(1)	69.77(11)
C(8)-C(9)-H(9)	126.1
C(10)-C(9)-H(9)	126.1
Fe(1)-C(9)-H(9)	125.9
C(6)-C(10)-C(9)	108.04(18)
C(6)-C(10)-Fe(1)	69.83(11)

C(9)-C(10)-Fe(1)	69.43(10)
C(6)-C(10)-H(10)	126.0
C(9)-C(10)-H(10)	126.0
Fe(1)-C(10)-H(10)	126.3
C(5)-Fe(1)-C(1)	40.96(8)
C(5)-Fe(1)-C(9)	170.54(8)
C(1)-Fe(1)-C(9)	147.83(8)
C(5)-Fe(1)-C(8)	131.25(9)
C(1)-Fe(1)-C(8)	169.79(9)
C(9)-Fe(1)-C(8)	40.65(8)
C(5)-Fe(1)-C(10)	147.35(8)
C(1)-Fe(1)-C(10)	115.09(8)
C(9)-Fe(1)-C(10)	40.81(8)
C(8)-Fe(1)-C(10)	68.37(8)
C(5)-Fe(1)-C(6)	115.41(8)
C(1)-Fe(1)-C(6)	107.63(8)
C(9)-Fe(1)-C(6)	68.34(8)
C(8)-Fe(1)-C(6)	68.30(8)
C(10)-Fe(1)-C(6)	40.38(8)
C(5)-Fe(1)-C(4)	40.86(8)
C(1)-Fe(1)-C(4)	68.75(8)
C(9)-Fe(1)-C(4)	131.73(8)
C(8)-Fe(1)-C(4)	109.44(8)
C(10)-Fe(1)-C(4)	170.61(8)
C(6)-Fe(1)-C(4)	148.30(8)
C(5)-Fe(1)-C(7)	108.31(9)
C(1)-Fe(1)-C(7)	130.38(8)
C(9)-Fe(1)-C(7)	68.40(9)
C(8)-Fe(1)-C(7)	40.60(8)
C(10)-Fe(1)-C(7)	68.26(8)
C(6)-Fe(1)-C(7)	40.66(8)
C(4)-Fe(1)-C(7)	116.49(8)
C(5)-Fe(1)-C(3)	68.46(8)
C(1)-Fe(1)-C(3)	68.54(8)
C(9)-Fe(1)-C(3)	109.45(8)
C(8)-Fe(1)-C(3)	117.08(8)
C(10)-Fe(1)-C(3)	131.53(8)
C(6)-Fe(1)-C(3)	169.70(8)
C(4)-Fe(1)-C(3)	40.48(8)
C(7)-Fe(1)-C(3)	148.94(8)
C(5)-Fe(1)-C(2)	68.98(8)
C(1)-Fe(1)-C(2)	40.98(8)
C(9)-Fe(1)-C(2)	115.92(8)
C(8)-Fe(1)-C(2)	148.69(9)
C(10)-Fe(1)-C(2)	108.07(8)
C(6)-Fe(1)-C(2)	130.20(8)

C(4)-Fe(1)-C(2)	68.74(7)
C(7)-Fe(1)-C(2)	169.29(8)
C(3)-Fe(1)-C(2)	40.80(7)

Symmetry transformations used to generate equivalent atoms:
#1 -x+1,-y,-z+1

Supporting Information Table 10

Anisotropic displacement parameters ($A^2 \times 10^3$) for biferrocene. The anisotropic displacement factor exponent takes the form:

$-2\ pi^2\ [\ h^2\ a^{*2}\ U11 + ... + 2\ h\ k\ a^*\ b^*\ U12\ ]$

	U11	U22	U33	U23	U13	U12
C(1)	21(1)	13(1)	21(1)	-3(1)	12(1)	-2(1)
C(2)	16(1)	14(1)	15(1)	-2(1)	8(1)	-5(1)
C(3)	15(1)	19(1)	14(1)	-1(1)	6(1)	-3(1)
C(4)	22(1)	23(1)	14(1)	-1(1)	10(1)	-5(1)
C(5)	24(1)	20(1)	21(1)	-6(1)	16(1)	-3(1)
C(6)	15(1)	21(1)	17(1)	-1(1)	5(1)	-1(1)
C(7)	18(1)	29(1)	24(1)	-1(1)	13(1)	-8(1)
C(8)	26(1)	16(1)	22(1)	1(1)	8(1)	-6(1)
C(9)	19(1)	19(1)	23(1)	-6(1)	9(1)	0(1)
C(10)	22(1)	23(1)	14(1)	-4(1)	9(1)	-4(1)
Fe(1)	13(1)	13(1)	13(1)	0(1)	7(1)	-1(1)

Supporting Information Table 11

Hydrogen coordinates (x 10^4) and isotropic displacement parameters (A^2 x 10^3) for biferrocene.

	x	y	z	U(eq)
H(1)	7516	-1506	5417	22
H(3)	3667	2099	3209	22
H(4)	5500	1996	2352	24
H(5)	7885	-231	3714	24
H(6)	10518	1485	7261	24
H(7)	10055	3353	5397	28
H(8)	7463	5295	4582	30
H(9)	6332	4628	5940	27
H(10)	8240	2279	7606	25

Supporting Information Table 12

Torsion angles [deg] for biferrocene.

C(5)-C(1)-C(2)-C(3)	-0.1(2)
Fe(1)-C(1)-C(2)-C(3)	59.16(12)
C(5)-C(1)-C(2)-C(2)#1	-178.9(2)
Fe(1)-C(1)-C(2)-C(2)#1	-119.7(2)
C(5)-C(1)-C(2)-Fe(1)	-59.22(13)
C(1)-C(2)-C(3)-C(4)	0.1(2)
C(2)#1-C(2)-C(3)-C(4)	178.9(2)
Fe(1)-C(2)-C(3)-C(4)	58.89(13)
C(1)-C(2)-C(3)-Fe(1)	-58.82(12)
C(2)#1-C(2)-C(3)-Fe(1)	120.0(2)
C(2)-C(3)-C(4)-C(5)	-0.1(2)
Fe(1)-C(3)-C(4)-C(5)	58.94(13)
C(2)-C(3)-C(4)-Fe(1)	-58.99(12)
C(3)-C(4)-C(5)-C(1)	0.0(2)
Fe(1)-C(4)-C(5)-C(1)	59.37(13)
C(3)-C(4)-C(5)-Fe(1)	-59.35(13)
C(2)-C(1)-C(5)-C(4)	0.0(2)
Fe(1)-C(1)-C(5)-C(4)	-59.61(13)
C(2)-C(1)-C(5)-Fe(1)	59.63(12)
C(10)-C(6)-C(7)-C(8)	-0.2(2)
Fe(1)-C(6)-C(7)-C(8)	59.20(13)
C(10)-C(6)-C(7)-Fe(1)	-59.41(13)
C(6)-C(7)-C(8)-C(9)	0.0(2)
Fe(1)-C(7)-C(8)-C(9)	59.25(13)
C(6)-C(7)-C(8)-Fe(1)	-59.22(13)
C(7)-C(8)-C(9)-C(10)	0.2(2)
Fe(1)-C(8)-C(9)-C(10)	59.64(13)
C(7)-C(8)-C(9)-Fe(1)	-59.48(13)
C(7)-C(6)-C(10)-C(9)	0.3(2)
Fe(1)-C(6)-C(10)-C(9)	-59.11(13)
C(7)-C(6)-C(10)-Fe(1)	59.42(13)
C(8)-C(9)-C(10)-C(6)	-0.3(2)
Fe(1)-C(9)-C(10)-C(6)	59.36(13)
C(8)-C(9)-C(10)-Fe(1)	-59.66(13)
C(4)-C(5)-Fe(1)-C(1)	119.11(17)
C(4)-C(5)-Fe(1)-C(9)	-41.5(5)
C(1)-C(5)-Fe(1)-C(9)	-160.6(5)
C(4)-C(5)-Fe(1)-C(8)	-70.29(15)
C(1)-C(5)-Fe(1)-C(8)	170.60(12)
C(4)-C(5)-Fe(1)-C(10)	172.32(14)
C(1)-C(5)-Fe(1)-C(10)	53.2(2)

C(4)-C(5)-Fe(1)-C(6)	-152.95(11)
C(1)-C(5)-Fe(1)-C(6)	87.94(13)
C(1)-C(5)-Fe(1)-C(4)	-119.11(17)
C(4)-C(5)-Fe(1)-C(7)	-109.61(12)
C(1)-C(5)-Fe(1)-C(7)	131.28(12)
C(4)-C(5)-Fe(1)-C(3)	37.46(11)
C(1)-C(5)-Fe(1)-C(3)	-81.64(12)
C(4)-C(5)-Fe(1)-C(2)	81.40(12)
C(1)-C(5)-Fe(1)-C(2)	-37.71(11)
C(2)-C(1)-Fe(1)-C(5)	-119.45(16)
C(5)-C(1)-Fe(1)-C(9)	174.12(14)
C(2)-C(1)-Fe(1)-C(9)	54.67(18)
C(5)-C(1)-Fe(1)-C(8)	-43.8(5)
C(2)-C(1)-Fe(1)-C(8)	-163.3(4)
C(5)-C(1)-Fe(1)-C(10)	-151.51(12)
C(2)-C(1)-Fe(1)-C(10)	89.04(12)
C(5)-C(1)-Fe(1)-C(6)	-108.72(12)
C(2)-C(1)-Fe(1)-C(6)	131.83(11)
C(5)-C(1)-Fe(1)-C(4)	37.83(12)
C(2)-C(1)-Fe(1)-C(4)	-81.63(12)
C(5)-C(1)-Fe(1)-C(7)	-69.48(14)
C(2)-C(1)-Fe(1)-C(7)	171.06(11)
C(5)-C(1)-Fe(1)-C(3)	81.44(12)
C(2)-C(1)-Fe(1)-C(3)	-38.02(11)
C(5)-C(1)-Fe(1)-C(2)	119.45(16)
C(8)-C(9)-Fe(1)-C(5)	-33.7(5)
C(10)-C(9)-Fe(1)-C(5)	-152.6(5)
C(8)-C(9)-Fe(1)-C(1)	170.37(14)
C(10)-C(9)-Fe(1)-C(1)	51.5(2)
C(10)-C(9)-Fe(1)-C(8)	-118.89(17)
C(8)-C(9)-Fe(1)-C(10)	118.89(17)
C(8)-C(9)-Fe(1)-C(6)	81.48(13)
C(10)-C(9)-Fe(1)-C(6)	-37.41(12)
C(8)-C(9)-Fe(1)-C(4)	-69.26(15)
C(10)-C(9)-Fe(1)-C(4)	171.84(12)
C(8)-C(9)-Fe(1)-C(7)	37.58(12)
C(10)-C(9)-Fe(1)-C(7)	-81.31(13)
C(8)-C(9)-Fe(1)-C(3)	-109.27(12)
C(10)-C(9)-Fe(1)-C(3)	131.84(12)
C(8)-C(9)-Fe(1)-C(2)	-153.13(11)
C(10)-C(9)-Fe(1)-C(2)	87.98(13)
C(9)-C(8)-Fe(1)-C(5)	173.03(11)
C(7)-C(8)-Fe(1)-C(5)	-67.60(15)
C(9)-C(8)-Fe(1)-C(1)	-149.8(4)
C(7)-C(8)-Fe(1)-C(1)	-30.5(5)
C(7)-C(8)-Fe(1)-C(9)	119.37(17)

C(9)-C(8)-Fe(1)-C(10)	-37.99(12)
C(7)-C(8)-Fe(1)-C(10)	81.39(13)
C(9)-C(8)-Fe(1)-C(6)	-81.58(12)
C(7)-C(8)-Fe(1)-C(6)	37.79(12)
C(9)-C(8)-Fe(1)-C(4)	132.25(12)
C(7)-C(8)-Fe(1)-C(4)	-108.37(13)
C(9)-C(8)-Fe(1)-C(7)	-119.37(17)
C(9)-C(8)-Fe(1)-C(3)	88.77(13)
C(7)-C(8)-Fe(1)-C(3)	-151.86(12)
C(9)-C(8)-Fe(1)-C(2)	51.45(19)
C(7)-C(8)-Fe(1)-C(2)	170.83(13)
C(6)-C(10)-Fe(1)-C(5)	52.6(2)
C(9)-C(10)-Fe(1)-C(5)	171.95(14)
C(6)-C(10)-Fe(1)-C(1)	88.03(13)
C(9)-C(10)-Fe(1)-C(1)	-152.62(12)
C(6)-C(10)-Fe(1)-C(9)	-119.35(17)
C(6)-C(10)-Fe(1)-C(8)	-81.51(13)
C(9)-C(10)-Fe(1)-C(8)	37.85(12)
C(9)-C(10)-Fe(1)-C(6)	119.35(17)
C(6)-C(10)-Fe(1)-C(4)	-159.8(4)
C(9)-C(10)-Fe(1)-C(4)	-40.4(5)
C(6)-C(10)-Fe(1)-C(7)	-37.66(12)
C(9)-C(10)-Fe(1)-C(7)	81.69(13)
C(6)-C(10)-Fe(1)-C(3)	170.85(11)
C(9)-C(10)-Fe(1)-C(3)	-69.80(15)
C(6)-C(10)-Fe(1)-C(2)	131.63(12)
C(9)-C(10)-Fe(1)-C(2)	-109.01(12)
C(10)-C(6)-Fe(1)-C(5)	-151.67(11)
C(7)-C(6)-Fe(1)-C(5)	88.90(13)
C(10)-C(6)-Fe(1)-C(1)	-108.25(12)
C(7)-C(6)-Fe(1)-C(1)	132.32(12)
C(10)-C(6)-Fe(1)-C(9)	37.80(12)
C(7)-C(6)-Fe(1)-C(9)	-81.63(13)
C(10)-C(6)-Fe(1)-C(8)	81.70(13)
C(7)-C(6)-Fe(1)-C(8)	-37.73(12)
C(7)-C(6)-Fe(1)-C(10)	-119.43(17)
C(10)-C(6)-Fe(1)-C(4)	173.84(14)
C(7)-C(6)-Fe(1)-C(4)	54.41(19)
C(10)-C(6)-Fe(1)-C(7)	119.43(17)
C(10)-C(6)-Fe(1)-C(3)	-41.7(5)
C(7)-C(6)-Fe(1)-C(3)	-161.2(4)
C(10)-C(6)-Fe(1)-C(2)	-68.48(14)
C(7)-C(6)-Fe(1)-C(2)	172.09(12)
C(3)-C(4)-Fe(1)-C(5)	119.35(16)
C(3)-C(4)-Fe(1)-C(1)	81.43(12)
C(5)-C(4)-Fe(1)-C(1)	-37.92(12)

C(3)-C(4)-Fe(1)-C(9)	-69.04(15)
C(5)-C(4)-Fe(1)-C(9)	171.61(12)
C(3)-C(4)-Fe(1)-C(8)	-109.29(12)
C(5)-C(4)-Fe(1)-C(8)	131.36(12)
C(3)-C(4)-Fe(1)-C(10)	-34.4(5)
C(5)-C(4)-Fe(1)-C(10)	-153.8(5)
C(3)-C(4)-Fe(1)-C(6)	170.78(13)
C(5)-C(4)-Fe(1)-C(6)	51.42(19)
C(3)-C(4)-Fe(1)-C(7)	-152.92(11)
C(5)-C(4)-Fe(1)-C(7)	87.73(13)
C(5)-C(4)-Fe(1)-C(3)	-119.35(16)
C(3)-C(4)-Fe(1)-C(2)	37.31(11)
C(5)-C(4)-Fe(1)-C(2)	-82.04(12)
C(8)-C(7)-Fe(1)-C(5)	132.93(12)
C(6)-C(7)-Fe(1)-C(5)	-107.97(12)
C(8)-C(7)-Fe(1)-C(1)	173.23(11)
C(6)-C(7)-Fe(1)-C(1)	-67.67(15)
C(8)-C(7)-Fe(1)-C(9)	-37.63(12)
C(6)-C(7)-Fe(1)-C(9)	81.47(13)
C(6)-C(7)-Fe(1)-C(8)	119.10(17)
C(8)-C(7)-Fe(1)-C(10)	-81.70(13)
C(6)-C(7)-Fe(1)-C(10)	37.40(12)
C(8)-C(7)-Fe(1)-C(6)	-119.10(17)
C(8)-C(7)-Fe(1)-C(4)	89.42(13)
C(6)-C(7)-Fe(1)-C(4)	-151.48(12)
C(8)-C(7)-Fe(1)-C(3)	54.5(2)
C(6)-C(7)-Fe(1)-C(3)	173.58(14)
C(8)-C(7)-Fe(1)-C(2)	-153.5(4)
C(6)-C(7)-Fe(1)-C(2)	-34.4(5)
C(4)-C(3)-Fe(1)-C(5)	-37.81(11)
C(2)-C(3)-Fe(1)-C(5)	82.36(12)
C(4)-C(3)-Fe(1)-C(1)	-81.99(12)
C(2)-C(3)-Fe(1)-C(1)	38.18(11)
C(4)-C(3)-Fe(1)-C(9)	132.34(12)
C(2)-C(3)-Fe(1)-C(9)	-107.49(12)
C(4)-C(3)-Fe(1)-C(8)	88.66(13)
C(2)-C(3)-Fe(1)-C(8)	-151.18(12)
C(4)-C(3)-Fe(1)-C(10)	172.92(12)
C(2)-C(3)-Fe(1)-C(10)	-66.91(15)
C(4)-C(3)-Fe(1)-C(6)	-151.9(4)
C(2)-C(3)-Fe(1)-C(6)	-31.7(5)
C(2)-C(3)-Fe(1)-C(4)	120.17(16)
C(4)-C(3)-Fe(1)-C(7)	52.2(2)
C(2)-C(3)-Fe(1)-C(7)	172.32(15)
C(4)-C(3)-Fe(1)-C(2)	-120.17(16)
C(3)-C(2)-Fe(1)-C(5)	-80.98(12)

C(1)-C(2)-Fe(1)-C(5)	37.70(11)
C(2)#1-C(2)-Fe(1)-C(5)	158.4(2)
C(3)-C(2)-Fe(1)-C(1)	-118.68(16)
C(2)#1-C(2)-Fe(1)-C(1)	120.7(3)
C(3)-C(2)-Fe(1)-C(9)	90.19(12)
C(1)-C(2)-Fe(1)-C(9)	-151.12(11)
C(2)#1-C(2)-Fe(1)-C(9)	-30.4(2)
C(3)-C(2)-Fe(1)-C(8)	55.69(19)
C(1)-C(2)-Fe(1)-C(8)	174.37(14)
C(2)#1-C(2)-Fe(1)-C(8)	-64.9(3)
C(3)-C(2)-Fe(1)-C(10)	133.59(12)
C(1)-C(2)-Fe(1)-C(10)	-107.73(11)
C(2)#1-C(2)-Fe(1)-C(10)	13.0(2)
C(3)-C(2)-Fe(1)-C(6)	172.93(11)
C(1)-C(2)-Fe(1)-C(6)	-68.39(14)
C(2)#1-C(2)-Fe(1)-C(6)	52.4(3)
C(3)-C(2)-Fe(1)-C(4)	-37.03(11)
C(1)-C(2)-Fe(1)-C(4)	81.65(12)
C(2)#1-C(2)-Fe(1)-C(4)	-157.6(2)
C(3)-C(2)-Fe(1)-C(7)	-158.2(4)
C(1)-C(2)-Fe(1)-C(7)	-39.6(5)
C(2)#1-C(2)-Fe(1)-C(7)	81.2(5)
C(1)-C(2)-Fe(1)-C(3)	118.68(16)
C(2)#1-C(2)-Fe(1)-C(3)	-120.6(3)

Symmetry transformations used to generate equivalent atoms:
#1 -x+1,-y,-z+1

Supporting Information Table 13

Crystal data and structure refinement for 3,4-diiodo-1-(triisopropylsilyl)pyrrole.

Identification code	a0059
Empirical formula	C13 H23 I2 N Si
Formula weight	475.21
Temperature	123(2) K
Wavelength	0.71075 A
Crystal system, space group	Monoclinic, P 21/c
Unit cell dimensions	a = 9.6249(6) A alpha = 90 deg. b = 21.7670(5) A beta = 107.464(8) deg. c = 8.7272(2) A gamma = 90 deg.
Volume	1744.12(12) A^3
Z, Calculated density	4, 1.810 Mg/m^3
Absorption coefficient	3.659 mm^-1
F(000)	912
Crystal size	0.38 x 0.09 x 0.09 mm
Theta range for data collection	3.08 to 27.29 deg.
Limiting indices	-11<=h<=12, -28<=k<=28, -11<=l<=11
Reflections collected / unique	11690 / 3908 [R(int) = 0.0185]
Completeness to theta = 27.29	99.7 %
Absorption correction	Semi-empirical from equivalents
Max. and min. transmission	1.000 and 0.686
Refinement method	Full-matrix least-squares on F^2
Data / restraints / parameters	3908 / 0 / 160

Goodness-of-fit on F^2	1.133
Final R indices [I>2sigma(I)]	R1 = 0.0211, wR2 = 0.0497
R indices (all data)	R1 = 0.0236, wR2 = 0.0506
Largest diff. peak and hole	1.419 and -0.338 e/A^-3

Supporting Information Table 14

Atomic coordinates (x 10^4) and equivalent isotropic displacement parameters (A^2 x 10^3) for 3,4-diiodo-1-(triisopropylsilyl)pyrrole. U(eq) is defined as one third of the trace of the orthogonalized Uij tensor.

	x	y	z	U(eq)
I(1)	-1570(1)	2684(1)	3421(1)	32(1)
I(2)	-3977(1)	3673(1)	5437(1)	29(1)
Si(1)	2251(1)	4073(1)	8839(1)	16(1)
N(1)	619(2)	3758(1)	7495(2)	18(1)
C(1)	548(2)	3365(1)	6234(2)	21(1)
C(2)	-872(2)	3271(1)	5361(2)	20(1)
C(3)	-1736(2)	3625(1)	6096(3)	19(1)
C(4)	-798(2)	3917(1)	7398(2)	18(1)
C(5)	1830(2)	4253(1)	10762(2)	21(1)
C(6)	3032(3)	4648(1)	11897(3)	29(1)
C(7)	1480(3)	3694(1)	11647(3)	35(1)
C(8)	2631(2)	4801(1)	7875(2)	20(1)
C(9)	1507(3)	5307(1)	7819(3)	29(1)
C(10)	2720(3)	4681(1)	6178(3)	35(1)
C(11)	3704(2)	3482(1)	8937(3)	24(1)
C(12)	5231(3)	3704(1)	9895(3)	37(1)
C(13)	3398(3)	2843(1)	9506(4)	42(1)

Supporting Information Table 15

Bond lengths [A] and angles [deg] for 3,4-diiodo-1-(triisopropylsilyl)pyrrole.

I(1)-C(2)	2.066(2)
I(2)-C(3)	2.061(2)
Si(1)-N(1)	1.7909(18)
Si(1)-C(8)	1.881(2)
Si(1)-C(5)	1.882(2)
Si(1)-C(11)	1.882(2)
N(1)-C(1)	1.379(3)
N(1)-C(4)	1.386(3)
C(1)-C(2)	1.366(3)
C(1)-H(1)	0.9500
C(2)-C(3)	1.420(3)
C(3)-C(4)	1.376(3)
C(4)-H(4)	0.9500
C(5)-C(7)	1.532(3)
C(5)-C(6)	1.539(3)
C(5)-H(5)	1.0000
C(6)-H(6A)	0.9800
C(6)-H(6B)	0.9800
C(6)-H(6C)	0.9800
C(7)-H(7A)	0.9800
C(7)-H(7B)	0.9800
C(7)-H(7C)	0.9800
C(8)-C(10)	1.531(3)
C(8)-C(9)	1.534(3)
C(8)-H(8)	1.0000
C(9)-H(9A)	0.9800
C(9)-H(9B)	0.9800
C(9)-H(9C)	0.9800
C(10)-H(10A)	0.9800
C(10)-H(10B)	0.9800
C(10)-H(10C)	0.9800
C(11)-C(13)	1.535(3)
C(11)-C(12)	1.535(3)
C(11)-H(11)	1.0000
C(12)-H(12A)	0.9800
C(12)-H(12B)	0.9800
C(12)-H(12C)	0.9800
C(13)-H(13A)	0.9800
C(13)-H(13B)	0.9800
C(13)-H(13C)	0.9800

N(1)-Si(1)-C(8)	106.25(9)
N(1)-Si(1)-C(5)	106.43(9)
C(8)-Si(1)-C(5)	110.27(9)
N(1)-Si(1)-C(11)	105.16(9)
C(8)-Si(1)-C(11)	110.71(10)
C(5)-Si(1)-C(11)	117.23(10)
C(1)-N(1)-C(4)	107.13(17)
C(1)-N(1)-Si(1)	125.75(14)
C(4)-N(1)-Si(1)	126.69(14)
C(2)-C(1)-N(1)	109.84(18)
C(2)-C(1)-H(1)	125.1
N(1)-C(1)-H(1)	125.1
C(1)-C(2)-C(3)	106.90(18)
C(1)-C(2)-I(1)	125.04(16)
C(3)-C(2)-I(1)	128.00(15)
C(4)-C(3)-C(2)	107.19(18)
C(4)-C(3)-I(2)	125.38(16)
C(2)-C(3)-I(2)	127.38(15)
C(3)-C(4)-N(1)	108.94(18)
C(3)-C(4)-H(4)	125.5
N(1)-C(4)-H(4)	125.5
C(7)-C(5)-C(6)	110.81(19)
C(7)-C(5)-Si(1)	115.02(15)
C(6)-C(5)-Si(1)	111.63(15)
C(7)-C(5)-H(5)	106.2
C(6)-C(5)-H(5)	106.2
Si(1)-C(5)-H(5)	106.2
C(5)-C(6)-H(6A)	109.5
C(5)-C(6)-H(6B)	109.5
H(6A)-C(6)-H(6B)	109.5
C(5)-C(6)-H(6C)	109.5
H(6A)-C(6)-H(6C)	109.5
H(6B)-C(6)-H(6C)	109.5
C(5)-C(7)-H(7A)	109.5
C(5)-C(7)-H(7B)	109.5
H(7A)-C(7)-H(7B)	109.5
C(5)-C(7)-H(7C)	109.5
H(7A)-C(7)-H(7C)	109.5
H(7B)-C(7)-H(7C)	109.5
C(10)-C(8)-C(9)	109.56(19)
C(10)-C(8)-Si(1)	111.36(15)
C(9)-C(8)-Si(1)	112.87(14)
C(10)-C(8)-H(8)	107.6
C(9)-C(8)-H(8)	107.6
Si(1)-C(8)-H(8)	107.6
C(8)-C(9)-H(9A)	109.5

C(8)-C(9)-H(9B)	109.5
H(9A)-C(9)-H(9B)	109.5
C(8)-C(9)-H(9C)	109.5
H(9A)-C(9)-H(9C)	109.5
H(9B)-C(9)-H(9C)	109.5
C(8)-C(10)-H(10A)	109.5
C(8)-C(10)-H(10B)	109.5
H(10A)-C(10)-H(10B)	109.5
C(8)-C(10)-H(10C)	109.5
H(10A)-C(10)-H(10C)	109.5
H(10B)-C(10)-H(10C)	109.5
C(13)-C(11)-C(12)	110.7(2)
C(13)-C(11)-Si(1)	114.92(17)
C(12)-C(11)-Si(1)	112.80(16)
C(13)-C(11)-H(11)	105.9
C(12)-C(11)-H(11)	105.9
Si(1)-C(11)-H(11)	105.9
C(11)-C(12)-H(12A)	109.5
C(11)-C(12)-H(12B)	109.5
H(12A)-C(12)-H(12B)	109.5
C(11)-C(12)-H(12C)	109.5
H(12A)-C(12)-H(12C)	109.5
H(12B)-C(12)-H(12C)	109.5
C(11)-C(13)-H(13A)	109.5
C(11)-C(13)-H(13B)	109.5
H(13A)-C(13)-H(13B)	109.5
C(11)-C(13)-H(13C)	109.5
H(13A)-C(13)-H(13C)	109.5
H(13B)-C(13)-H(13C)	109.5

Symmetry transformations used to generate equivalent atoms:

Supporting Information Table 16

Anisotropic displacement parameters (A^2 x 10^3) for 3,4-diiodo-1-(triisopropylsilyl)pyrrole. The anisotropic displacement factor exponent takes the form: -2 pi^2 [h^2 a*^2 U11 + ... + 2 h k a* b* U12]

	U11	U22	U33	U23	U13	U12
I(1)	38(1)	28(1)	24(1)	-11(1)	2(1)	-2(1)
I(2)	17(1)	32(1)	34(1)	-1(1)	3(1)	-3(1)
Si(1)	15(1)	17(1)	15(1)	-1(1)	4(1)	2(1)
N(1)	17(1)	20(1)	18(1)	-3(1)	4(1)	1(1)
C(1)	22(1)	20(1)	20(1)	-2(1)	8(1)	2(1)
C(2)	26(1)	17(1)	15(1)	-1(1)	5(1)	-1(1)
C(3)	18(1)	18(1)	21(1)	2(1)	4(1)	-1(1)
C(4)	19(1)	16(1)	20(1)	-1(1)	6(1)	1(1)
C(5)	23(1)	22(1)	17(1)	1(1)	7(1)	1(1)
C(6)	31(1)	35(1)	19(1)	-6(1)	5(1)	-1(1)
C(7)	53(2)	31(1)	27(1)	3(1)	19(1)	-2(1)
C(8)	19(1)	22(1)	21(1)	1(1)	7(1)	-1(1)
C(9)	34(1)	22(1)	32(1)	6(1)	13(1)	5(1)
C(10)	52(2)	32(1)	29(1)	4(1)	23(1)	2(1)
C(11)	21(1)	26(1)	25(1)	-2(1)	5(1)	7(1)
C(12)	21(1)	48(2)	36(1)	-7(1)	1(1)	10(1)
C(13)	43(2)	26(1)	55(2)	7(1)	12(1)	14(1)

Supporting Information Table 17

Hydrogen coordinates (x 10^4) and isotropic displacement parameters (A^2 x 10^3) for 3,4-diiodo-1-(triisopropylsilyl)pyrrole.

	x	y	z	U(eq)
H(1)	1365	3187	6005	25
H(4)	-1077	4185	8113	22
H(5)	931	4512	10456	25
H(6A)	3947	4416	12216	43
H(6B)	2750	4754	12854	43
H(6C)	3164	5025	11342	43
H(7A)	1116	3832	12524	53
H(7B)	2365	3449	12088	53
H(7C)	736	3442	10896	53
H(8)	3603	4957	8536	24
H(9A)	532	5157	7232	43
H(9B)	1736	5669	7272	43
H(9C)	1535	5418	8916	43
H(10A)	2918	5068	5708	53
H(10B)	1793	4511	5511	53
H(10C)	3506	4388	6229	53
H(11)	3727	3427	7808	29
H(12A)	5957	3403	9798	55
H(12B)	5285	3750	11029	55
H(12C)	5428	4101	9472	55
H(13A)	3556	2851	10668	63
H(13B)	4056	2543	9254	63
H(13C)	2386	2728	8957	63

Supporting Information Table 18

Torsion angles [deg] for 3,4-diiodo-1-(triisopropylsilyl)pyrrole.

C(8)-Si(1)-N(1)-C(1)	87.87(18)
C(5)-Si(1)-N(1)-C(1)	-154.60(17)
C(11)-Si(1)-N(1)-C(1)	-29.56(19)
C(8)-Si(1)-N(1)-C(4)	-83.60(19)
C(5)-Si(1)-N(1)-C(4)	33.9(2)
C(11)-Si(1)-N(1)-C(4)	158.98(18)
C(4)-N(1)-C(1)-C(2)	-0.5(2)
Si(1)-N(1)-C(1)-C(2)	-173.39(14)
N(1)-C(1)-C(2)-C(3)	0.6(2)
N(1)-C(1)-C(2)-I(1)	-176.62(14)
C(1)-C(2)-C(3)-C(4)	-0.4(2)
I(1)-C(2)-C(3)-C(4)	176.70(15)
C(1)-C(2)-C(3)-I(2)	-177.88(15)
I(1)-C(2)-C(3)-I(2)	-0.8(3)
C(2)-C(3)-C(4)-N(1)	0.1(2)
I(2)-C(3)-C(4)-N(1)	177.61(14)
C(1)-N(1)-C(4)-C(3)	0.3(2)
Si(1)-N(1)-C(4)-C(3)	173.05(14)
N(1)-Si(1)-C(5)-C(7)	64.38(19)
C(8)-Si(1)-C(5)-C(7)	179.22(17)
C(11)-Si(1)-C(5)-C(7)	-52.9(2)
N(1)-Si(1)-C(5)-C(6)	-168.25(15)
C(8)-Si(1)-C(5)-C(6)	-53.42(18)
C(11)-Si(1)-C(5)-C(6)	74.46(18)
N(1)-Si(1)-C(8)-C(10)	-55.35(18)
C(5)-Si(1)-C(8)-C(10)	-170.30(16)
C(11)-Si(1)-C(8)-C(10)	58.32(19)
N(1)-Si(1)-C(8)-C(9)	68.37(17)
C(5)-Si(1)-C(8)-C(9)	-46.58(18)
C(11)-Si(1)-C(8)-C(9)	-177.96(16)
N(1)-Si(1)-C(11)-C(13)	-58.2(2)
C(8)-Si(1)-C(11)-C(13)	-172.55(18)
C(5)-Si(1)-C(11)-C(13)	59.8(2)
N(1)-Si(1)-C(11)-C(12)	173.59(17)
C(8)-Si(1)-C(11)-C(12)	59.2(2)
C(5)-Si(1)-C(11)-C(12)	-68.4(2)

Symmetry transformations used to generate equivalent atoms:

Supporting Information Table 19

Crystal data and structure refinement for 3,4-bis(ferrocenyl)-1-(triisopropylsilyl)pyrrole.

Identification code	shelxl	
Empirical formula	C33 H41 Fe2 N Si	
Formula weight	591.46	
Temperature	123(2) K	
Wavelength	0.71075 A	
Crystal system, space group	?, ?	
Unit cell dimensions	a = 7.3670(3) A	alpha = 110.563(8) deg.
	b = 12.3067(5) A	beta = 98.491(7) deg.
	c = 17.1322(12) A	gamma = 94.446(7) deg.
Volume	1424.25(13) A^3	
Z, Calculated density	2, 1.379 Mg/m^3	
Absorption coefficient	1.083 mm^{-1}	
F(000)	624	
Crystal size	0.27 x 0.04 x 0.04 mm	
Theta range for data collection	3.12 to 26.37 deg.	
Limiting indices	-9<=h<=9, -15<=k<=15, -21<=l<=21	
Reflections collected / unique	44317 / 5821 [R(int) = 0.1344]	
Completeness to theta = 26.37	99.8 %	
Max. and min. transmission	0.9631 and 0.7615	
Refinement method	Full-matrix least-squares on F^2	
Data / restraints / parameters	5821 / 0 / 340	
Goodness-of-fit on F^2	1.090	

Final R indices [I>2sigma(I)] $R_1 = 0.0555$, $wR_2 = 0.1280$

R indices (all data) $R_1 = 0.0779$, $wR_2 = 0.1409$

Largest diff. peak and hole 0.678 and -0.886 $e.A^{-3}$

Supporting Information Table 20

Atomic coordinates (x 10^4) and equivalent isotropic displacement parameters (A^2 x 10^3) for 3,4-bis(ferrocenyl)-1-(triisopropylsilyl)pyrrole.

U(eq) is defined as one third of the trace of the orthogonalized Uij tensor.

	x	y	z	U(eq)
C(1)	9192(5)	6092(3)	1648(2)	27(1)
C(2)	8945(5)	5734(3)	2305(2)	27(1)
C(3)	9749(5)	6713(3)	3074(2)	26(1)
C(4)	10409(5)	7590(3)	2836(2)	27(1)
C(5)	8036(5)	4574(3)	2192(2)	25(1)
C(6)	6532(5)	3887(3)	1527(2)	28(1)
C(7)	6140(5)	2780(3)	1605(2)	32(1)
C(8)	7391(5)	2766(3)	2313(2)	31(1)
C(9)	8556(5)	3868(3)	2678(2)	28(1)
C(10)	4922(5)	5607(3)	3378(2)	34(1)
C(11)	3447(5)	4854(3)	2730(2)	36(1)
C(12)	3189(5)	3784(4)	2865(2)	38(1)
C(13)	4495(5)	3872(4)	3586(2)	36(1)
C(14)	5570(5)	4997(3)	3905(2)	34(1)
C(15)	9810(5)	6791(3)	3959(2)	25(1)
C(16)	10897(5)	6201(3)	4403(2)	30(1)
C(17)	10521(5)	6536(3)	5243(2)	31(1)
C(18)	9233(5)	7352(3)	5336(2)	31(1)
C(19)	8800(5)	7506(3)	4543(2)	28(1)
C(20)	13670(5)	8717(3)	4639(2)	32(1)
C(21)	14412(5)	8336(3)	5295(2)	34(1)
C(22)	13665(5)	8936(3)	6028(2)	35(1)
C(23)	12462(5)	9678(3)	5821(2)	34(1)
C(24)	12468(5)	9550(3)	4965(2)	33(1)
C(25)	11595(5)	9565(3)	2030(2)	34(1)
C(26)	9828(7)	10125(4)	2128(3)	50(1)
C(27)	12975(6)	10267(4)	1731(3)	45(1)
C(28)	13538(5)	7412(3)	1280(2)	33(1)
C(29)	14786(6)	7726(4)	2149(2)	41(1)
C(30)	13371(6)	6090(3)	771(2)	41(1)
C(31)	9721(5)	7462(3)	292(2)	33(1)
C(32)	10475(6)	8044(4)	-278(2)	46(1)
C(33)	7663(6)	7591(5)	286(3)	54(1)
N(1)	10094(4)	7237(3)	1956(2)	28(1)

Si(1)	11221(1)	7941(1)	1374(1)	27(1)
Fe(1)	5829(1)	4096(1)	2677(1)	26(1)
Fe(2)	11577(1)	7969(1)	5028(1)	27(1)

Supporting Information Table 21

Bond lengths [A] and angles [deg] for 3,4-bis(ferrocenyl)-1-(triisopropylsilyl)pyrrole.

C(1)-C(2)	1.374(5)
C(1)-N(1)	1.391(4)
C(1)-H(1)	0.9500
C(2)-C(3)	1.443(5)
C(2)-C(5)	1.465(5)
C(3)-C(4)	1.361(5)
C(3)-C(15)	1.480(4)
C(4)-N(1)	1.392(4)
C(4)-H(4)	0.9500
C(5)-C(6)	1.430(5)
C(5)-C(9)	1.435(5)
C(5)-Fe(1)	2.067(3)
C(6)-C(7)	1.426(5)
C(6)-Fe(1)	2.045(3)
C(6)-H(6)	0.9500
C(7)-C(8)	1.418(5)
C(7)-Fe(1)	2.036(4)
C(7)-H(7)	0.9500
C(8)-C(9)	1.426(5)
C(8)-Fe(1)	2.045(4)
C(8)-H(8)	0.9500
C(9)-Fe(1)	2.050(4)
C(9)-H(9)	0.9500
C(10)-C(14)	1.419(5)
C(10)-C(11)	1.427(5)
C(10)-Fe(1)	2.051(4)
C(10)-H(10)	0.9500
C(11)-C(12)	1.418(5)
C(11)-Fe(1)	2.049(4)
C(11)-H(11)	0.9500
C(12)-C(13)	1.416(6)
C(12)-Fe(1)	2.047(4)
C(12)-H(12)	0.9500
C(13)-C(14)	1.419(5)
C(13)-Fe(1)	2.044(4)
C(13)-H(13)	0.9500
C(14)-Fe(1)	2.050(3)
C(14)-H(14)	0.9500
C(15)-C(19)	1.425(5)
C(15)-C(16)	1.430(5)
C(15)-Fe(2)	2.071(3)

C(16)-C(17)	1.426(5)
C(16)-Fe(2)	2.042(4)
C(16)-H(16)	0.9500
C(17)-C(18)	1.420(5)
C(17)-Fe(2)	2.044(4)
C(17)-H(17)	0.9500
C(18)-C(19)	1.430(5)
C(18)-Fe(2)	2.045(4)
C(18)-H(18)	0.9500
C(19)-Fe(2)	2.046(4)
C(19)-H(19)	0.9500
C(20)-C(21)	1.418(5)
C(20)-C(24)	1.425(5)
C(20)-Fe(2)	2.046(4)
C(20)-H(20)	0.9500
C(21)-C(22)	1.429(5)
C(21)-Fe(2)	2.050(4)
C(21)-H(21)	0.9500
C(22)-C(23)	1.417(5)
C(22)-Fe(2)	2.055(3)
C(22)-H(22)	0.9500
C(23)-C(24)	1.420(5)
C(23)-Fe(2)	2.053(4)
C(23)-H(23)	0.9500
C(24)-Fe(2)	2.049(4)
C(24)-H(24)	0.9500
C(25)-C(26)	1.523(6)
C(25)-C(27)	1.539(5)
C(25)-Si(1)	1.891(4)
C(25)-H(25)	1.0000
C(26)-H(26A)	0.9800
C(26)-H(26B)	0.9800
C(26)-H(26C)	0.9800
C(27)-H(27A)	0.9800
C(27)-H(27B)	0.9800
C(27)-H(27C)	0.9800
C(28)-C(29)	1.532(5)
C(28)-C(30)	1.538(5)
C(28)-Si(1)	1.883(4)
C(28)-H(28)	1.0000
C(29)-H(29A)	0.9800
C(29)-H(29B)	0.9800
C(29)-H(29C)	0.9800
C(30)-H(30A)	0.9800
C(30)-H(30B)	0.9800
C(30)-H(30C)	0.9800

C(31)-C(33)	1.535(5)
C(31)-C(32)	1.537(5)
C(31)-Si(1)	1.879(3)
C(31)-H(31)	1.0000
C(32)-H(32A)	0.9800
C(32)-H(32B)	0.9800
C(32)-H(32C)	0.9800
C(33)-H(33A)	0.9800
C(33)-H(33B)	0.9800
C(33)-H(33C)	0.9800
N(1)-Si(1)	1.782(3)

C(2)-C(1)-N(1)	110.7(3)
C(2)-C(1)-H(1)	124.6
N(1)-C(1)-H(1)	124.6
C(1)-C(2)-C(3)	106.0(3)
C(1)-C(2)-C(5)	124.2(3)
C(3)-C(2)-C(5)	129.8(3)
C(4)-C(3)-C(2)	106.9(3)
C(4)-C(3)-C(15)	125.4(3)
C(2)-C(3)-C(15)	127.7(3)
C(3)-C(4)-N(1)	110.8(3)
C(3)-C(4)-H(4)	124.6
N(1)-C(4)-H(4)	124.6
C(6)-C(5)-C(9)	106.6(3)
C(6)-C(5)-C(2)	125.9(3)
C(9)-C(5)-C(2)	127.3(3)
C(6)-C(5)-Fe(1)	68.83(19)
C(9)-C(5)-Fe(1)	69.0(2)
C(2)-C(5)-Fe(1)	130.6(2)
C(7)-C(6)-C(5)	108.6(3)
C(7)-C(6)-Fe(1)	69.2(2)
C(5)-C(6)-Fe(1)	70.47(19)
C(7)-C(6)-H(6)	125.7
C(5)-C(6)-H(6)	125.7
Fe(1)-C(6)-H(6)	126.2
C(8)-C(7)-C(6)	108.2(3)
C(8)-C(7)-Fe(1)	70.0(2)
C(6)-C(7)-Fe(1)	69.9(2)
C(8)-C(7)-H(7)	125.9
C(6)-C(7)-H(7)	125.9
Fe(1)-C(7)-H(7)	125.8
C(7)-C(8)-C(9)	107.7(3)
C(7)-C(8)-Fe(1)	69.3(2)
C(9)-C(8)-Fe(1)	69.8(2)
C(7)-C(8)-H(8)	126.1

C(9)-C(8)-H(8)	126.1
Fe(1)-C(8)-H(8)	126.3
C(8)-C(9)-C(5)	108.8(3)
C(8)-C(9)-Fe(1)	69.4(2)
C(5)-C(9)-Fe(1)	70.2(2)
C(8)-C(9)-H(9)	125.6
C(5)-C(9)-H(9)	125.6
Fe(1)-C(9)-H(9)	126.3
C(14)-C(10)-C(11)	108.1(3)
C(14)-C(10)-Fe(1)	69.7(2)
C(11)-C(10)-Fe(1)	69.6(2)
C(14)-C(10)-H(10)	125.9
C(11)-C(10)-H(10)	125.9
Fe(1)-C(10)-H(10)	126.4
C(12)-C(11)-C(10)	107.7(3)
C(12)-C(11)-Fe(1)	69.7(2)
C(10)-C(11)-Fe(1)	69.7(2)
C(12)-C(11)-H(11)	126.2
C(10)-C(11)-H(11)	126.2
Fe(1)-C(11)-H(11)	126.0
C(13)-C(12)-C(11)	108.1(4)
C(13)-C(12)-Fe(1)	69.6(2)
C(11)-C(12)-Fe(1)	69.8(2)
C(13)-C(12)-H(12)	125.9
C(11)-C(12)-H(12)	125.9
Fe(1)-C(12)-H(12)	126.2
C(12)-C(13)-C(14)	108.3(4)
C(12)-C(13)-Fe(1)	69.9(2)
C(14)-C(13)-Fe(1)	69.9(2)
C(12)-C(13)-H(13)	125.8
C(14)-C(13)-H(13)	125.8
Fe(1)-C(13)-H(13)	125.9
C(10)-C(14)-C(13)	107.8(3)
C(10)-C(14)-Fe(1)	69.8(2)
C(13)-C(14)-Fe(1)	69.5(2)
C(10)-C(14)-H(14)	126.1
C(13)-C(14)-H(14)	126.1
Fe(1)-C(14)-H(14)	126.1
C(19)-C(15)-C(16)	106.7(3)
C(19)-C(15)-C(3)	125.6(3)
C(16)-C(15)-C(3)	127.7(3)
C(19)-C(15)-Fe(2)	68.81(19)
C(16)-C(15)-Fe(2)	68.57(19)
C(3)-C(15)-Fe(2)	126.5(2)
C(17)-C(16)-C(15)	108.6(3)
C(17)-C(16)-Fe(2)	69.7(2)

C(15)-C(16)-Fe(2)	70.73(19)
C(17)-C(16)-H(16)	125.7
C(15)-C(16)-H(16)	125.7
Fe(2)-C(16)-H(16)	125.5
C(18)-C(17)-C(16)	108.3(3)
C(18)-C(17)-Fe(2)	69.7(2)
C(16)-C(17)-Fe(2)	69.5(2)
C(18)-C(17)-H(17)	125.9
C(16)-C(17)-H(17)	125.9
Fe(2)-C(17)-H(17)	126.5
C(17)-C(18)-C(19)	107.2(3)
C(17)-C(18)-Fe(2)	69.7(2)
C(19)-C(18)-Fe(2)	69.6(2)
C(17)-C(18)-H(18)	126.4
C(19)-C(18)-H(18)	126.4
Fe(2)-C(18)-H(18)	125.9
C(15)-C(19)-C(18)	109.2(3)
C(15)-C(19)-Fe(2)	70.7(2)
C(18)-C(19)-Fe(2)	69.5(2)
C(15)-C(19)-H(19)	125.4
C(18)-C(19)-H(19)	125.4
Fe(2)-C(19)-H(19)	126.0
C(21)-C(20)-C(24)	108.0(3)
C(21)-C(20)-Fe(2)	69.9(2)
C(24)-C(20)-Fe(2)	69.8(2)
C(21)-C(20)-H(20)	126.0
C(24)-C(20)-H(20)	126.0
Fe(2)-C(20)-H(20)	125.9
C(20)-C(21)-C(22)	107.8(3)
C(20)-C(21)-Fe(2)	69.6(2)
C(22)-C(21)-Fe(2)	69.8(2)
C(20)-C(21)-H(21)	126.1
C(22)-C(21)-H(21)	126.1
Fe(2)-C(21)-H(21)	126.1
C(23)-C(22)-C(21)	108.2(3)
C(23)-C(22)-Fe(2)	69.7(2)
C(21)-C(22)-Fe(2)	69.5(2)
C(23)-C(22)-H(22)	125.9
C(21)-C(22)-H(22)	125.9
Fe(2)-C(22)-H(22)	126.5
C(22)-C(23)-C(24)	107.9(3)
C(22)-C(23)-Fe(2)	69.9(2)
C(24)-C(23)-Fe(2)	69.6(2)
C(22)-C(23)-H(23)	126.0
C(24)-C(23)-H(23)	126.0
Fe(2)-C(23)-H(23)	126.0

C(23)-C(24)-C(20)	108.1(3)
C(23)-C(24)-Fe(2)	69.9(2)
C(20)-C(24)-Fe(2)	69.5(2)
C(23)-C(24)-H(24)	125.9
C(20)-C(24)-H(24)	125.9
Fe(2)-C(24)-H(24)	126.2
C(26)-C(25)-C(27)	110.8(3)
C(26)-C(25)-Si(1)	114.9(3)
C(27)-C(25)-Si(1)	112.8(3)
C(26)-C(25)-H(25)	105.8
C(27)-C(25)-H(25)	105.8
Si(1)-C(25)-H(25)	105.8
C(25)-C(26)-H(26A)	109.5
C(25)-C(26)-H(26B)	109.5
H(26A)-C(26)-H(26B)	109.5
C(25)-C(26)-H(26C)	109.5
H(26A)-C(26)-H(26C)	109.5
H(26B)-C(26)-H(26C)	109.5
C(25)-C(27)-H(27A)	109.5
C(25)-C(27)-H(27B)	109.5
H(27A)-C(27)-H(27B)	109.5
C(25)-C(27)-H(27C)	109.5
H(27A)-C(27)-H(27C)	109.5
H(27B)-C(27)-H(27C)	109.5
C(29)-C(28)-C(30)	110.0(3)
C(29)-C(28)-Si(1)	112.0(3)
C(30)-C(28)-Si(1)	112.9(3)
C(29)-C(28)-H(28)	107.2
C(30)-C(28)-H(28)	107.2
Si(1)-C(28)-H(28)	107.2
C(28)-C(29)-H(29A)	109.5
C(28)-C(29)-H(29B)	109.5
H(29A)-C(29)-H(29B)	109.5
C(28)-C(29)-H(29C)	109.5
H(29A)-C(29)-H(29C)	109.5
H(29B)-C(29)-H(29C)	109.5
C(28)-C(30)-H(30A)	109.5
C(28)-C(30)-H(30B)	109.5
H(30A)-C(30)-H(30B)	109.5
C(28)-C(30)-H(30C)	109.5
H(30A)-C(30)-H(30C)	109.5
H(30B)-C(30)-H(30C)	109.5
C(33)-C(31)-C(32)	109.8(3)
C(33)-C(31)-Si(1)	115.3(3)
C(32)-C(31)-Si(1)	112.8(3)
C(33)-C(31)-H(31)	106.1

C(32)-C(31)-H(31)	106.1
Si(1)-C(31)-H(31)	106.1
C(31)-C(32)-H(32A)	109.5
C(31)-C(32)-H(32B)	109.5
H(32A)-C(32)-H(32B)	109.5
C(31)-C(32)-H(32C)	109.5
H(32A)-C(32)-H(32C)	109.5
H(32B)-C(32)-H(32C)	109.5
C(31)-C(33)-H(33A)	109.5
C(31)-C(33)-H(33B)	109.5
H(33A)-C(33)-H(33B)	109.5
C(31)-C(33)-H(33C)	109.5
H(33A)-C(33)-H(33C)	109.5
H(33B)-C(33)-H(33C)	109.5
C(1)-N(1)-C(4)	105.6(3)
C(1)-N(1)-Si(1)	126.6(2)
C(4)-N(1)-Si(1)	125.4(3)
N(1)-Si(1)-C(31)	106.57(16)
N(1)-Si(1)-C(28)	107.93(16)
C(31)-Si(1)-C(28)	109.78(17)
N(1)-Si(1)-C(25)	106.49(15)
C(31)-Si(1)-C(25)	116.54(17)
C(28)-Si(1)-C(25)	109.15(17)
C(7)-Fe(1)-C(13)	124.68(16)
C(7)-Fe(1)-C(8)	40.66(14)
C(13)-Fe(1)-C(8)	107.66(15)
C(7)-Fe(1)-C(6)	40.92(14)
C(13)-Fe(1)-C(6)	161.71(16)
C(8)-Fe(1)-C(6)	68.57(14)
C(7)-Fe(1)-C(12)	107.53(16)
C(13)-Fe(1)-C(12)	40.49(16)
C(8)-Fe(1)-C(12)	120.99(16)
C(6)-Fe(1)-C(12)	124.85(15)
C(7)-Fe(1)-C(11)	120.91(15)
C(13)-Fe(1)-C(11)	68.20(16)
C(8)-Fe(1)-C(11)	156.07(15)
C(6)-Fe(1)-C(11)	107.56(15)
C(12)-Fe(1)-C(11)	40.52(15)
C(7)-Fe(1)-C(14)	161.54(15)
C(13)-Fe(1)-C(14)	40.57(15)
C(8)-Fe(1)-C(14)	124.79(14)
C(6)-Fe(1)-C(14)	156.21(15)
C(12)-Fe(1)-C(14)	68.25(16)
C(11)-Fe(1)-C(14)	68.39(15)
C(7)-Fe(1)-C(9)	68.39(14)
C(13)-Fe(1)-C(9)	121.38(15)

C(8)-Fe(1)-C(9)	40.75(14)
C(6)-Fe(1)-C(9)	68.25(14)
C(12)-Fe(1)-C(9)	156.41(16)
C(11)-Fe(1)-C(9)	161.73(15)
C(14)-Fe(1)-C(9)	107.84(14)
C(7)-Fe(1)-C(10)	156.43(15)
C(13)-Fe(1)-C(10)	68.08(16)
C(8)-Fe(1)-C(10)	161.67(15)
C(6)-Fe(1)-C(10)	121.14(15)
C(12)-Fe(1)-C(10)	68.18(16)
C(11)-Fe(1)-C(10)	40.73(15)
C(14)-Fe(1)-C(10)	40.48(15)
C(9)-Fe(1)-C(10)	124.92(15)
C(7)-Fe(1)-C(5)	68.87(14)
C(13)-Fe(1)-C(5)	156.36(15)
C(8)-Fe(1)-C(5)	68.89(14)
C(6)-Fe(1)-C(5)	40.70(13)
C(12)-Fe(1)-C(5)	161.49(15)
C(11)-Fe(1)-C(5)	124.53(15)
C(14)-Fe(1)-C(5)	120.92(15)
C(9)-Fe(1)-C(5)	40.78(13)
C(10)-Fe(1)-C(5)	107.43(15)
C(16)-Fe(2)-C(17)	40.85(13)
C(16)-Fe(2)-C(18)	68.72(15)
C(17)-Fe(2)-C(18)	40.64(15)
C(16)-Fe(2)-C(19)	68.17(14)
C(17)-Fe(2)-C(19)	68.23(15)
C(18)-Fe(2)-C(19)	40.92(14)
C(16)-Fe(2)-C(20)	114.55(15)
C(17)-Fe(2)-C(20)	146.67(15)
C(18)-Fe(2)-C(20)	171.47(15)
C(19)-Fe(2)-C(20)	131.77(14)
C(16)-Fe(2)-C(24)	147.16(14)
C(17)-Fe(2)-C(24)	171.42(14)
C(18)-Fe(2)-C(24)	132.62(15)
C(19)-Fe(2)-C(24)	109.96(15)
C(20)-Fe(2)-C(24)	40.71(15)
C(16)-Fe(2)-C(21)	107.58(16)
C(17)-Fe(2)-C(21)	115.07(15)
C(18)-Fe(2)-C(21)	147.43(15)
C(19)-Fe(2)-C(21)	169.88(14)
C(20)-Fe(2)-C(21)	40.51(14)
C(24)-Fe(2)-C(21)	68.25(15)
C(16)-Fe(2)-C(23)	170.52(14)
C(17)-Fe(2)-C(23)	132.07(14)
C(18)-Fe(2)-C(23)	109.75(15)

C(19)-Fe(2)-C(23)	117.26(15)
C(20)-Fe(2)-C(23)	68.39(15)
C(24)-Fe(2)-C(23)	40.52(14)
C(21)-Fe(2)-C(23)	68.35(16)
C(16)-Fe(2)-C(22)	131.14(15)
C(17)-Fe(2)-C(22)	108.92(15)
C(18)-Fe(2)-C(22)	116.17(14)
C(19)-Fe(2)-C(22)	148.81(14)
C(20)-Fe(2)-C(22)	68.22(15)
C(24)-Fe(2)-C(22)	67.98(15)
C(21)-Fe(2)-C(22)	40.74(15)
C(23)-Fe(2)-C(22)	40.35(15)
C(16)-Fe(2)-C(15)	40.70(13)
C(17)-Fe(2)-C(15)	68.61(13)
C(18)-Fe(2)-C(15)	68.87(13)
C(19)-Fe(2)-C(15)	40.51(13)
C(20)-Fe(2)-C(15)	108.06(14)
C(24)-Fe(2)-C(15)	115.90(14)
C(21)-Fe(2)-C(15)	130.44(15)
C(23)-Fe(2)-C(15)	148.35(15)
C(22)-Fe(2)-C(15)	169.82(15)

Symmetry transformations used to generate equivalent atoms:
#1 -x+1,-y,-z+1

Supporting Information Table 22

Anisotropic displacement parameters ($A^2 \times 10^3$) for 3,4-bis(ferrocenyl)-1-(triisopropylsilyl)pyrrole. The anisotropic displacement factor exponent takes the form:

$-2\ pi^2\ [\ h^2\ a^{*2}\ U11 + ... + 2\ h\ k\ a^*\ b^*\ U12\ ]$

	U11	U22	U33	U23	U13	U12
C(1)	27(2)	31(2)	22(2)	9(1)	4(1)	2(2)
C(2)	22(2)	35(2)	27(2)	13(2)	6(1)	7(2)
C(3)	26(2)	29(2)	21(2)	9(1)	2(1)	2(2)
C(4)	29(2)	30(2)	20(2)	7(1)	4(1)	5(2)
C(5)	26(2)	28(2)	21(2)	8(1)	7(1)	5(2)
C(6)	32(2)	29(2)	23(2)	9(1)	7(2)	3(2)
C(7)	32(2)	32(2)	29(2)	7(2)	6(2)	-1(2)
C(8)	34(2)	29(2)	33(2)	13(2)	8(2)	7(2)
C(9)	28(2)	32(2)	26(2)	11(2)	7(2)	7(2)
C(10)	35(2)	30(2)	37(2)	9(2)	12(2)	8(2)
C(11)	31(2)	41(2)	35(2)	13(2)	8(2)	8(2)
C(12)	31(2)	40(2)	40(2)	11(2)	10(2)	-0(2)
C(13)	37(2)	39(2)	44(2)	21(2)	21(2)	14(2)
C(14)	34(2)	40(2)	28(2)	10(2)	8(2)	12(2)
C(15)	28(2)	23(2)	21(2)	6(1)	2(1)	-1(2)
C(16)	35(2)	29(2)	24(2)	9(2)	5(2)	2(2)
C(17)	37(2)	33(2)	21(2)	12(2)	1(2)	-3(2)
C(18)	31(2)	36(2)	22(2)	5(2)	9(2)	-1(2)
C(19)	28(2)	25(2)	27(2)	7(1)	4(1)	-2(2)
C(20)	31(2)	35(2)	29(2)	13(2)	6(2)	-1(2)
C(21)	28(2)	38(2)	37(2)	17(2)	2(2)	-2(2)
C(22)	34(2)	41(2)	23(2)	11(2)	-3(2)	-5(2)
C(23)	36(2)	30(2)	28(2)	5(2)	1(2)	-8(2)
C(24)	37(2)	30(2)	30(2)	13(2)	2(2)	-1(2)
C(25)	41(2)	31(2)	29(2)	11(2)	7(2)	5(2)
C(26)	62(3)	42(3)	46(2)	12(2)	15(2)	21(2)
C(27)	58(3)	34(2)	44(2)	16(2)	7(2)	-4(2)
C(28)	34(2)	36(2)	29(2)	13(2)	5(2)	3(2)
C(29)	34(2)	49(3)	38(2)	16(2)	1(2)	9(2)
C(30)	45(2)	36(2)	40(2)	10(2)	13(2)	10(2)
C(31)	35(2)	39(2)	25(2)	16(2)	1(2)	3(2)
C(32)	50(3)	62(3)	32(2)	25(2)	11(2)	8(2)
C(33)	36(2)	82(4)	51(3)	35(3)	-1(2)	3(2)

N(1)	30(2)	31(2)	20(1)	9(1)	3(1)	1(1)
Si(1)	30(1)	29(1)	22(1)	10(1)	4(1)	3(1)
Fe(1)	26(1)	28(1)	26(1)	10(1)	5(1)	4(1)
Fe(2)	28(1)	28(1)	21(1)	7(1)	3(1)	1(1)

Supporting Information Table 23

Hydrogen coordinates (x 10^4) and isotropic displacement parameters (A^2 x 10^3) for 3,4-bis(ferrocenyl)-1-(triisopropylsilyl)pyrrole.

	x	y	z	U(eq)
H(1)	8799	5622	1064	33
H(4)	11003	8341	3219	32
H(6)	5900	4128	1104	34
H(7)	5203	2159	1244	39
H(8)	7444	2135	2510	37
H(9)	9519	4097	3162	33
H(10)	5388	6383	3445	41
H(11)	2762	5037	2288	43
H(12)	2294	3124	2529	46
H(13)	4630	3278	3817	44
H(14)	6548	5289	4385	41
H(16)	11730	5674	4177	36
H(17)	11043	6260	5667	37
H(18)	8750	7727	5832	37
H(19)	7970	8005	4424	33
H(20)	13929	8463	4081	38
H(21)	15256	7781	5254	41
H(22)	13930	8851	6562	41
H(23)	11772	10175	6190	41
H(24)	11789	9949	4662	39
H(25)	12193	9645	2614	41
H(26A)	10123	10912	2569	60
H(26B)	8946	9643	2291	60
H(26C)	9278	10179	1589	60
H(27A)	12436	10247	1167	55
H(27B)	14127	9919	1703	55
H(27C)	13239	11081	2132	55
H(28)	14169	7827	965	39
H(29A)	14175	7371	2490	49
H(29B)	15012	8580	2441	49
H(29C)	15969	7428	2073	49
H(30A)	14612	5858	755	49
H(30B)	12711	5913	191	49
H(30C)	12684	5656	1043	49
H(31)	9771	6605	15	39
H(32A)	9820	7640	-865	55

H(32B)	11803	7993	-249	55
H(32C)	10283	8869	-83	55
H(33A)	7519	8424	481	65
H(33B)	7201	7242	665	65
H(33C)	6957	7189	-292	65

Supporting Information Table 24

Torsion angles [deg] for 3,4-bis(ferrocenyl)-1-(triisopropylsilyl)pyrrole.

N(1)-C(1)-C(2)-C(3)	-0.2(4)
N(1)-C(1)-C(2)-C(5)	179.9(3)
C(1)-C(2)-C(3)-C(4)	0.4(4)
C(5)-C(2)-C(3)-C(4)	-179.7(3)
C(1)-C(2)-C(3)-C(15)	178.5(3)
C(5)-C(2)-C(3)-C(15)	-1.6(6)
C(2)-C(3)-C(4)-N(1)	-0.5(4)
C(15)-C(3)-C(4)-N(1)	-178.6(3)
C(1)-C(2)-C(5)-C(6)	-33.7(5)
C(3)-C(2)-C(5)-C(6)	146.5(4)
C(1)-C(2)-C(5)-C(9)	141.0(4)
C(3)-C(2)-C(5)-C(9)	-38.8(6)
C(1)-C(2)-C(5)-Fe(1)	-125.6(3)
C(3)-C(2)-C(5)-Fe(1)	54.5(5)
C(9)-C(5)-C(6)-C(7)	0.0(4)
C(2)-C(5)-C(6)-C(7)	175.6(3)
Fe(1)-C(5)-C(6)-C(7)	-58.8(2)
C(9)-C(5)-C(6)-Fe(1)	58.9(2)
C(2)-C(5)-C(6)-Fe(1)	-125.5(3)
C(5)-C(6)-C(7)-C(8)	-0.1(4)
Fe(1)-C(6)-C(7)-C(8)	-59.8(3)
C(5)-C(6)-C(7)-Fe(1)	59.6(2)
C(6)-C(7)-C(8)-C(9)	0.2(4)
Fe(1)-C(7)-C(8)-C(9)	-59.5(2)
C(6)-C(7)-C(8)-Fe(1)	59.7(2)
C(7)-C(8)-C(9)-C(5)	-0.2(4)
Fe(1)-C(8)-C(9)-C(5)	-59.4(2)
C(7)-C(8)-C(9)-Fe(1)	59.2(3)
C(6)-C(5)-C(9)-C(8)	0.1(4)
C(2)-C(5)-C(9)-C(8)	-175.4(3)
Fe(1)-C(5)-C(9)-C(8)	58.9(2)
C(6)-C(5)-C(9)-Fe(1)	-58.8(2)
C(2)-C(5)-C(9)-Fe(1)	125.7(3)
C(14)-C(10)-C(11)-C(12)	0.3(4)
Fe(1)-C(10)-C(11)-C(12)	59.5(3)
C(14)-C(10)-C(11)-Fe(1)	-59.3(3)
C(10)-C(11)-C(12)-C(13)	-0.3(4)
Fe(1)-C(11)-C(12)-C(13)	59.3(3)
C(10)-C(11)-C(12)-Fe(1)	-59.6(3)
C(11)-C(12)-C(13)-C(14)	0.2(4)
Fe(1)-C(12)-C(13)-C(14)	59.6(3)

C(11)-C(12)-C(13)-Fe(1)	-59.4(3)
C(11)-C(10)-C(14)-C(13)	-0.2(4)
Fe(1)-C(10)-C(14)-C(13)	-59.4(3)
C(11)-C(10)-C(14)-Fe(1)	59.2(2)
C(12)-C(13)-C(14)-C(10)	0.0(4)
Fe(1)-C(13)-C(14)-C(10)	59.6(3)
C(12)-C(13)-C(14)-Fe(1)	-59.5(3)
C(4)-C(3)-C(15)-C(19)	67.4(5)
C(2)-C(3)-C(15)-C(19)	-110.4(4)
C(4)-C(3)-C(15)-C(16)	-111.2(4)
C(2)-C(3)-C(15)-C(16)	71.1(5)
C(4)-C(3)-C(15)-Fe(2)	-21.3(5)
C(2)-C(3)-C(15)-Fe(2)	160.9(3)
C(19)-C(15)-C(16)-C(17)	1.1(4)
C(3)-C(15)-C(16)-C(17)	179.9(3)
Fe(2)-C(15)-C(16)-C(17)	59.6(2)
C(19)-C(15)-C(16)-Fe(2)	-58.5(2)
C(3)-C(15)-C(16)-Fe(2)	120.3(4)
C(15)-C(16)-C(17)-C(18)	-1.2(4)
Fe(2)-C(16)-C(17)-C(18)	59.1(3)
C(15)-C(16)-C(17)-Fe(2)	-60.3(2)
C(16)-C(17)-C(18)-C(19)	0.8(4)
Fe(2)-C(17)-C(18)-C(19)	59.7(2)
C(16)-C(17)-C(18)-Fe(2)	-59.0(3)
C(16)-C(15)-C(19)-C(18)	-0.7(4)
C(3)-C(15)-C(19)-C(18)	-179.5(3)
Fe(2)-C(15)-C(19)-C(18)	-59.0(2)
C(16)-C(15)-C(19)-Fe(2)	58.3(2)
C(3)-C(15)-C(19)-Fe(2)	-120.5(3)
C(17)-C(18)-C(19)-C(15)	0.0(4)
Fe(2)-C(18)-C(19)-C(15)	59.7(2)
C(17)-C(18)-C(19)-Fe(2)	-59.8(3)
C(24)-C(20)-C(21)-C(22)	0.0(4)
Fe(2)-C(20)-C(21)-C(22)	-59.6(3)
C(24)-C(20)-C(21)-Fe(2)	59.6(3)
C(20)-C(21)-C(22)-C(23)	0.3(4)
Fe(2)-C(21)-C(22)-C(23)	-59.2(3)
C(20)-C(21)-C(22)-Fe(2)	59.5(3)
C(21)-C(22)-C(23)-C(24)	-0.4(4)
Fe(2)-C(22)-C(23)-C(24)	-59.4(3)
C(21)-C(22)-C(23)-Fe(2)	59.0(3)
C(22)-C(23)-C(24)-C(20)	0.4(4)
Fe(2)-C(23)-C(24)-C(20)	-59.2(3)
C(22)-C(23)-C(24)-Fe(2)	59.6(3)
C(21)-C(20)-C(24)-C(23)	-0.3(4)
Fe(2)-C(20)-C(24)-C(23)	59.4(3)

C(21)-C(20)-C(24)-Fe(2)	-59.7(3)
C(2)-C(1)-N(1)-C(4)	0.0(4)
C(2)-C(1)-N(1)-Si(1)	163.0(2)
C(3)-C(4)-N(1)-C(1)	0.3(4)
C(3)-C(4)-N(1)-Si(1)	-163.0(3)
C(1)-N(1)-Si(1)-C(31)	39.9(3)
C(4)-N(1)-Si(1)-C(31)	-160.2(3)
C(1)-N(1)-Si(1)-C(28)	-78.0(3)
C(4)-N(1)-Si(1)-C(28)	82.0(3)
C(1)-N(1)-Si(1)-C(25)	164.9(3)
C(4)-N(1)-Si(1)-C(25)	-35.1(3)
C(33)-C(31)-Si(1)-N(1)	50.3(3)
C(32)-C(31)-Si(1)-N(1)	177.6(3)
C(33)-C(31)-Si(1)-C(28)	167.0(3)
C(32)-C(31)-Si(1)-C(28)	-65.8(3)
C(33)-C(31)-Si(1)-C(25)	-68.3(4)
C(32)-C(31)-Si(1)-C(25)	58.9(3)
C(29)-C(28)-Si(1)-N(1)	-61.4(3)
C(30)-C(28)-Si(1)-N(1)	63.4(3)
C(29)-C(28)-Si(1)-C(31)	-177.1(3)
C(30)-C(28)-Si(1)-C(31)	-52.4(3)
C(29)-C(28)-Si(1)-C(25)	54.0(3)
C(30)-C(28)-Si(1)-C(25)	178.8(3)
C(26)-C(25)-Si(1)-N(1)	-66.1(3)
C(27)-C(25)-Si(1)-N(1)	165.6(3)
C(26)-C(25)-Si(1)-C(31)	52.6(3)
C(27)-C(25)-Si(1)-C(31)	-75.7(3)
C(26)-C(25)-Si(1)-C(28)	177.6(3)
C(27)-C(25)-Si(1)-C(28)	49.3(3)
C(8)-C(7)-Fe(1)-C(13)	-76.2(3)
C(6)-C(7)-Fe(1)-C(13)	164.7(2)
C(6)-C(7)-Fe(1)-C(8)	-119.1(3)
C(8)-C(7)-Fe(1)-C(6)	119.1(3)
C(8)-C(7)-Fe(1)-C(12)	-117.5(2)
C(6)-C(7)-Fe(1)-C(12)	123.4(2)
C(8)-C(7)-Fe(1)-C(11)	-159.7(2)
C(6)-C(7)-Fe(1)-C(11)	81.1(3)
C(8)-C(7)-Fe(1)-C(14)	-43.8(6)
C(6)-C(7)-Fe(1)-C(14)	-162.9(4)
C(8)-C(7)-Fe(1)-C(9)	37.9(2)
C(6)-C(7)-Fe(1)-C(9)	-81.3(2)
C(8)-C(7)-Fe(1)-C(10)	167.1(4)
C(6)-C(7)-Fe(1)-C(10)	47.9(5)
C(8)-C(7)-Fe(1)-C(5)	81.8(2)
C(6)-C(7)-Fe(1)-C(5)	-37.3(2)
C(12)-C(13)-Fe(1)-C(7)	-75.7(3)

C(14)-C(13)-Fe(1)-C(7)	164.9(2)
C(12)-C(13)-Fe(1)-C(8)	-117.3(2)
C(14)-C(13)-Fe(1)-C(8)	123.3(2)
C(12)-C(13)-Fe(1)-C(6)	-42.3(6)
C(14)-C(13)-Fe(1)-C(6)	-161.7(4)
C(14)-C(13)-Fe(1)-C(12)	-119.4(3)
C(12)-C(13)-Fe(1)-C(11)	37.6(2)
C(14)-C(13)-Fe(1)-C(11)	-81.8(2)
C(12)-C(13)-Fe(1)-C(14)	119.4(3)
C(12)-C(13)-Fe(1)-C(9)	-159.9(2)
C(14)-C(13)-Fe(1)-C(9)	80.8(2)
C(12)-C(13)-Fe(1)-C(10)	81.6(3)
C(14)-C(13)-Fe(1)-C(10)	-37.8(2)
C(12)-C(13)-Fe(1)-C(5)	165.1(3)
C(14)-C(13)-Fe(1)-C(5)	45.7(4)
C(9)-C(8)-Fe(1)-C(7)	119.0(3)
C(7)-C(8)-Fe(1)-C(13)	123.1(2)
C(9)-C(8)-Fe(1)-C(13)	-117.9(2)
C(7)-C(8)-Fe(1)-C(6)	-37.9(2)
C(9)-C(8)-Fe(1)-C(6)	81.1(2)
C(7)-C(8)-Fe(1)-C(12)	80.8(3)
C(9)-C(8)-Fe(1)-C(12)	-160.2(2)
C(7)-C(8)-Fe(1)-C(11)	47.2(5)
C(9)-C(8)-Fe(1)-C(11)	166.2(3)
C(7)-C(8)-Fe(1)-C(14)	164.5(2)
C(9)-C(8)-Fe(1)-C(14)	-76.4(3)
C(7)-C(8)-Fe(1)-C(9)	-119.0(3)
C(7)-C(8)-Fe(1)-C(10)	-163.5(4)
C(9)-C(8)-Fe(1)-C(10)	-44.4(6)
C(7)-C(8)-Fe(1)-C(5)	-81.7(2)
C(9)-C(8)-Fe(1)-C(5)	37.3(2)
C(5)-C(6)-Fe(1)-C(7)	-119.8(3)
C(7)-C(6)-Fe(1)-C(13)	-43.7(6)
C(5)-C(6)-Fe(1)-C(13)	-163.6(4)
C(7)-C(6)-Fe(1)-C(8)	37.7(2)
C(5)-C(6)-Fe(1)-C(8)	-82.1(2)
C(7)-C(6)-Fe(1)-C(12)	-75.9(3)
C(5)-C(6)-Fe(1)-C(12)	164.2(2)
C(7)-C(6)-Fe(1)-C(11)	-117.2(2)
C(5)-C(6)-Fe(1)-C(11)	122.9(2)
C(7)-C(6)-Fe(1)-C(14)	166.7(3)
C(5)-C(6)-Fe(1)-C(14)	46.8(4)
C(7)-C(6)-Fe(1)-C(9)	81.7(2)
C(5)-C(6)-Fe(1)-C(9)	-38.2(2)
C(7)-C(6)-Fe(1)-C(10)	-159.7(2)
C(5)-C(6)-Fe(1)-C(10)	80.5(2)

C(7)-C(6)-Fe(1)-C(5)	119.8(3)
C(13)-C(12)-Fe(1)-C(7)	123.3(2)
C(11)-C(12)-Fe(1)-C(7)	-117.4(2)
C(11)-C(12)-Fe(1)-C(13)	119.3(3)
C(13)-C(12)-Fe(1)-C(8)	80.9(3)
C(11)-C(12)-Fe(1)-C(8)	-159.8(2)
C(13)-C(12)-Fe(1)-C(6)	165.1(2)
C(11)-C(12)-Fe(1)-C(6)	-75.6(3)
C(13)-C(12)-Fe(1)-C(11)	-119.3(3)
C(13)-C(12)-Fe(1)-C(14)	-37.6(2)
C(11)-C(12)-Fe(1)-C(14)	81.7(2)
C(13)-C(12)-Fe(1)-C(9)	47.3(5)
C(11)-C(12)-Fe(1)-C(9)	166.6(3)
C(13)-C(12)-Fe(1)-C(10)	-81.3(2)
C(11)-C(12)-Fe(1)-C(10)	38.0(2)
C(13)-C(12)-Fe(1)-C(5)	-161.0(4)
C(11)-C(12)-Fe(1)-C(5)	-41.7(5)
C(12)-C(11)-Fe(1)-C(7)	80.8(3)
C(10)-C(11)-Fe(1)-C(7)	-160.4(2)
C(12)-C(11)-Fe(1)-C(13)	-37.6(2)
C(10)-C(11)-Fe(1)-C(13)	81.3(2)
C(12)-C(11)-Fe(1)-C(8)	46.9(5)
C(10)-C(11)-Fe(1)-C(8)	165.8(3)
C(12)-C(11)-Fe(1)-C(6)	123.5(2)
C(10)-C(11)-Fe(1)-C(6)	-117.6(2)
C(10)-C(11)-Fe(1)-C(12)	118.8(3)
C(12)-C(11)-Fe(1)-C(14)	-81.4(2)
C(10)-C(11)-Fe(1)-C(14)	37.5(2)
C(12)-C(11)-Fe(1)-C(9)	-162.8(4)
C(10)-C(11)-Fe(1)-C(9)	-44.0(5)
C(12)-C(11)-Fe(1)-C(10)	-118.8(3)
C(12)-C(11)-Fe(1)-C(5)	165.2(2)
C(10)-C(11)-Fe(1)-C(5)	-76.0(3)
C(10)-C(14)-Fe(1)-C(7)	-161.6(4)
C(13)-C(14)-Fe(1)-C(7)	-42.6(6)
C(10)-C(14)-Fe(1)-C(13)	-119.0(3)
C(10)-C(14)-Fe(1)-C(8)	165.1(2)
C(13)-C(14)-Fe(1)-C(8)	-75.9(3)
C(10)-C(14)-Fe(1)-C(6)	46.9(5)
C(13)-C(14)-Fe(1)-C(6)	165.9(3)
C(10)-C(14)-Fe(1)-C(12)	-81.4(2)
C(13)-C(14)-Fe(1)-C(12)	37.5(2)
C(10)-C(14)-Fe(1)-C(11)	-37.7(2)
C(13)-C(14)-Fe(1)-C(11)	81.3(2)
C(10)-C(14)-Fe(1)-C(9)	123.3(2)
C(13)-C(14)-Fe(1)-C(9)	-117.7(2)

C(13)-C(14)-Fe(1)-C(10)	119.0(3)
C(10)-C(14)-Fe(1)-C(5)	80.6(3)
C(13)-C(14)-Fe(1)-C(5)	-160.5(2)
C(8)-C(9)-Fe(1)-C(7)	-37.8(2)
C(5)-C(9)-Fe(1)-C(7)	82.3(2)
C(8)-C(9)-Fe(1)-C(13)	80.6(2)
C(5)-C(9)-Fe(1)-C(13)	-159.4(2)
C(5)-C(9)-Fe(1)-C(8)	120.1(3)
C(8)-C(9)-Fe(1)-C(6)	-82.0(2)
C(5)-C(9)-Fe(1)-C(6)	38.08(19)
C(8)-C(9)-Fe(1)-C(12)	46.6(4)
C(5)-C(9)-Fe(1)-C(12)	166.7(3)
C(8)-C(9)-Fe(1)-C(11)	-162.0(4)
C(5)-C(9)-Fe(1)-C(11)	-42.0(5)
C(8)-C(9)-Fe(1)-C(14)	123.0(2)
C(5)-C(9)-Fe(1)-C(14)	-116.9(2)
C(8)-C(9)-Fe(1)-C(10)	164.4(2)
C(5)-C(9)-Fe(1)-C(10)	-75.5(2)
C(8)-C(9)-Fe(1)-C(5)	-120.1(3)
C(14)-C(10)-Fe(1)-C(7)	165.5(4)
C(11)-C(10)-Fe(1)-C(7)	46.1(5)
C(14)-C(10)-Fe(1)-C(13)	37.8(2)
C(11)-C(10)-Fe(1)-C(13)	-81.6(2)
C(14)-C(10)-Fe(1)-C(8)	-42.1(6)
C(11)-C(10)-Fe(1)-C(8)	-161.5(4)
C(14)-C(10)-Fe(1)-C(6)	-159.9(2)
C(11)-C(10)-Fe(1)-C(6)	80.7(3)
C(14)-C(10)-Fe(1)-C(12)	81.6(2)
C(11)-C(10)-Fe(1)-C(12)	-37.8(2)
C(14)-C(10)-Fe(1)-C(11)	119.4(3)
C(11)-C(10)-Fe(1)-C(14)	-119.4(3)
C(14)-C(10)-Fe(1)-C(9)	-76.0(3)
C(11)-C(10)-Fe(1)-C(9)	164.6(2)
C(14)-C(10)-Fe(1)-C(5)	-117.5(2)
C(11)-C(10)-Fe(1)-C(5)	123.1(2)
C(6)-C(5)-Fe(1)-C(7)	37.5(2)
C(9)-C(5)-Fe(1)-C(7)	-81.0(2)
C(2)-C(5)-Fe(1)-C(7)	157.3(3)
C(6)-C(5)-Fe(1)-C(13)	167.2(3)
C(9)-C(5)-Fe(1)-C(13)	48.7(4)
C(2)-C(5)-Fe(1)-C(13)	-73.0(5)
C(6)-C(5)-Fe(1)-C(8)	81.3(2)
C(9)-C(5)-Fe(1)-C(8)	-37.3(2)
C(2)-C(5)-Fe(1)-C(8)	-158.9(3)
C(9)-C(5)-Fe(1)-C(6)	-118.5(3)
C(2)-C(5)-Fe(1)-C(6)	119.8(4)

C(6)-C(5)-Fe(1)-C(12)	-44.6(5)
C(9)-C(5)-Fe(1)-C(12)	-163.1(4)
C(2)-C(5)-Fe(1)-C(12)	75.2(6)
C(6)-C(5)-Fe(1)-C(11)	-76.2(2)
C(9)-C(5)-Fe(1)-C(11)	165.3(2)
C(2)-C(5)-Fe(1)-C(11)	43.6(4)
C(6)-C(5)-Fe(1)-C(14)	-159.9(2)
C(9)-C(5)-Fe(1)-C(14)	81.5(2)
C(2)-C(5)-Fe(1)-C(14)	-40.2(4)
C(6)-C(5)-Fe(1)-C(9)	118.5(3)
C(2)-C(5)-Fe(1)-C(9)	-121.7(4)
C(6)-C(5)-Fe(1)-C(10)	-117.8(2)
C(9)-C(5)-Fe(1)-C(10)	123.7(2)
C(2)-C(5)-Fe(1)-C(10)	2.0(3)
C(15)-C(16)-Fe(2)-C(17)	119.3(3)
C(17)-C(16)-Fe(2)-C(18)	-37.4(2)
C(15)-C(16)-Fe(2)-C(18)	81.9(2)
C(17)-C(16)-Fe(2)-C(19)	-81.5(2)
C(15)-C(16)-Fe(2)-C(19)	37.8(2)
C(17)-C(16)-Fe(2)-C(20)	151.2(2)
C(15)-C(16)-Fe(2)-C(20)	-89.5(2)
C(17)-C(16)-Fe(2)-C(24)	-174.8(3)
C(15)-C(16)-Fe(2)-C(24)	-55.5(4)
C(17)-C(16)-Fe(2)-C(21)	108.2(2)
C(15)-C(16)-Fe(2)-C(21)	-132.5(2)
C(17)-C(16)-Fe(2)-C(23)	45.1(10)
C(15)-C(16)-Fe(2)-C(23)	164.4(9)
C(17)-C(16)-Fe(2)-C(22)	69.4(3)
C(15)-C(16)-Fe(2)-C(22)	-171.3(2)
C(17)-C(16)-Fe(2)-C(15)	-119.3(3)
C(18)-C(17)-Fe(2)-C(16)	-119.7(3)
C(16)-C(17)-Fe(2)-C(18)	119.7(3)
C(18)-C(17)-Fe(2)-C(19)	-38.4(2)
C(16)-C(17)-Fe(2)-C(19)	81.4(2)
C(18)-C(17)-Fe(2)-C(20)	-172.7(2)
C(16)-C(17)-Fe(2)-C(20)	-52.9(3)
C(18)-C(17)-Fe(2)-C(24)	41.1(10)
C(16)-C(17)-Fe(2)-C(24)	160.8(9)
C(18)-C(17)-Fe(2)-C(21)	152.1(2)
C(16)-C(17)-Fe(2)-C(21)	-88.2(2)
C(18)-C(17)-Fe(2)-C(23)	69.3(3)
C(16)-C(17)-Fe(2)-C(23)	-170.9(2)
C(18)-C(17)-Fe(2)-C(22)	108.4(2)
C(16)-C(17)-Fe(2)-C(22)	-131.8(2)
C(18)-C(17)-Fe(2)-C(15)	-82.1(2)
C(16)-C(17)-Fe(2)-C(15)	37.6(2)

C(17)-C(18)-Fe(2)-C(16)	37.6(2)
C(19)-C(18)-Fe(2)-C(16)	-80.8(2)
C(19)-C(18)-Fe(2)-C(17)	-118.4(3)
C(17)-C(18)-Fe(2)-C(19)	118.4(3)
C(17)-C(18)-Fe(2)-C(20)	151.7(9)
C(19)-C(18)-Fe(2)-C(20)	33.4(10)
C(17)-C(18)-Fe(2)-C(24)	-172.3(2)
C(19)-C(18)-Fe(2)-C(24)	69.3(3)
C(17)-C(18)-Fe(2)-C(21)	-52.0(4)
C(19)-C(18)-Fe(2)-C(21)	-170.4(3)
C(17)-C(18)-Fe(2)-C(23)	-132.4(2)
C(19)-C(18)-Fe(2)-C(23)	109.2(2)
C(17)-C(18)-Fe(2)-C(22)	-89.0(2)
C(19)-C(18)-Fe(2)-C(22)	152.7(2)
C(17)-C(18)-Fe(2)-C(15)	81.4(2)
C(19)-C(18)-Fe(2)-C(15)	-37.0(2)
C(15)-C(19)-Fe(2)-C(16)	-38.0(2)
C(18)-C(19)-Fe(2)-C(16)	82.3(2)
C(15)-C(19)-Fe(2)-C(17)	-82.1(2)
C(18)-C(19)-Fe(2)-C(17)	38.1(2)
C(15)-C(19)-Fe(2)-C(18)	-120.2(3)
C(15)-C(19)-Fe(2)-C(20)	66.1(3)
C(18)-C(19)-Fe(2)-C(20)	-173.7(2)
C(15)-C(19)-Fe(2)-C(24)	106.9(2)
C(18)-C(19)-Fe(2)-C(24)	-132.9(2)
C(15)-C(19)-Fe(2)-C(21)	29.0(9)
C(18)-C(19)-Fe(2)-C(21)	149.2(8)
C(15)-C(19)-Fe(2)-C(23)	150.6(2)
C(18)-C(19)-Fe(2)-C(23)	-89.2(2)
C(15)-C(19)-Fe(2)-C(22)	-172.9(3)
C(18)-C(19)-Fe(2)-C(22)	-52.7(4)
C(18)-C(19)-Fe(2)-C(15)	120.2(3)
C(21)-C(20)-Fe(2)-C(16)	-88.7(2)
C(24)-C(20)-Fe(2)-C(16)	152.3(2)
C(21)-C(20)-Fe(2)-C(17)	-53.6(3)
C(24)-C(20)-Fe(2)-C(17)	-172.7(2)
C(21)-C(20)-Fe(2)-C(18)	160.5(9)
C(24)-C(20)-Fe(2)-C(18)	41.5(10)
C(21)-C(20)-Fe(2)-C(19)	-170.6(2)
C(24)-C(20)-Fe(2)-C(19)	70.3(3)
C(21)-C(20)-Fe(2)-C(24)	119.0(3)
C(24)-C(20)-Fe(2)-C(21)	-119.0(3)
C(21)-C(20)-Fe(2)-C(23)	81.5(2)
C(24)-C(20)-Fe(2)-C(23)	-37.5(2)
C(21)-C(20)-Fe(2)-C(22)	38.0(2)
C(24)-C(20)-Fe(2)-C(22)	-81.1(2)

C(21)-C(20)-Fe(2)-C(15)	-132.0(2)
C(24)-C(20)-Fe(2)-C(15)	109.0(2)
C(23)-C(24)-Fe(2)-C(16)	-170.6(3)
C(20)-C(24)-Fe(2)-C(16)	-51.3(4)
C(23)-C(24)-Fe(2)-C(17)	32.7(11)
C(20)-C(24)-Fe(2)-C(17)	152.1(9)
C(23)-C(24)-Fe(2)-C(18)	68.3(3)
C(20)-C(24)-Fe(2)-C(18)	-172.3(2)
C(23)-C(24)-Fe(2)-C(19)	109.0(2)
C(20)-C(24)-Fe(2)-C(19)	-131.6(2)
C(23)-C(24)-Fe(2)-C(20)	-119.4(3)
C(23)-C(24)-Fe(2)-C(21)	-81.7(2)
C(20)-C(24)-Fe(2)-C(21)	37.7(2)
C(20)-C(24)-Fe(2)-C(23)	119.4(3)
C(23)-C(24)-Fe(2)-C(22)	-37.6(2)
C(20)-C(24)-Fe(2)-C(22)	81.8(2)
C(23)-C(24)-Fe(2)-C(15)	152.7(2)
C(20)-C(24)-Fe(2)-C(15)	-87.9(2)
C(20)-C(21)-Fe(2)-C(16)	107.5(2)
C(22)-C(21)-Fe(2)-C(16)	-133.6(2)
C(20)-C(21)-Fe(2)-C(17)	150.8(2)
C(22)-C(21)-Fe(2)-C(17)	-90.3(2)
C(20)-C(21)-Fe(2)-C(18)	-174.7(2)
C(22)-C(21)-Fe(2)-C(18)	-55.8(4)
C(20)-C(21)-Fe(2)-C(19)	43.8(9)
C(22)-C(21)-Fe(2)-C(19)	162.8(8)
C(22)-C(21)-Fe(2)-C(20)	118.9(3)
C(20)-C(21)-Fe(2)-C(24)	-37.9(2)
C(22)-C(21)-Fe(2)-C(24)	81.1(2)
C(20)-C(21)-Fe(2)-C(23)	-81.6(2)
C(22)-C(21)-Fe(2)-C(23)	37.3(2)
C(20)-C(21)-Fe(2)-C(22)	-118.9(3)
C(20)-C(21)-Fe(2)-C(15)	68.3(3)
C(22)-C(21)-Fe(2)-C(15)	-172.8(2)
C(22)-C(23)-Fe(2)-C(16)	28.5(10)
C(24)-C(23)-Fe(2)-C(16)	147.6(9)
C(22)-C(23)-Fe(2)-C(17)	67.2(3)
C(24)-C(23)-Fe(2)-C(17)	-173.8(2)
C(22)-C(23)-Fe(2)-C(18)	107.5(2)
C(24)-C(23)-Fe(2)-C(18)	-133.4(2)
C(22)-C(23)-Fe(2)-C(19)	151.6(2)
C(24)-C(23)-Fe(2)-C(19)	-89.3(2)
C(22)-C(23)-Fe(2)-C(20)	-81.4(2)
C(24)-C(23)-Fe(2)-C(20)	37.7(2)
C(22)-C(23)-Fe(2)-C(24)	-119.1(3)
C(22)-C(23)-Fe(2)-C(21)	-37.6(2)

C(24)-C(23)-Fe(2)-C(21)	81.4(2)
C(24)-C(23)-Fe(2)-C(22)	119.1(3)
C(22)-C(23)-Fe(2)-C(15)	-171.0(3)
C(24)-C(23)-Fe(2)-C(15)	-51.9(4)
C(23)-C(22)-Fe(2)-C(16)	-174.0(2)
C(21)-C(22)-Fe(2)-C(16)	66.4(3)
C(23)-C(22)-Fe(2)-C(17)	-133.7(2)
C(21)-C(22)-Fe(2)-C(17)	106.8(2)
C(23)-C(22)-Fe(2)-C(18)	-90.2(2)
C(21)-C(22)-Fe(2)-C(18)	150.3(2)
C(23)-C(22)-Fe(2)-C(19)	-54.7(4)
C(21)-C(22)-Fe(2)-C(19)	-174.2(3)
C(23)-C(22)-Fe(2)-C(20)	81.8(2)
C(21)-C(22)-Fe(2)-C(20)	-37.7(2)
C(23)-C(22)-Fe(2)-C(24)	37.8(2)
C(21)-C(22)-Fe(2)-C(24)	-81.8(2)
C(23)-C(22)-Fe(2)-C(21)	119.6(3)
C(21)-C(22)-Fe(2)-C(23)	-119.6(3)
C(23)-C(22)-Fe(2)-C(15)	152.2(8)
C(21)-C(22)-Fe(2)-C(15)	32.6(9)
C(19)-C(15)-Fe(2)-C(16)	118.9(3)
C(3)-C(15)-Fe(2)-C(16)	-121.8(4)
C(19)-C(15)-Fe(2)-C(17)	81.1(2)
C(16)-C(15)-Fe(2)-C(17)	-37.8(2)
C(3)-C(15)-Fe(2)-C(17)	-159.6(3)
C(19)-C(15)-Fe(2)-C(18)	37.4(2)
C(16)-C(15)-Fe(2)-C(18)	-81.5(2)
C(3)-C(15)-Fe(2)-C(18)	156.7(3)
C(16)-C(15)-Fe(2)-C(19)	-118.9(3)
C(3)-C(15)-Fe(2)-C(19)	119.3(4)
C(19)-C(15)-Fe(2)-C(20)	-134.2(2)
C(16)-C(15)-Fe(2)-C(20)	106.9(2)
C(3)-C(15)-Fe(2)-C(20)	-14.9(3)
C(19)-C(15)-Fe(2)-C(24)	-90.9(2)
C(16)-C(15)-Fe(2)-C(24)	150.2(2)
C(3)-C(15)-Fe(2)-C(24)	28.4(3)
C(19)-C(15)-Fe(2)-C(21)	-173.6(2)
C(16)-C(15)-Fe(2)-C(21)	67.5(3)
C(3)-C(15)-Fe(2)-C(21)	-54.2(4)
C(19)-C(15)-Fe(2)-C(23)	-56.3(4)
C(16)-C(15)-Fe(2)-C(23)	-175.2(3)
C(3)-C(15)-Fe(2)-C(23)	63.1(4)
C(19)-C(15)-Fe(2)-C(22)	158.9(8)
C(16)-C(15)-Fe(2)-C(22)	40.0(9)
C(3)-C(15)-Fe(2)-C(22)	-81.8(9)

Symmetry transformations used to generate equivalent atoms:
#1 -x+1,-y,-z+1